14

A Comparison of Sediment Transport Models for Combined Current and Wave Flows

by

John Piero Gambino

Submitted to the Department of Civil and Environmental Engineering
in partial fulfillment of the requirements for the degree of

Master of Science in Civil and Environmental Engineering

at the

MASSACHUSETTS INSTITUTE OF TECHNOLOGY

February 1998

Author .....
Department of Civil and Environmental Engineering
January 29, 1998

Certified by .....
Ole S. Madsen
Professor, Department of Civil and Environmental Engineering
Thesis Supervisor

Accepted by .....
Joseph M. Sussman
Chairman, Departmental Committee on Graduate Studies
Department of Civil and Environmental Engineering

A Comparison of Sediment Transport Models for Combined Current and Wave Flows

by

John Piero Gambino

Submitted to the Department of Civil and Environmental Engineering
on January 29, 1998, in partial fulfillment of the
requirements for the degree of
Master of Science in Civil and Environmental Engineering

Abstract

Three models that predict sediment transport in combined wave-current flows were compared to determine which does the best job of modeling sediment transport in the coastal environment. The models compared were derived by Ackers and White (1973), Bailard (1981), and Madsen (1997). The Ackers and White model was derived for steady unidirectional flow and was modified by Scheffner (1996) to account for waves.

The assumptions made by the three models were analyzed and compared, and subsequently the predictions of the three models were also compared to determine the differences between the models. The analysis was first done for steady unidirectional flows to pinpoint differences in the models that were not specific to the combined wave-current flow. Major differences were found between the Madsen model and other two on how suspended load transport was calculated. These differences were magnified greatly when the predictions for combined wave-current flows were analyzed.

Analysis of the methods used by the different models indicate that the Madsen model does the best job of predicting sediment transport and that in the presence of large waves the other two models will over-predict the amount of sediment transport because of their deficiencies in accounting for the influence of waves in the calculation of suspended load transport.

Thesis Supervisor: Ole S. Madsen
Title: Professor, Department of Civil and Environmental Engineering

Acknowledgments

I would like to begin by thanking my advisor, Ole Madsen, for the all guidance he has given me throughout my 6 years at MIT. I know that I would have had a much tougher time going through MIT had it not been for his influence. He is a great professor and friend.

I am also very grateful to all of the friends who have shared my MIT experiences and even though many have moved on to new lives, they will never be forgotten. I would especially like to thank Paulo Salles and Sanjay Pahuja (an expert in the properties of sand) for their eagerness to help me with any problem that I faced, especially the academic ones.

Most importantly, I would like to thank my family. I dedicate this thesis to my parents, for all their love and support and to my sister Maria. I would finally like to thank my cousin Nico for his advice about college, and his encouragement to become an engineer, despite the fact that he probably will not be able to understand much of this thesis.

Contents

1.0 Introduction

The modeling of sediment transport in the coastal environment is complex and quite difficult. There are many factors that can influence sediment transport: waves, longshore currents, sediment size and density, storms and the slope of the bed. Predicting sediment transport is made even more difficult by the fact that these factors are highly variable, changing from one day to the next. Despite all of these difficulties, many models that try to predict sediment transport from these variables have been published. Knowing the sediment transport rate is quite useful because it helps to predict how often a harbor needs to be dredged, or how long a cap over a dumped contaminant can last before it is eroded away. It is also important in determining how beaches change due to waves, which is especially important to people who live close to or on a beach.

This paper examines three models of sediment transport, comparing how they account for each of the different variables that influence sediment transport and by analyzing the predictions made by these models when these variables change. The models examined are from Ackers and White (1973), Bailard (1981) and Madsen (1997). Linear waves are assumed for the analysis, without breaking, which makes the analysis valid for areas outside of the surf zone. Since the prediction of sediment transport is at best an estimate, compounded by the fact that we are trying to model the real coastal environment which is constantly changing, the exact answers are not known, so the patterns and trends of the predictions are looked at instead, to explain how and why each model predicts what is does.

This paper begins by reviewing each model, first for unidirectional flows and then for combined wave-current flows, summarizing the method of calculation used and the assumptions made by each model. The analysis begins by comparing the predictions made by the models for steady unidirectional flows, and then they are compared for combined wave-current flows. This is

done to examine why the models predict different results; to see whether they differ in their basic predictions of sediment transport in steady unidirectional flows or whether the differences are due to how they account for waves.

2.0 The Different Models for Pure Current

2.1 Ackers and White

The Ackers and White model for sediment transport is developed from a theory given by Ackers (1972). Ackers and White (1973) are seeking to develop a new framework for the analysis of transport data. In order to calculate the stream's transporting power, they are using the average stream velocity instead of the shear velocity. Dimensional analysis is used and the theory avoids refinements that the authors believe do not add much to the accuracy of the model.

Ackers and White (1973) state that there are seven variables needed to calculate the sediment transport of a unidirectional flow: sediment diameter; specific gravity of the sediment; mean velocity of the flow; shear velocity (which can be determined from the velocity distribution of the flow or the depth/slope relationship); depth of flow; kinematic viscosity of the fluid; and the acceleration due to gravity. The sediment transport rate (Q_s) in a steady unidirectional flow is given by

$$Q_s = C\left(\frac{F_{gr}}{A} - 1.0\right)^m dU\left(\frac{U}{U_*}\right)^n \tag{1}$$

Where d = median sediment diameter (d_{50})

U = depth-averaged current velocity

U_* = shear velocity

F_{gr} = sediment mobility number

A, C, m, and n are dimensionless variables calculated from equations 3 through 10.

The result, Q_s, is in units of volume per length per time. In order to use this equation, the dimensionless grain diameter, which is the cube root of the ratio of immersed weight to viscous forces, applicable to both coarse, transitional and fine sediments, needs to be calculated. Coarse sediment is sediment that is transported mainly as bedload while fine sediment is transported mainly as suspended load. The dimensionless grain diameter is given by

$$D_{gr} = d\left[g\frac{(s-1)}{\upsilon^2}\right]^{1/3} \tag{2}$$

Where g = acceleration due to gravity

s = specific gravity of the sediment

υ = the kinematic viscosity of the fluid

Once the dimensionless grain diameter is calculated, the following variables can be determined:

If $D_{gr} > 60.0$,

$$n = 0 \tag{3}$$

$$m = 1.5 \tag{4}$$

$$A = 0.17 \tag{5}$$

$$C = 0.025 \tag{6}$$

If $1.0 < D_{gr} \leq 60.0$,

$$n = 1.00 - 0.56 \log (D_{gr}) \tag{7}$$

$$m = (9.66 / D_{gr}) + 1.34 \tag{8}$$

$$A = (0.23/\sqrt{D_{gr}}) + 0.14 \tag{9}$$

$$\log C = 2.86 \log (D_{gr}) - (\log D_{gr})^2 - 3.53 \tag{10}$$

The shear velocity can be found if the Chezy coefficient is calculated. The formula given below for the Chezy coefficient (C_z) is valid only for metric units. C_z and the number 18 are in units of meters$^{1/2}$ / second. Once the Chezy coefficient is calculated, the shear velocity, U_*, can be calculated (Scheffner 1996).

$$C_z = 18 \log\left(12\frac{h}{d}\right) \tag{11}$$

$$U_* = U\frac{\sqrt{g}}{C_z} \tag{12}$$

h = flow depth

U = average flow velocity

Dimensionless expressions for sediment transport were derived using the stream power concept, which bases transport on the available power of the flow. There are different transport modes, depending on whether the sediment is coarse or fine. For fine sediment, the total stream power is

used to determine the power per unit area available while for coarse sediment, the power per unit area of the bed is the product of net grain shear and shear velocity. This leads to the development of a term for the efficiency of the transport. Ackers and White hypothesize that efficiency is dependent on the sediment mobility number, which is "the ratio of the shear force on unit area of the bed to the immersed weight of a layer of grains" (1973). The sediment mobility number is given by

$$F_{gr} = \frac{U_*^n}{\sqrt{gd(s-1)}}\left[\frac{U}{\sqrt{32}\log\left(\frac{\Theta h}{d}\right)}\right]^{1-n} \tag{13}$$

Theta (Θ) was determined experimentally from flume data and Θ should be set equal to 10. Once the sediment mobility number is calculated, all the variables needed for equation 1 are known and the sediment transport can be calculated. Equation 1 can be used for a range of sediment diameters from 0.04 mm to 4 mm (0.00004 m to 0.004 m).

2.2 Bailard

The basis for the Bailard model of sediment transport comes from the energetics-based total load sediment transport model for streams developed by Bagnold (1966). The Bagnold method is an attempt from the general to the particular and the uncertainties about turbulence effects, such as those of boundary roughness, form drag, and sediment transport, on the flow resistance have been avoided by treating the mean flow velocity and the tractive force as independent, or given, variables. Bagnold justifies this by stating that "the objective is to predict the transport of

solids by the fluid flow and not to attempt to predict fluid flow itself, which lies within the proper province of the hydraulic engineer" (Bagnold 1966).

Bagnold's model is applicable to streams and rivers with the following four restrictions: steady open-channel flow by gravity; unlimited availability of transportable solids; the concentration of transported solids, by immersed weight, is sufficiently small that the contribution of the tangential gravity pull on the solids to the applied tractive stress can be neglected; and the system considered is defined as statistically steady and as representative not of conditions at a single crossection but average conditions along a length of channel sufficient to include all repetitive irregularities of slope, crossection, and boundary.

Bagnold states that there are two ways by which sediment can be transported: through bedload and through suspended load. Bedload is supported by the bed via grain to grain interactions, while suspended load is supported by the fluid via turbulent diffusion. In either case, energy is used by the stream to transport the sediment. For steady flow, Bailard (1981) used Bagnold's theory to develop the following total load sediment transport equation:

$$i = i_B + i_S = \left(\frac{\varepsilon_B}{\tan\phi - \tan\beta} + \frac{\varepsilon_S}{(W/U) - \varepsilon_S \tan\beta} \right) \Omega \tag{14}$$

where i is the immersed weight per unit width per unit time, the subscript B refers to bedload and the subscript S refers to suspended load. β is the slope of the stream bed, ϕ is the internal angle of friction for the sediment, W is the fall velocity of the sediment (given by equation 45), ε is the load efficiency, U is the mean velocity of the stream, and Ω is the rate of energy dissipation of the stream, given by

$$\Omega = \tau U = \rho C_f |U|^3 \tag{15}$$

where τ is the shear stress at the bed, ρ is the density of water and C_f is a friction coefficient, taken equal to 0.003 from experimental data. Bagnold (1966) found the load efficiencies experimentally, and for stream flow found ε_B roughly equal to 0.13, ε_S roughly equal to 0.01, and tan ϕ can be taken as roughly equal to 40°. The immersed weight per unit width per unit time (i) can be related to the sediment transport, Q_s, by

$$i = (s-1)\rho g Q_s \tag{16}$$

where s is the specific gravity of the sediment. Bailard's (1981) derivation of equation 14 leads to a different result for the suspended load transport than the one Bagnold developed. Bailard begins with the analysis of a simple two dimensional flow over a plane bed with slope tan β. The depth of the flow is h, and the velocity is a function of z, expressed as $\vec{u}(z)$. The z coordinate is perpendicular to the bed while the x coordinate is directed downslope (parallel to the flow). The rate of energy dissipation of the stream, Ω_{stream}, is given by

$$\Omega_{\text{stream}} = \int_0^h \rho_a g \sin\beta \vec{u} \bullet \hat{i} dz \tag{17}$$

$$\rho_a = (\rho_s - \rho)N + \rho \tag{18}$$

where ρ_a is the apparent density of the water (accounting for the inclusion of sediment in the water), N is the local volume concentration of solids, and ρ is the density of pure water. Combining equations 17 and 18 yields:

$$\Omega_{\text{stream}} = (\rho_s - \rho) g \sin\beta \int_0^h N\vec{u} \bullet \hat{i} dz + \Omega \tag{19}$$

Ω is the sediment-free stream power, given by equation 15. According to Bagnold (1966), the immersed weight suspended sediment transport rate per unit area bed, $\vec{i}_s$ is defined by

$$\vec{i}_s = (\rho_s - \rho) g \cos\beta \int_0^h N\vec{u} dz \tag{20}$$

According to Bagnold (1966), the rate of energy dissipation per unit area of bed associated with this transport of sediment, Ω_{sed}, is equal to the sediment load times its fall velocity:

$$\Omega_{\text{sed}} = (\rho_s - \rho) g \cos\beta W \int_0^h N dz \tag{21}$$

Where W is the sediment fall velocity. Combining equations 20 and 21 yields:

$$\Omega_{\text{sed}} = \frac{|\vec{i}_s| W}{\bar{u}} \tag{22}$$

$$\bar{u} = \frac{\left| \int_0^h N\vec{u} dz \right|}{\int_0^h N dz} \tag{23}$$

A critical aspect of Bagnold's model is his hypothesis that the rate of energy dissipation associated with the suspended sediment transport is related to the total rate of energy production of the stream through a constant of suspended load efficiency, ε_S (Bailard, 1981). This can be expressed with the following equation:

$$\Omega_{\text{sed}} = \varepsilon_s \Omega_{\text{stream}} \tag{24}$$

By combining equations 19, 20, 22, and 23, and assuming $\bar{u} = U$ (the depth-averaged velocity), Bailard obtains the equation for the magnitude of the suspended sediment transport rate:

$$\left|\vec{i}_s\right| = \varepsilon_s \frac{U}{W}(\tan\beta \vec{i}_S \cdot \hat{i} + \Omega) \tag{25}$$

It is important to note that this result is not identical the one derived by Bagnold. Rearranging equation 25 yields a result that can be compared to Bagnold's:

$$\left|\vec{i}_s\right| = \frac{\varepsilon_s \Omega}{[(W/U) - \varepsilon_s \tan\beta]} \tag{26}$$

While Bagnold's paper yields the following equation:

$$\left|\vec{i}_s\right| = \frac{\varepsilon_s \Omega (1 - \varepsilon_B)}{[(W/U) - \tan\beta]} \tag{27}$$

Bagnold derived this result while assuming that the stream power contribution from the suspended sediment load contributes directly to the suspended sediment transport rate instead of through an efficiency factor (which is what Bailard assumes). There is hardly a difference between equations 26 and 27 for small bedslopes, which is fine for river flow, but this is not the case for equilibrium beach profiles. If U exceeds $W/\tan\beta$, equation 27 predicts negative or infinite transport, which is obviously incorrect. Equations 15 and 26 correct for this by including ε_S in the denominator. Since $1/\varepsilon_S$ is roughly equal to 41, it is quite difficult for equation 26 to yield negative or infinite transport. Since the ultimate purpose of this paper is to compare flows including both waves and current in the coastal environment, the Bailard result will be used.

There is one other difference between Bagnold's and Bailard's derivations. Bagnold multiplies the suspended load transport by $1-\varepsilon_B$, because the energy that has been dissipated in bedload

transport cannot go into suspended load. Bailard simply incorporates this into his ε_S, so there is a slight difference between Bagnold's ε_S and Bailard's ε_S. Bagnold states that equation 27 is equal to 0 for laminar flow.

2.3 Madsen

The Madsen model (1997) takes into account the formation of dunes and other effects that the flow may have on the bed surface, but since the other models do not take this into account, I am going to neglect this aspect (only for pure current, however) of the Madsen model in order to make a more logical comparison of the models. This will enable me to eliminate this added feature of this model as a potential source of differences with the other models.

The following variables are needed to begin the calculation of sediment transport in a steady unidirectional flow (such as a river):

U_c = the current velocity at a specified height (z_r) above the bottom

z_r = the height were the current velocity is specified

h = water depth

d = median sediment diameter (d_{50})

ρ_s = sediment density (assumed = 2, 650 kg/m^3 for quartz)

$\rho_w = \rho$ = water density (assumed = 1, 025 kg/m^3 for seawater)

β = slope of bottom measured from horizontal (positive if flow is downhill)

υ = kinematic viscosity of fluid (molecular = 10^{-6} m^2/sec for seawater)

$\kappa = 0.4$

If U_c at z_r is not given, it can be calculated if the depth-averaged current velocity is known. I used metric units for all of my calculations. All lengths are in meters, times in seconds, velocities in meters per second, stresses in pascals, etc.

Many of the variables in the equations contain subscripts. The meaning of these subscripts are listed below:

$()_b$ = conditions at the bottom

$()_c$ = quantity associated with current

$()_{cr}$ = quantity associated with critical conditions for initiation of sediment motion

Since we are dealing with flows over a plane bed, the Nikuradse equivalent bottom roughness, k_n, is equal to the sediment diameter, d. The first thing we need to know is whether the flow is rough turbulent or smooth turbulent:

If $k_n U_{*c}/\nu > 3.3$, the flow is rough turbulent and

$$z_o = \frac{k_n}{30} \tag{28}$$

If $k_n U_{*c}/\nu < 3.3$, the flow is smooth turbulent and

$$z_o = \nu/9U_{*c} \tag{29}$$

This leads to the calculation of the shear velocity (U_{*c}) and current friction factor (f_c):

$$U_{*c} = U_c\sqrt{\frac{f_c}{2}} \tag{30}$$

$$f_c = \left(\frac{1}{4\log\left(\frac{z_r}{z_o}\right)} \right)^2 \tag{31}$$

Unfortunately, U_{*c} has different solutions according to whether the flow is rough turbulent or not because this affects the computation of z_o. Another problem is the fact that it is not known whether the flow is rough turbulent or smooth turbulent unless U_{*c} is known, which is one of the variables that we are solving for. To solve these equations, it is assumed that the flow is rough turbulent, and then the condition is checked after the calculation. If the flow is indeed rough turbulent, the solution remains the same. If, however, the flow proves to be smooth turbulent, equations 29 through 31 need to be solved iteratively.

Knowing U_{*c} enables the total shear stress to be calculated:

$$\tau = \rho U_{*c}^2 \tag{32}$$

2.3.a Bedload Transport

The Shields Parameter can be calculated from:

$$\psi = \frac{\tau}{(s-1)\rho g d} \tag{33}$$

where $s = \rho_s/\rho_w$. For transport to occur, the Shields parameter calculated in equation 33 must be greater than a critical Shields parameter. The following equations calculate the critical Shields parameter:

$$S_* = \frac{d}{4\nu}\sqrt{((s-1)gd)} \tag{34}$$

If $S_* < 0.8$

$$\psi_{cr} = 0.1 S_*^{-2/7} \tag{35}$$

If $S_* > 300$

$$\psi_{cr} = 0.06 \tag{36}$$

If $0.8 < S_* < 300$

$$\psi_{cr} = \frac{0.24}{4^{2/3} S_*^{2/3}} + 0.055\left(1 - e^{-4^{2/3}\frac{S_*^{2/3}}{50}}\right) \tag{37}$$

This value for the critical Shields parameter does not take slope into effect. The complete parameter, $\psi_{cr.\beta}$, is presented by

$$\psi_{cr.\beta} = \cos\beta\left(1 - \frac{\tan\beta}{\tan\phi_s}\right)\psi_{cr} \tag{38}$$

Where $\phi_s \approx 50°$. A generalized form of the Meyer-Peter and Muller bedload transport formula allows the bedload to be calculated:

$$F(\beta) = \cos\beta\left(1 - \frac{\tan\beta}{\tan\phi_m}\right) \tag{39}$$

Where $\phi_m \approx 30°$

$$\Phi_B = \frac{q_{SB}}{d\sqrt{(s-1)gd}} = \frac{8}{F(\beta)}(\psi - F(\beta)\psi_{cr})^{3/2} \quad (40)$$

Where q_{SB} is the bedload. Note that for transport to begin, the Shields parameter must be greater than the critical Shields parameter (accounting for slope). If ψ is less than $\psi_{cr,\beta}$, there will be no transport. The reason why the bedload formula has a different internal angle of friction (ϕ_m versus ϕ_s) is because the angle of kinetic (moving) friction must be overcome during transport while for the initiation of motion, the angle of static friction must be surpassed.

2.3.b Suspended Load Transport

The calculation of the suspended load transport begins with the calculation of the sediment reference concentration:

$$C_a = (0.4C_b)\frac{q_{SB}}{U_s a} \quad (41)$$

Where C_b is the concentration in the bottom (Ξ is the sediment porosity, assumed = 0.35),

$$C_b = 1 - \Xi \approx 0.65 \quad (42)$$

$$a = 7d \quad (43)$$

$$U_s = 11.6U_{*c} \quad (44)$$

The fall velocity, W, can be calculated from knowledge of S_* (which is given by equation 34):

$$W = \frac{\sqrt{(s-1)gd}}{\frac{5.1}{S_*} + 0.9} \tag{45}$$

The next step is to calculate the suspended sediment concentration:

$$C(z) = C_a\left(\frac{z}{a}\right)^{-Z} \tag{46}$$

$$Z = \frac{W}{\kappa U_{*c}} \tag{47}$$

This leads to the equation for suspended load transport:

$$q_{sS} = 0.4C_b[I_1(a^*, Z)\ln h/z_o - I_2(a^*, Z)] \tag{48}$$

Where

$$a^* = \frac{a}{h} \tag{49}$$

$$I_1 = 0.216\frac{(a^*)^{z-1} - 1}{1 - Z} \tag{50}$$

$$I_2 = 0.216\frac{\ln a^*}{1 - Z} + \frac{I_1}{1 - Z} \tag{51}$$

3.0 Comparison of the Models for Pure Current

3.1 Description of the Differences

The Ackers and White model (1973) is the simplest of the three. It does not specifically calculate a bedload and suspended load, like the Madsen (1997) and Bailard (1981) models. This model is limited by the fact that it does not take bed slope into effect, which may not be important for river beds, where the slope is usually small, but this cannot be assumed correct for the coastal environment, where equilibrium bed slopes are generally steeper than river beds. The Ackers and White model was derived using an energetics approach.

The Bailard model, like Ackers and White's, is derived using an energetics approach. Unlike the other two models, however, it does not take water depth into account when calculating transport. Another difference between this model and the others is the fact that it does not incorporate a critical shear stress for the initiation of motion. Both the Madsen model and the Ackers and White model give no transport until a critical shear stress is reached, which makes physical sense. The Bailard model will always give a transport, no matter how small the shear stress. The Bailard model also relies on experimental data for the calculation of the parameters ε_S, ε_B, and C_f, which are needed to calculate the transport.

The Madsen model is unique in its accounting for changes in the bed surface due to the flow (though this is neglected for the pure current comparison). Unlike a laboratory, where the bed may contain immovable roughness elements, real beds change because of the flow, and this changes the flow's boundary layer and total transport. The Madsen model was derived using a mechanics approach. Like the Bailard model, the Madsen model gives two components of the

transport: a bedload and a suspended load, and takes bedslope into effect. The Madsen model, like the Ackers and White model, takes water depth into account and incorporates a critical Shields parameter that must be overcome in order for any transport to occur.

3.2 Discussion

In order to compare the models numerically, I programmed the three models and ran them with the same set of conditions.The Madsen model was modified to neglect changes in the bed due to the flow. Since the Ackers and White model does not account for bed slope, it was taken as zero for all of the runs. The water depth was set at 5 meters, but runs were also performed at a water depth of 2.5 meters to check if the Bailard model could neglect water depth without a large error. Transport was compared for three different grain diameters: 0.1 mm, 0.2 mm and 0.5 mm. Tables 1 and 2, given on pages 23 and 24, contain the output of these runs for all three models. For each of these conditions, transport was plotted versus current velocity. These figures are presented after the tables. As expected, transport increased with increasing current velocity for every single grain diameter and model. This occurred because with everything else held constant, increasing the flow velocity increases the shear on the bed and therefore the transport.

The first analysis I performed was to determine the effect of water depth on the transport for the Ackers and White model and the Madsen model. Figures 1 through 3 (pages 25 through 27) reveal that for all three grain sizes, transport increases as the water depth decreases for the Ackers and White model, while Figures 4 through 6 (pages 28 through 30) show the results for the Madsen model: the change in transport depends on the sediment size.

When the water depth decreases, the Chezy coefficient also decreases. Since the Chezy

coefficient is used to calculate the shear velocity and is in the denominator of equation 12, this serves to increase the shear velocity in the Ackers and White model. An increased shear velocity leads to a greater sediment transport.

Table 1

Total Transport Versus Grain Size and Depth Averaged Current Velocity, depth = 5 m.

Case #	Vc (m/sec)	d (mm)	Madsen Total Load (m^3/m*sec)	Ackers & White Total Load (m^3/m*sec)	Bailard Total Load (m^3/m*sec)
1	0.37	0.1	0	0	1.22554E-05
2	0.38	0.1	1.70779E-08	4.50052E-15	1.36008E-05
3	0.5	0.1	3.40001E-06	8.44351E-09	3.98589E-05
4	0.6	0.1	2.02127E-05	2.03591E-07	8.16573E-05
5	0.75	0.1	0.000136492	3.53246E-06	0.000196932
6	0.8	0.1	0.000226982	7.1938E-06	0.00025415
7	0.9	0.1	0.000548536	2.41488E-05	0.000405002
8	1	0.1	0.001152578	6.62074E-05	0.00061473
9	1.2	0.1	0.003947541	0.000335313	0.001266752
10	1.4	0.1	0.010471126	0.001207404	0.00233629
11	0.38	0.2	0	0	4.32738E-06
12	0.39	0.2	1.26925E-09	0	4.76527E-06
13	0.5	0.2	5.88167E-07	3.18143E-08	1.20626E-05
14	0.6	0.2	1.95439E-06	5.61782E-07	2.40188E-05
15	0.75	0.2	6.03565E-06	5.17487E-06	5.62127E-05
16	0.8	0.2	8.14627E-06	8.77888E-06	7.1984E-05
17	0.9	0.2	1.40142E-05	2.12839E-05	0.000113207
18	1	0.2	2.30587E-05	4.40313E-05	0.000169989
19	1.2	0.2	5.95482E-05	0.00013974	0.000344537
20	1.4	0.2	0.000151946	0.000344773	0.000627773
21	0.44	0.5	0	0	3.83587E-06
22	0.45	0.5	6.37291E-09	0	4.149E-06
23	0.6	0.5	1.51138E-06	5.72398E-07	1.1456E-05
24	0.75	0.5	5.177E-06	6.41933E-06	2.55418E-05
25	0.9	0.5	1.14343E-05	2.20867E-05	4.96083E-05
26	1	0.5	1.73364E-05	4.01104E-05	7.30541E-05
27	1.2	0.5	3.41879E-05	0.000100227	0.000143532
28	1.4	0.5	5.92814E-05	0.000201364	0.000255387
29	1.6	0.5	9.47408E-05	0.000354473	0.000422213
30	1.8	0.5	0.000143175	0.000570743	0.000659528

Table 2

Total Transport Versus Grain Size and Flow Velocity, depth = 2.5 m.

Case #	Vc (m/sec)	d (mm)	Madsen Total Load (m^3/m*sec)	Ackers & White Total Load (m^3/m*sec)	Bailard Total Load (m^3/m*sec)
1	0.37	0.1	7.5933E-08	2.73297E-13	1.22554E-05
2	0.38	0.1	1.56398E-07	2.8401E-12	1.36008E-05
3	0.5	0.1	5.39471E-06	2.23099E-08	3.98589E-05
4	0.6	0.1	2.72187E-05	3.9517E-07	8.16573E-05
5	0.75	0.1	0.000156057	5.81739E-06	0.000196932
6	0.8	0.1	0.000248718	1.14996E-05	0.00025415
7	0.9	0.1	0.000559253	3.69809E-05	0.000405002
8	1	0.1	0.001108142	9.84441E-05	0.00061473
9	1.2	0.1	0.00353607	0.000480064	0.001266752
10	1.4	0.1	0.008762145	0.001688886	0.00233629
11	0.38	0.2	2.35026E-08	0	4.32738E-06
12	0.39	0.2	5.36783E-08	0	4.76527E-06
13	0.5	0.2	8.93687E-07	8.6669E-08	1.20626E-05
14	0.6	0.2	2.66239E-06	9.77082E-07	2.40188E-05
15	0.75	0.2	7.86407E-06	7.53848E-06	5.62127E-05
16	0.8	0.2	1.05808E-05	1.2426E-05	7.1984E-05
17	0.9	0.2	1.82536E-05	2.89474E-05	0.000113207
18	1	0.2	3.03538E-05	5.83258E-05	0.000169989
19	1.2	0.2	8.03477E-05	0.000179146	0.000344537
20	1.4	0.2	0.00020532	0.000433457	0.000627773
21	0.44	0.5	6.85692E-08	0	3.83587E-06
22	0.45	0.5	1.2427E-07	0	4.149E-06
23	0.6	0.5	2.22614E-06	1.25176E-06	1.1456E-05
24	0.75	0.5	6.85658E-06	9.30826E-06	2.55418E-05
25	0.9	0.5	1.46224E-05	2.89802E-05	4.96083E-05
26	1	0.5	2.19084E-05	5.09146E-05	7.30541E-05
27	1.2	0.5	4.26714E-05	0.000122512	0.000143532
28	1.4	0.5	7.36238E-05	0.00024104	0.000255387
29	1.6	0.5	0.000117539	0.000418712	0.000422213
30	1.8	0.5	0.000177922	0.000668004	0.000659528

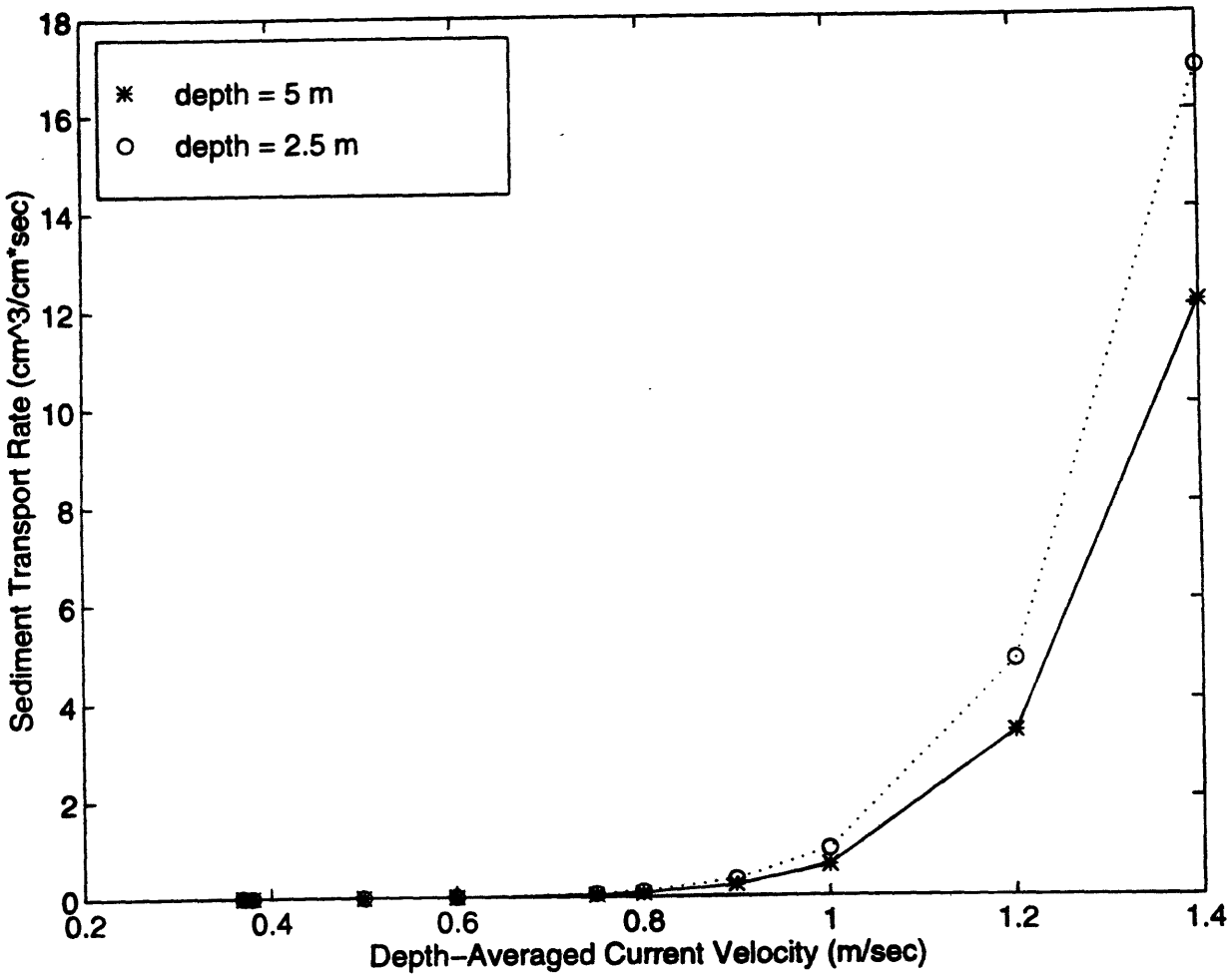

Figure 1. The Ackers and White model, total sediment transport rate versus depth-averaged current velocity for 0.1 mm diameter grains.

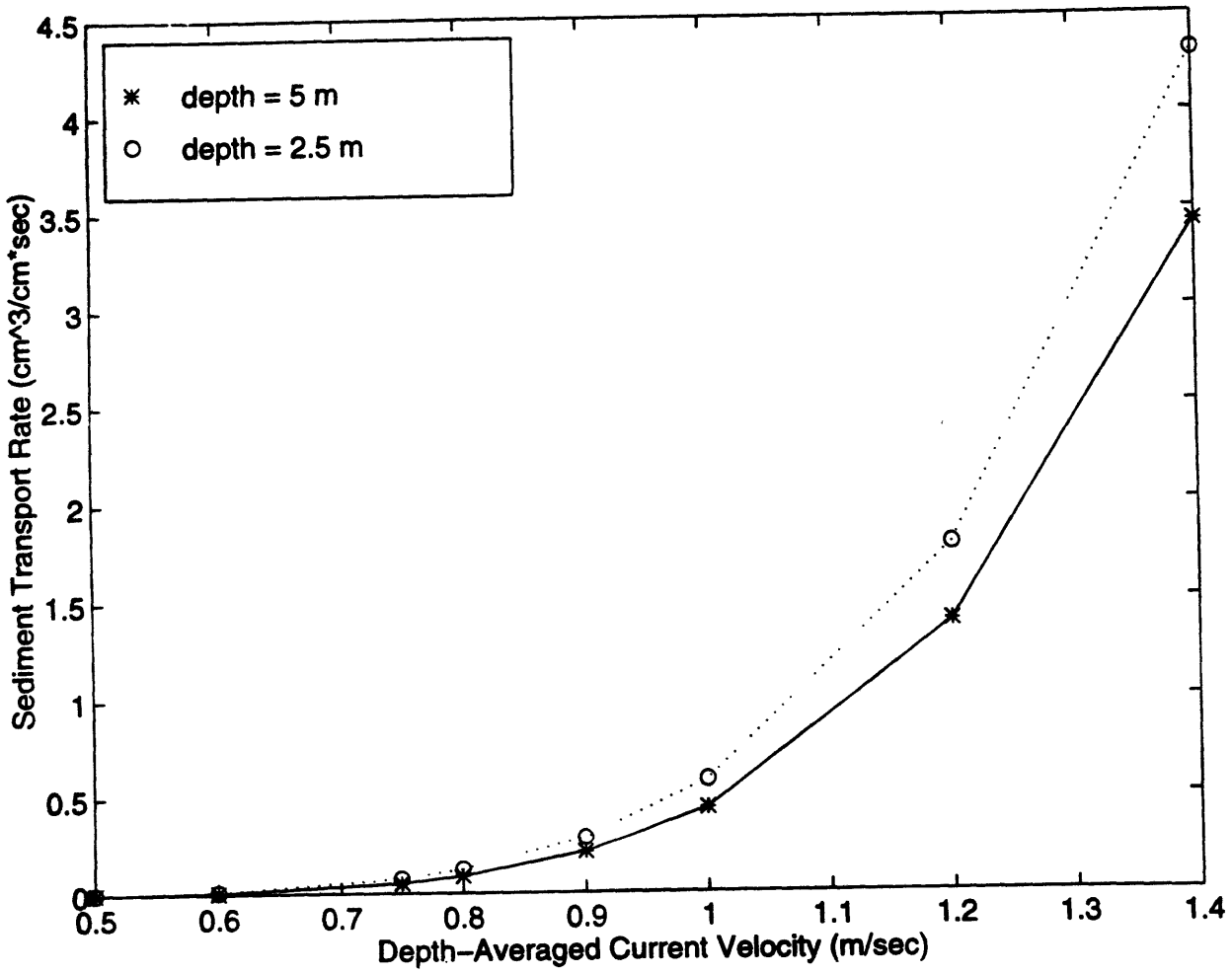

Figure 2. The Ackers and White model, total sediment transport rate versus depth-averaged current velocity for 0.2 mm diameter grains.

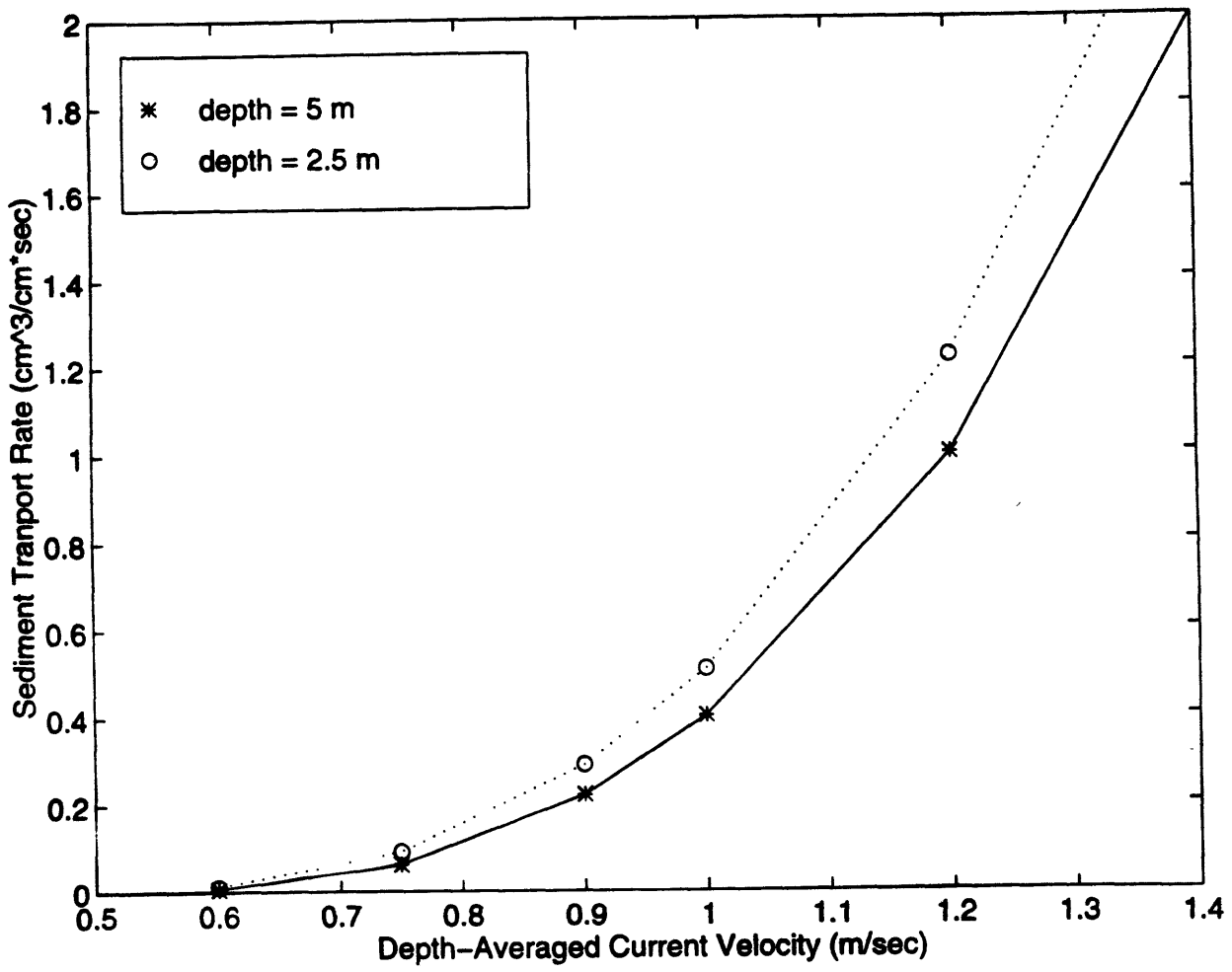

Figure 3. The Ackers and White model, total sediment transport rate versus depth-averaged current velocity for 0.5 mm diameter grains.

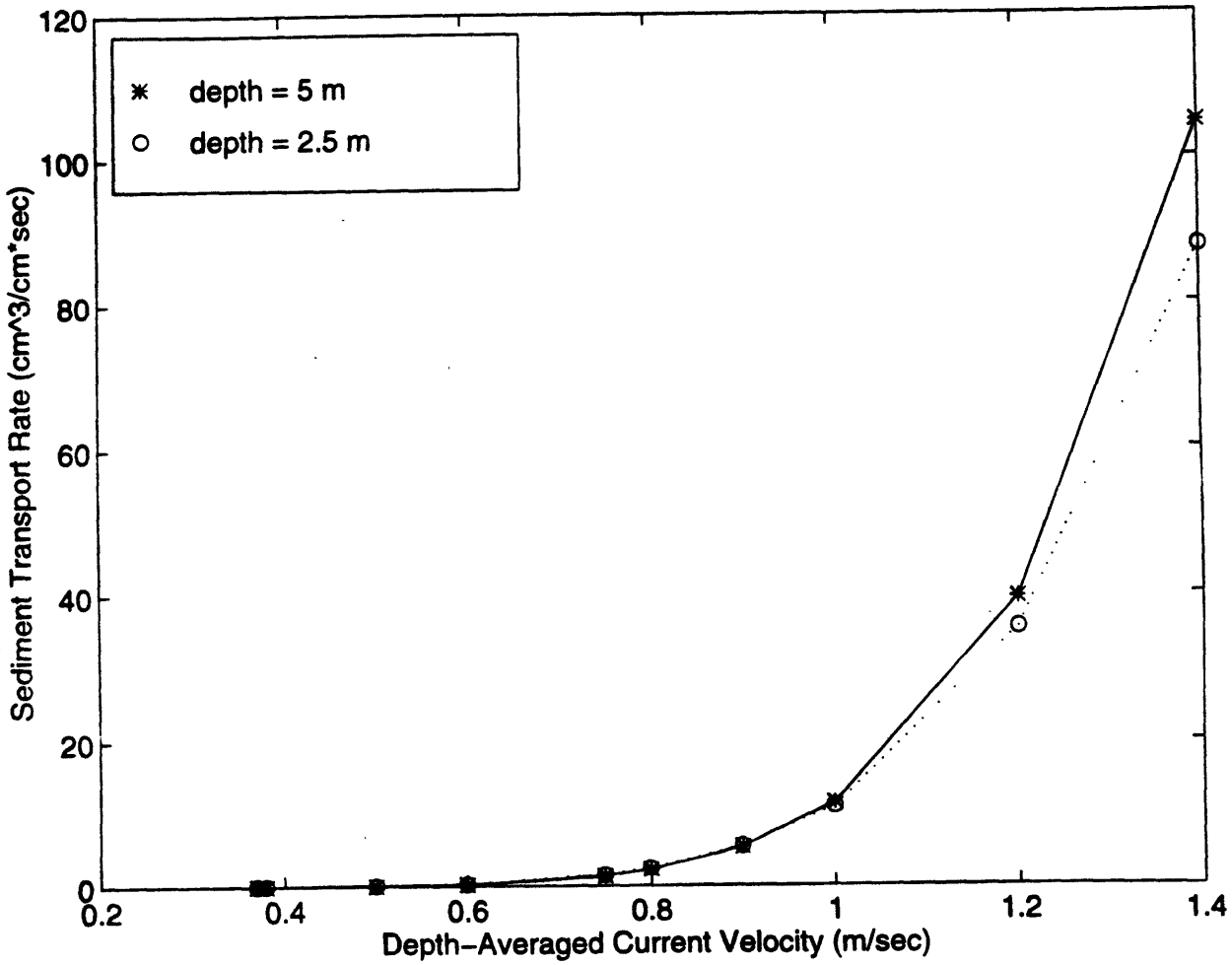

Figure 4. The Madsen model, total sediment transport rate versus depth-averaged current velocity for 0.1 mm diameter grains.

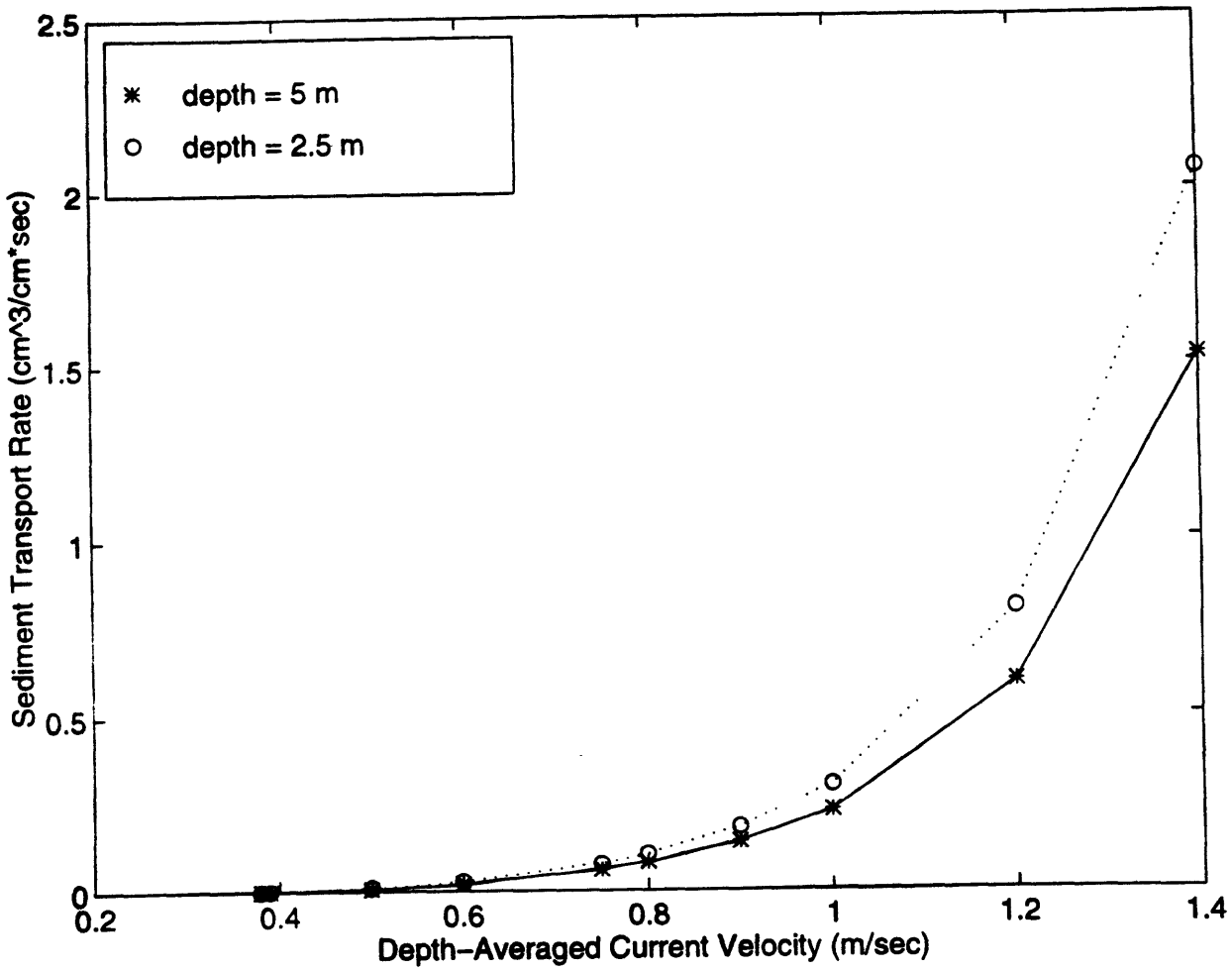

Figure 5. The Madsen model, total sediment transport rate versus depth averaged-current velocity for 0.2 mm diameter grains.

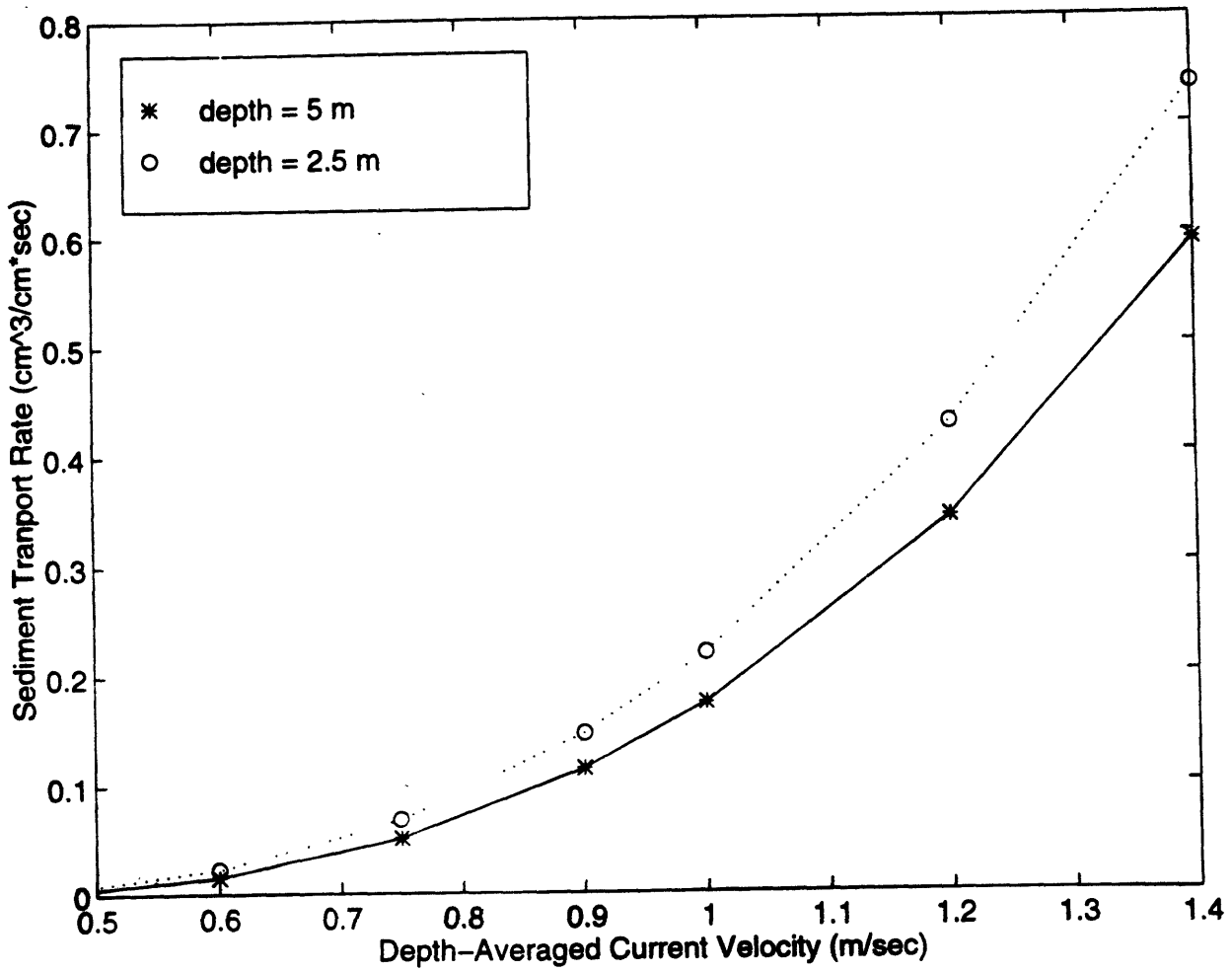

Figure 6. The Madsen model, total sediment transport rate versus depth averaged-current velocity for 0.5 mm diameter grains.

The effect of water depth is more complex in the Madsen model. The decreased water depth decreases the height above the bed where the given velocity is occurring, increasing the shear stress and the bedload. This is the same result as the Ackers and White model, but the suspended load reacts differently to the decreased depth. The decreased water depth lowers the total amount of sediment that can be held in suspension. With less sediment in suspension, there is less transport. This is especially true for small sediment, because suspended load comprises more of the total transport for fine grains than it does for large grains. Suspended load also depends on the shear stress, and an increased shear stress results in an increased suspended load. In the Madsen model, suspended load also increases with decreased depth, except for the 0.1 mm grains (figure 4). Figures 7 through 9 (pages 32 through 34) break down the Madsen transport into suspended load and bedload. Figure 7 reveals that at high enough current velocities, suspended load actually decreases with the smaller depth, despite the fact that the bedload increases, because the 0.1 mm sediment is small enough to have a large suspended load. Such a large suspended load will be more affected by a decrease in the water depth.

At very low flow velocities (less than 0.3 m/sec) only the Bailard model yields a transport because the flow is not strong enough to initiate movement according to the other two models. Table 1 (page 23) contains the output for the three models (at 5 meter depth). Table 1 reveals that the Madsen model predicts initiation of motion at lower flow rates than the Ackers and White model for the 0.2 mm and 0.5 mm grain sizes.

Figures 10 through 12 (pages 35 through 37) plot the sediment transport for each sediment size, for a flow depth of 5 meters. The plots show that the Madsen model is the most sensitive to grain size. When the sediment is small, the Madsen model predicts the largest transport of the three models, while the opposite is true for the larger grains: the Madsen model predicts the low-

est transport.

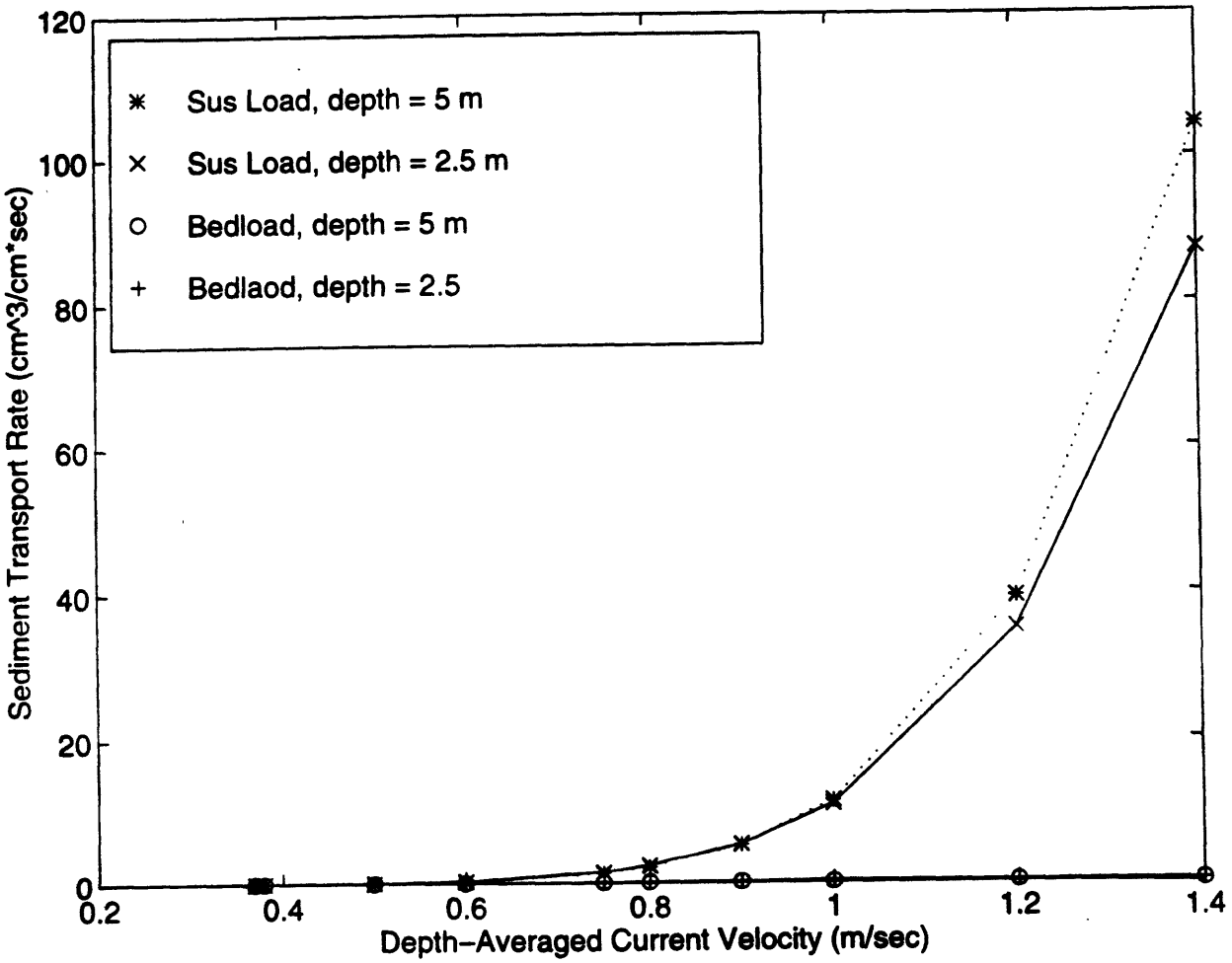

Figure 7. The Madsen model, break down of the total sediment transport rate versus depth-averaged current velocity for 0.1 mm diameter sediment.

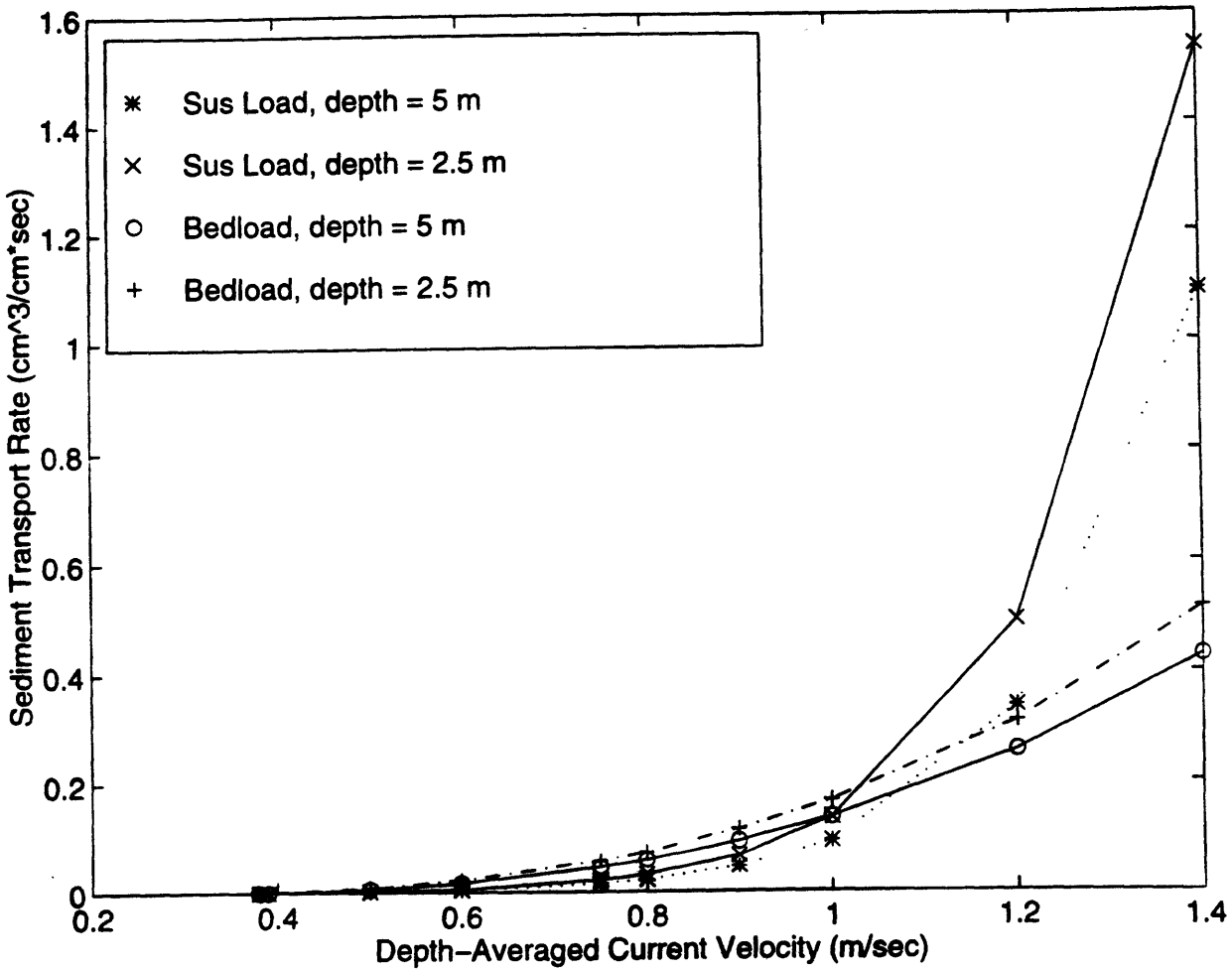

Figure 8. The Madsen model, break down of the total sediment transport rate versus depth-averaged current velocity for 0.2 mm diameter sediment.

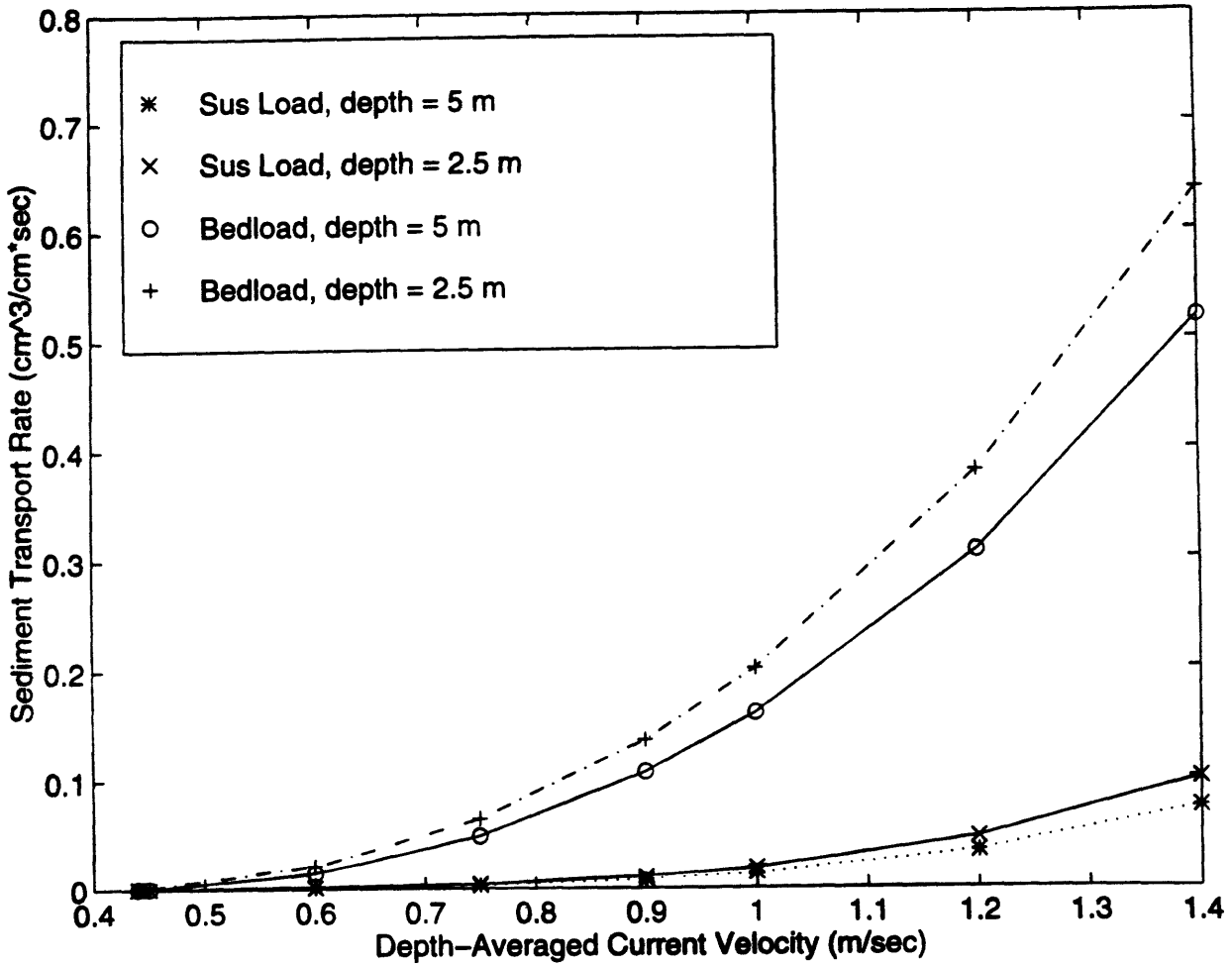

Figure 9. The Madsen model, break down of the total sediment transport rate versus depth-averaged current velocity for 0.5 mm diameter sediment.

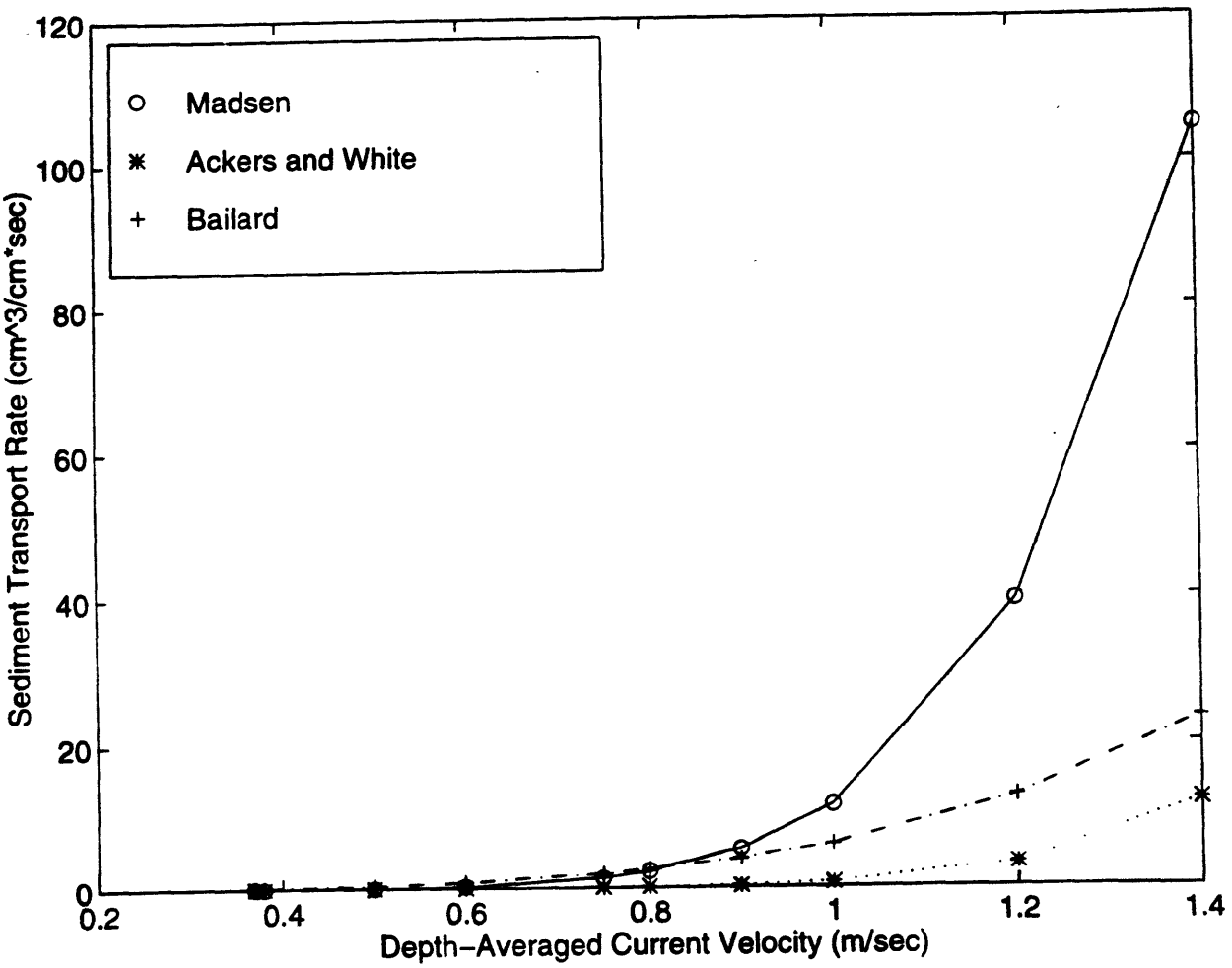

Figure 10. The total sediment transport rate versus depth-averaged current velocity for 0.1 mm diameter sediment and a flow depth of 5 m.

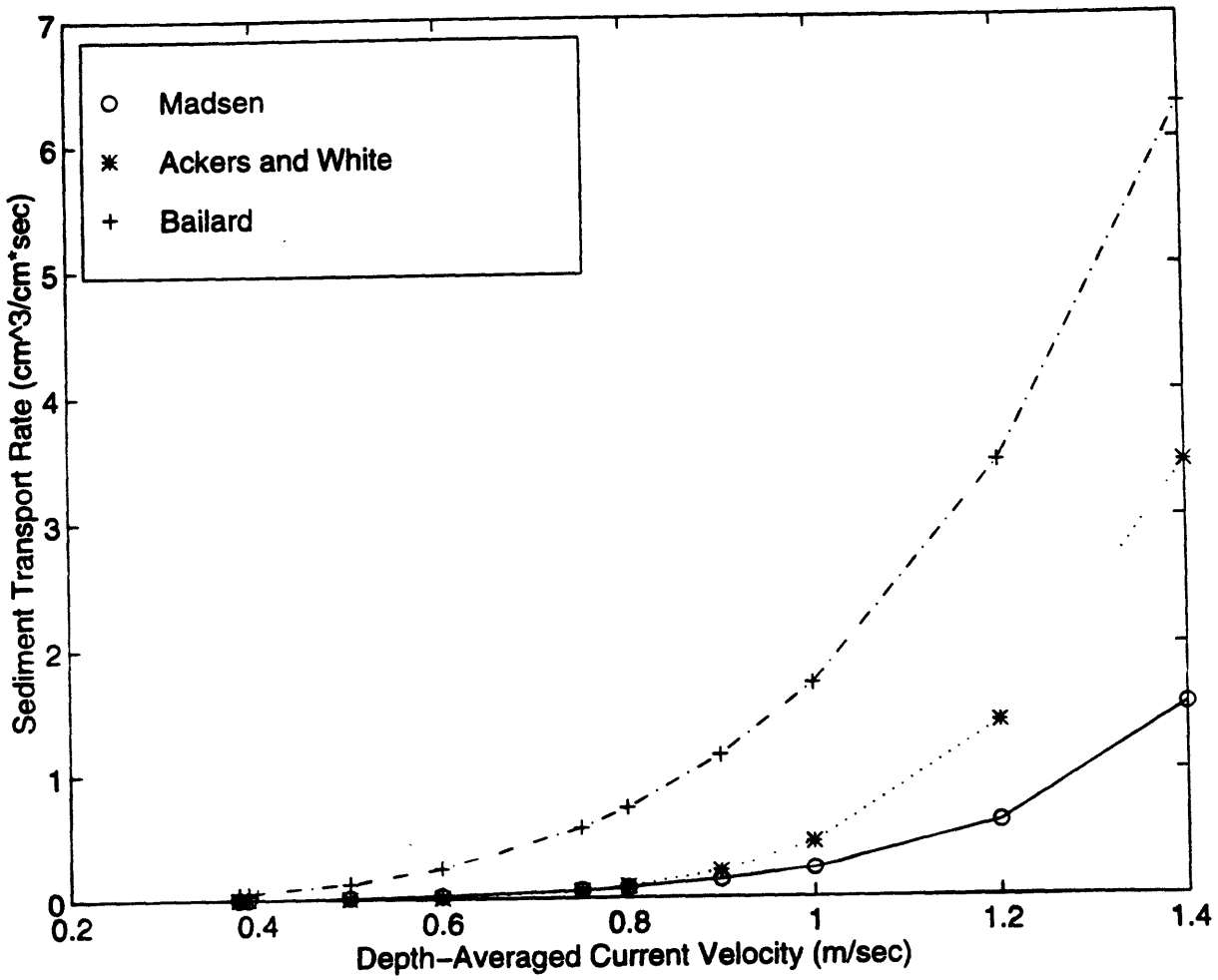

Figure 11. The total sediment transport rate versus depth-averaged current velocity for 0.2 mm diameter sediment and a flow depth of 5 m.

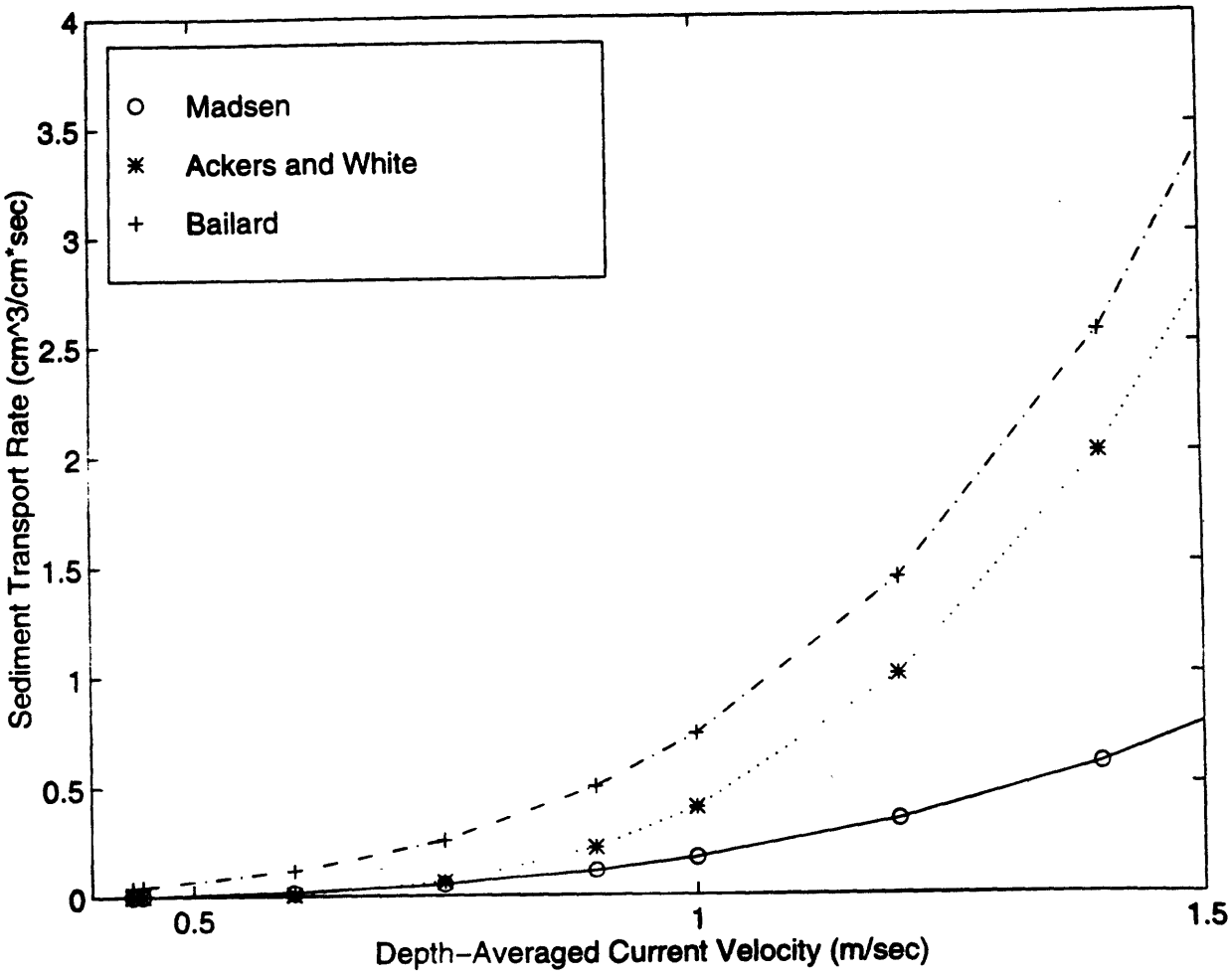

Figure 12. The total sediment transport rate versus depth-averaged current velocity for 0.5 mm diameter sediment and a flow depth of 5 m.

Figures 13 through 15 (pages 39 through 41) break down the total transport of the Bailard and Madsen models into suspended load and bed load. These figures show that the main difference between these two models is in the suspended load. Suspended load is very dependent on grain size in the Madsen model, and this leads to the high fluctuations in the transport (mainly because of the change in suspended load) based on grain size. The Bailard suspended load is more constant; it is less dependent on grain size than the Madsen model. For all three grain sizes, suspended load is greater than the bedload based on the Bailard model (except at very low flow rates). This is not the case for the Madsen model, where Bedload dominates for the larger grains because large grains are less likely to be held in suspension by the water column.

Each model predicts a large increase in transport for increasing flow velocities. The Madsen model predicts the largest increase with flow velocity for the smallest sediment examined, mainly because of the increased suspended load, while the Ackers and White model predicts the largest increase for the larger sediments. While the Madsen model is the most sensitive to grain size, the Ackers and White model is the most sensitive to current velocity.

The Bailard model appears to be the least sensitive to changes in current velocity and grain size. It usually predicts the largest transport rates, regardless of the conditions. The other models, however, vary greatly according to the given conditions, with the Madsen model predicting very high transport only for fine sediment, and the Ackers and White model predicting a large transport for high flow conditions and large sediment. Examination of Tables 1 and 2 reveal that the Bailard model is within the range of the other two models for the two depths, indicating that for average flow depths, the Bailard model's omission of water depth may not be that significant. It should be stressed, however, that the Bailard model would overestimate the suspended load for fine sediments if the flow depth was very low because it would assume that the suspended sediment would

extend up the water column until the suspended sediment concentration reached zero, which would happen at a significant height above the bottom. This, however, cannot happen because of the low flow depth.

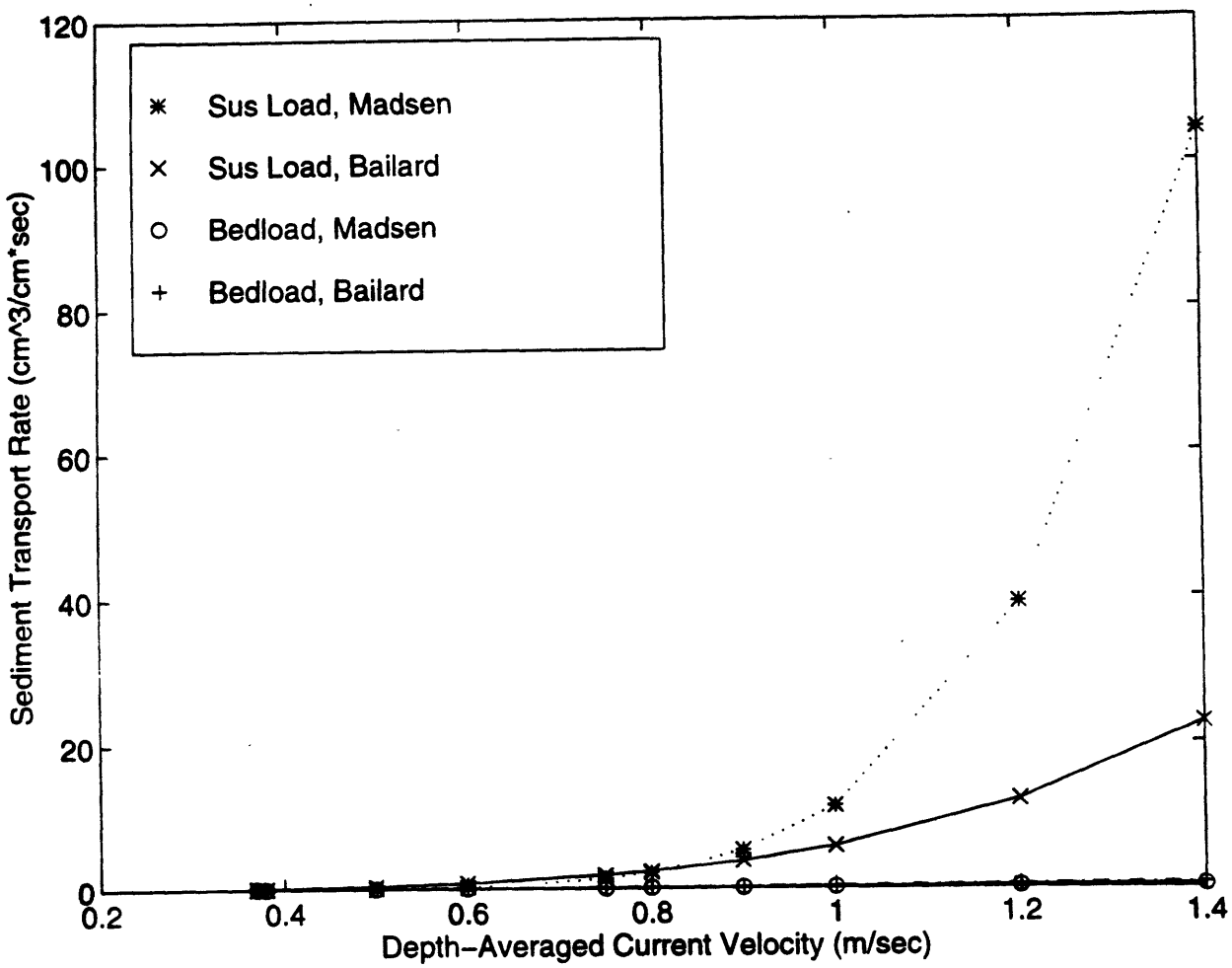

Figure 13. Break down of the total sediment transport rate versus depth-averaged current velocity for the Madsen and Bailard models. Taken for 0.1 mm diameter sediment and 5 m flow depth.

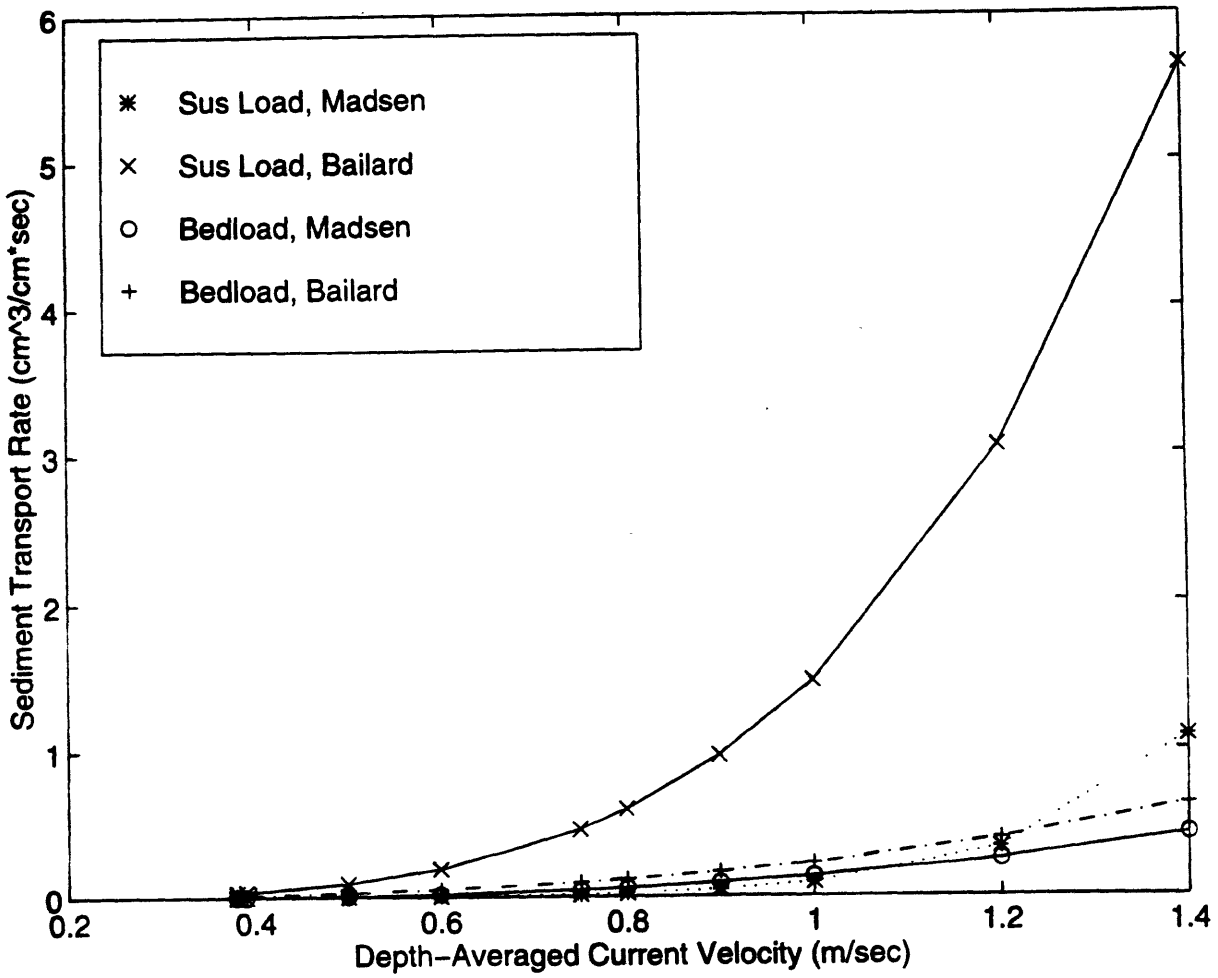

Figure 14. Break down of the total sediment transport rate versus depth-averaged current velocity for the Madsen and Bailard models. Taken for 0.2 mm diameter sediment and 5 m flow depth.

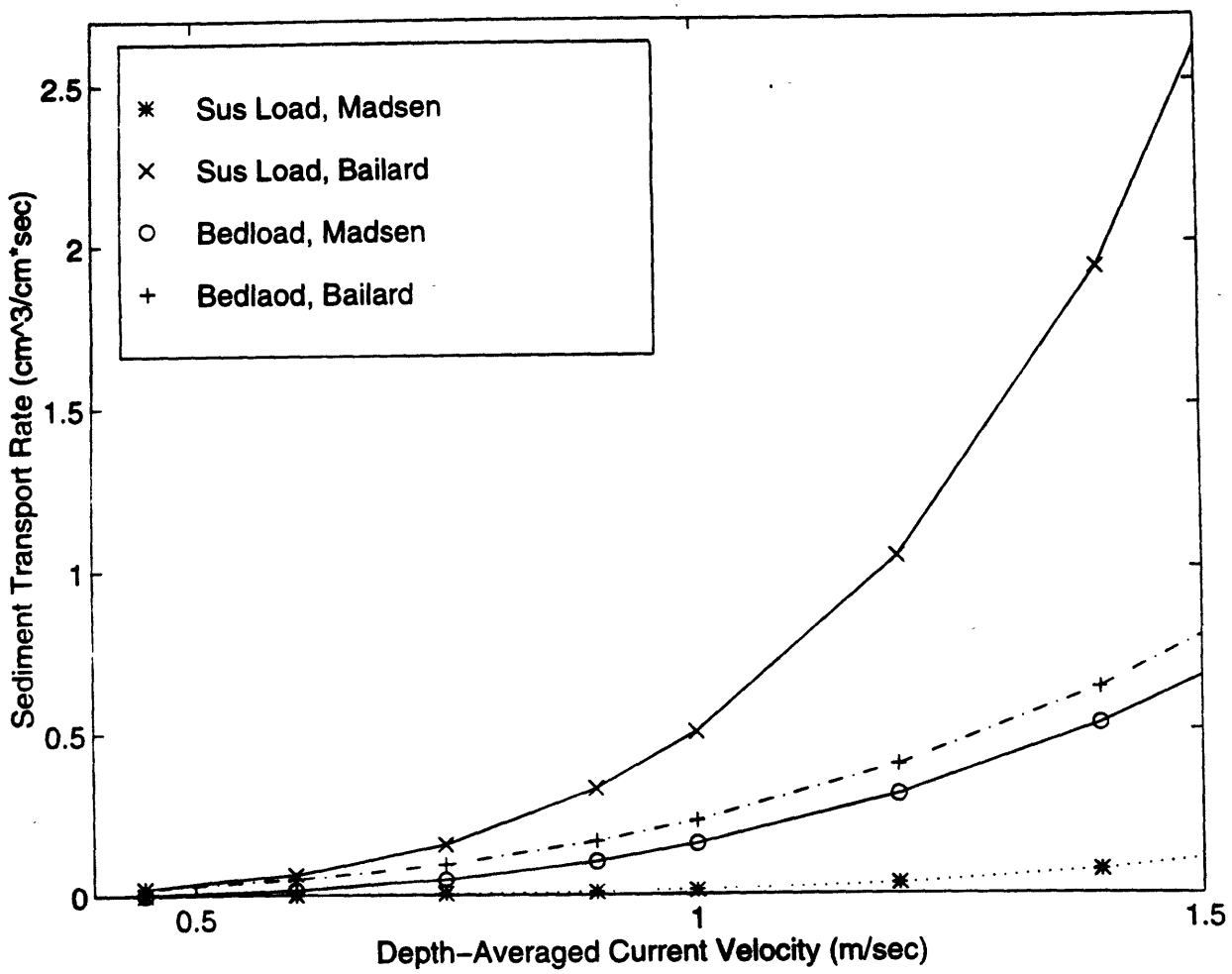

Figure 15. Break down of the total sediment transport rate versus depth-averaged current velocity for the Madsen and Bailard models. Taken for 0.5 mm diameter sediment and 5 m flow depth.

Closer analysis of Tables 1 and 2 on pages 23 and 24 reveals a major difference between the Ackers and White model and the other two. The Madsen model and the Bailard model predict larger transport the smaller the grain size. The Ackers and White model does not predict the same result. When the sediment is small, it requires less of a shear in order to initiate movement and transport. This, however, is not the only mechanism at work when the grain diameter is changed: a smaller sediment has a smaller roughness and therefore experiences a smaller shear stress from the flow. The criteria for motion, however, is determined by the Shields parameter (given by equation 33). This relationship involves the shear stress in the numerator and the sediment diameter in the denominator. Since the shear stress does not increase as rapidly as the grain diameter, the Shields parameter does not increase with increased diameter, like the shear stress does. The critical Shields parameter, however, also decreases with increased sediment diameter, and since the bedload is related to the difference between the critical Shields parameter and the Shields parameter, this leaves no clear cut answer as to whether the bedload increases or decreases with increased sediment diameter. Inspection of Tables 3 and 4 (pages 44 and 45), which break down the Madsen and Bailard models according to bedload and suspended load, reveals this pattern. There is no strict relationship between bedload and grain diameter; at low current velocities, there is more bedload for the finer sediment, and the opposite is true for the high current velocities. This makes sense because the shear stress is related to the velocity squared, and therefore the effect of increasing the roughness is more important at higher flow rates. The Ackers and White data follows this pattern: more transport for fine sediment at low flow conditions, and more transport for the large sediment at high flow conditions.

The suspended load, on the other hand, always decreases with increased sediment size, despite the fact that suspended load is related to bedload. The water column holds small sediment

in suspension much better than large sediment, and at high flow rates there is a lot of fine sediment in suspension, which contributes to a large suspended load. Therefore, in the Madsen and Bailard models, suspended load outweighs the bedload at large flow rates, enabling the total load to decrease with increased sediment diameter. The Bailard and Madsen models' pattern of decreased transport for coarser sediment is more applicable to real world applications because sediments are rarely well sorted, and the flow feels only one roughness. Therefore, both the fine and coarse sediments are going to feel the same shear stress, and the fine sediment is going to move before the coarse sediment.

Overall, the models agree best for low to medium flow conditions, with great divergence occurring only after current velocities exceeding 1 m/sec are reached. For everything but fine sediment, it is usually the Madsen model that predicts the lowest transport, but this assessment is not entirely accurate because the Madsen model is intended to incorporate the formation of bedforms, which increases the roughness and also the transport. It is also impossible to judge which of the three models does the best job at predicting the actual transport in rivers by looking at the magnitude of each result.

The exact answer is not known, which is why numerous models exist. The best way to examine the models is to analyze the patterns of the change in transport each model predicts for changes in the flow or sediment characteristics. The Bailard and Madsen models appear to do a better job of incorporating all of the factors and changes that occur in transport, with the Madsen model being better adept at predicting suspended load transport because of its incorporation of the flow depth, and both the Madsen and the Ackers and White models doing a better job than the Bailard model at very low flow rates, where the flow is near the critical stage to initiate sediment motion.

Table 3

Bedload and Suspended Load Transport Versus Grain Size and Depth Averaged Current Velocity.

The Madsen and Bailard Models. Flow depth = 5 m.

Case #	Vc (m/sec)	d (mm)	Madsen Bedload (m^3/m*sec)	Bailard Bedload (m^3/m*sec)	Madsen Sus Load (m^3/m*sec)	Bailard Sus Load (m^3/m*sec)
1	0.37	0.1	0	1.16562E-06	0	1.10898E-05
2	0.38	0.1	7.44358E-09	1.26271E-06	9.63436E-09	1.23381E-05
3	0.5	0.1	6.06181E-07	2.87649E-06	2.79383E-06	3.69824E-05
4	0.6	0.1	1.65761E-06	4.97057E-06	1.85551E-05	7.66867E-05
5	0.75	0.1	4.25196E-06	9.70814E-06	0.00013224	0.000187223
6	0.8	0.1	5.41636E-06	1.17821E-05	0.000221566	0.000242368
7	0.9	0.1	8.23963E-06	1.67757E-05	0.000540297	0.000388227
8	1	0.1	1.17726E-05	2.30119E-05	0.001140805	0.000591719
9	1.2	0.1	2.1733E-05	3.97645E-05	0.003925808	0.001226988
10	1.4	0.1	3.62658E-05	6.31446E-05	0.01043486	0.002273146
11	0.38	0.2	0	1.26271E-06	0	3.06468E-06
12	0.39	0.2	1.15012E-09	1.36504E-06	1.19128E-10	3.40023E-06
13	0.5	0.2	5.10419E-07	2.87649E-06	7.77478E-08	9.18608E-06
14	0.6	0.2	1.61911E-06	4.97057E-06	3.35281E-07	1.90483E-05
15	0.75	0.2	4.56816E-06	9.70814E-06	1.46749E-06	4.65045E-05
16	0.8	0.2	5.93788E-06	1.17821E-05	2.20839E-06	6.02019E-05
17	0.9	0.2	9.33296E-06	1.67757E-05	4.68128E-06	9.64318E-05
18	1	0.2	1.36884E-05	2.30119E-05	9.37028E-06	0.000146977
19	1.2	0.2	2.56983E-05	3.97645E-05	3.38499E-05	0.000304772
20	1.4	0.2	4.28088E-05	6.31446E-05	0.000109137	0.000564628
21	0.44	0.5	0	1.96024E-06	0	1.87563E-06
22	0.45	0.5	6.16849E-09	2.09696E-06	2.04417E-10	2.05204E-06
23	0.6	0.5	1.44466E-06	4.97057E-06	6.67234E-08	6.48547E-06
24	0.75	0.5	4.88183E-06	9.70814E-06	2.95172E-07	1.58337E-05
25	0.9	0.5	1.06252E-05	1.67757E-05	8.09084E-07	3.28327E-05
26	1	0.5	1.59417E-05	2.30119E-05	1.39469E-06	5.00422E-05
27	1.2	0.5	3.07274E-05	3.97645E-05	3.46056E-06	0.000103767
28	1.4	0.5	5.19265E-05	6.31446E-05	7.35489E-06	0.000192242
29	1.6	0.5	8.05978E-05	9.42567E-05	1.41431E-05	0.000327956
30	1.8	0.5	0.000117803	0.000134205	2.53721E-05	0.000525323

Table 4

Bedload and Suspended Load Transport Versus Grain Size and Depth Averaged Current Velocity.

The Madsen and Bailard Models. Flow depth = 2.5 m.

Case #	Vc (m/sec)	d (mm)	Madsen Bedload (m^3/m*sec)	Bailard Bedload (m^3/m*sec)	Madsen Sus Load (m^3/m*sec)	Bailard Sus Load (m^3/m*sec)
1	0.37	0.1	3.13878E-08	1.16562E-06	4.45452E-08	1.10898E-05
2	0.38	0.1	6.05349E-08	1.26271E-06	9.58631E-08	1.23381E-05
3	0.5	0.1	8.61202E-07	2.87649E-06	4.53351E-06	3.69824E-05
4	0.6	0.1	2.14253E-06	4.97057E-06	2.50762E-05	7.66867E-05
5	0.75	0.1	5.23137E-06	9.70814E-06	0.000150825	0.000187223
6	0.8	0.1	6.60583E-06	1.17821E-05	0.000242113	0.000242368
7	0.9	0.1	9.92415E-06	1.67757E-05	0.000549329	0.000388227
8	1	0.1	1.40596E-05	2.30119E-05	0.001094082	0.000591719
9	1.2	0.1	2.60425E-05	3.97645E-05	0.003510028	0.001226988
10	1.4	0.1	4.32165E-05	6.31446E-05	0.008718929	0.002273146
11	0.38	0.2	2.11993E-08	1.26271E-06	2.30338E-09	3.06468E-06
12	0.39	0.2	4.82297E-08	1.36504E-06	5.44864E-09	3.40023E-06
13	0.5	0.2	7.65709E-07	2.87649E-06	1.27978E-07	9.18608E-06
14	0.6	0.2	2.16497E-06	4.97057E-06	4.97419E-07	1.90483E-05
15	0.75	0.2	5.76079E-06	9.70814E-06	2.10328E-06	4.65045E-05
16	0.8	0.2	7.41625E-06	1.17821E-05	3.16457E-06	6.02019E-05
17	0.9	0.2	1.15033E-05	1.67757E-05	6.75021E-06	9.64318E-05
18	1	0.2	1.67282E-05	2.30119E-05	1.36256E-05	0.000146977
19	1.2	0.2	3.10887E-05	3.97645E-05	4.9259E-05	0.000304772
20	1.4	0.2	5.14975E-05	6.31446E-05	0.000153823	0.000564628
21	0.44	0.5	6.62734E-08	1.96024E-06	2.29572E-09	1.87563E-06
22	0.45	0.5	1.20005E-07	2.09696E-06	4.26464E-09	2.05204E-06
23	0.6	0.5	2.12075E-06	4.97057E-06	1.05381E-07	6.48547E-06
24	0.75	0.5	6.4364E-06	9.70814E-06	4.20182E-07	1.58337E-05
25	0.9	0.5	1.35075E-05	1.67757E-05	1.11486E-06	3.28327E-05
26	1	0.5	2.0006E-05	2.30119E-05	1.90246E-06	5.00422E-05
27	1.2	0.5	3.79918E-05	3.97645E-05	4.67968E-06	0.000103767
28	1.4	0.5	6.36872E-05	6.31446E-05	9.93662E-06	0.000192242
29	1.6	0.5	9.83676E-05	9.42567E-05	1.91713E-05	0.000327956
30	1.8	0.5	0.000143312	0.000134205	3.46098E-05	0.000525323

4.0 How the Models Account for Waves

4.1 Ackers and White

Scheffner (1996) extends the Ackers and White model for sediment transport to flows containing both current and waves. This modification is achieved by augmenting the depth-averaged current velocity to account for waves. This is a very simple modification, and it begins with the calculation of the angular frequency (ω) of the wave motion.

$$\omega = \frac{2\pi}{T} \tag{52}$$

The orbital excursion amplitude (A_o) is computed knowing the angular frequency:

$$A_o = \frac{U_o}{\omega} \tag{53}$$

The bottom friction coefficient (f_w) is calculated next:

$$f_w = \exp\left[-5.977 + 5.213\left(\frac{d}{A_o}\right)^{0.194}\right] \tag{54}$$

This leads to the calculation of ξ, given by

$$\xi = C_z\sqrt{\left(\frac{f_w}{2g}\right)} \tag{55}$$

Where C_z is the Chezy coefficient, given by equation 11. Before any calculations can be performed, the following variables must be known:

T = wave period

h = water depth

g = the acceleration due to gravity

d = median sediment diameter (d_{50})

U_o = the maximum wave orbital velocity

U = the depth averaged current velocity

A "new" depth averaged velocity (U_{wc}), which is defined to implicitly account for the effect of the presence of waves, can be calculated once ξ is known:

$$U_{wc} = U\sqrt{\left[1.0 + 0.5\left(\xi\frac{U_o}{U}\right)^2\right]} \tag{56}$$

U_{wc} can be viewed as an equivalent current velocity in a flow without waves that would produce the same transport as the combined wave-current problem. The Scheffner paper (1996) is unclear as to whether this new velocity replaces both current velocities in equation 1 or only the one in the parenthesis. Since Scheffner makes no distinction between the two current velocities in equation 1, U_{wc} replaced both current velocities in the calculations preformed during the analysis. This new current velocity allows the combined wave-current problem to be analyzed in the same manner as a steady unidirectional flow. The Ackers and White model for pure current flow can be used (equations 1 through 13) with the only difference being that the current velocity is replaced with U_{wc}. Therefore, the only change for the combined wave-current flow is that the average current velocity is augmented to account for the waves. This new velocity can also be used to calculate the total shear stress on the bottom:

$$\tau = \rho U_{wc}^2 \frac{g}{C_z^2} \tag{57}$$

4.2 Bailard

Bailard extends equation 14 to combined unsteady (waves) and steady flows. He time averages the transport equation to produce an expression for the time-averaged transport expressed in terms of volume per unit width per unit time. The cross-shore transport (Q_x) is given by

$$Q_x = K_B\left\{\langle|\vec{U}|^2\tilde{U}\rangle + \langle|\vec{U}|^2\overline{U}\rangle - \frac{\tan\beta}{\tan\phi}\langle|\vec{U}|^3\rangle\right\} + K_S\left\{\langle|\vec{U}|^3\tilde{U}\rangle + \langle|\vec{U}|^3\overline{U}\rangle - \frac{\varepsilon_S}{W}\tan\beta\langle|\vec{U}|^5\rangle\right\} \tag{58}$$

And the longshore transport (Q_y) is given by

$$Q_y = K_B\left\{\langle|\vec{U}|^2\tilde{V}\rangle + \langle|\vec{U}|^2\overline{V}\rangle - \frac{\tan\beta}{\tan\phi}\langle|\vec{U}|^3\rangle\right\} + K_S\left\{\langle|\vec{U}|^3\tilde{V}\rangle + \langle|\vec{U}|^3\overline{V}\rangle - \frac{\varepsilon_S}{W}\tan\beta\langle|\vec{U}|^5\rangle\right\} \tag{59}$$

Where $\vec{U}$ = the total velocity vector (cross-shore and longshore)

$\overline{U}$ = the mean component of the cross-shore velocity

$\tilde{U}$ = the oscillatory component of the cross-shore velocity

$\overline{V}$ = the mean component of the long shore velocity

$\tilde{V}$ = the oscillatory component of the long shore velocity

$\tan\beta$ = the cross-shore beach slope

and $\langle\ \rangle$ indicates time averaging, given by

$$\langle x \rangle = \frac{1}{T}\int_0^T x dt \tag{60}$$

The coefficients K_B and K_S are defined as

$$K_B = \frac{\rho}{\rho_s - \rho}\frac{C_f}{g}\frac{\varepsilon_B}{\tan\phi} \tag{61}$$

$$K_S = \frac{\rho}{\rho_s - \rho}\frac{C_f}{g}\frac{\varepsilon_S}{W} \tag{62}$$

Since the Ackers and White model does not have beach slope as an input, I am going to compare the models on a flat bed ($\beta = 0$). I am also going to have the waves approach the shore at a 90^o angle (there is no longshore component of the wave motion) because the Scheffner model cannot account for the angle of wave incidence. This enables equations 58 and 59 to be simplified to

$$Q_x = K_B\left\{\langle|\vec{U}|^2\tilde{U}\rangle + \langle|\vec{U}|^2\bar{U}\rangle\right\} + K_S\left\{\langle|\vec{U}|^3\tilde{U}\rangle + \langle|\vec{U}|^3\bar{U}\rangle\right\} \tag{63}$$

$$Q_y = K_B\left\{\langle|\vec{U}|^2\bar{V}\rangle\right\} + K_S\left\{\langle|\vec{U}|^3\bar{V}\rangle\right\} \tag{64}$$

For combined wave and current flows, Bailard (1981) sets $C_f = 0.003$, $\varepsilon_B = 0.1$, and $\varepsilon_S = 0.02$. In order to time average equations 63 and 64, the velocity vectors need to be expressed in

terms of the average current velocity (U) and the maximum wave orbital velocity (U_o).

$$B = \cos\phi_{wc} \tag{65}$$

$$D = \sin\phi_{wc} \tag{66}$$

$$\overline{U} = U\cos\phi_{wc} = UB \tag{67}$$

$$\tilde{U} = U_o\cos\omega t \tag{68}$$

$$\overline{V} = U\sin\phi_{wc} = UD \tag{69}$$

$$\left|\vec{U}\right| = \sqrt{[U^2 + U_o^2(\cos\omega t)^2 + 2U_o U\cos\omega t\cos\phi_{wc}]} \tag{70}$$

Where t is time and ϕ_{wc} is the angle between wave propagation and current direction. The x axis is in the same direction as wave propagation while the y axis is perpendicular to the wave. U_x is the component of the water velocity that travels in the same direction as the wave motion (cross-shore) while U_y is the component of the water velocity that travels perpendicular to the wave motion (longshore). Since I am only comparing cases where the waves are approaching the shore directly ($\alpha = 0$), the x component of the total fluid velocity is the total wave velocity, $U_o\cos\omega t$ plus the x component of the current velocity, $U\cos\phi_{wc}$ or UB. The y component is simply $U\sin\phi_{wc}$, or UD. This is given by

$$U_x = U_o\cos\omega t + UB \tag{71}$$

$$U_y = UD \tag{72}$$

since $|\vec{U}| = \sqrt{U_x^2 + U_y^2}$ and

$$U_x^2 = U^2B^2 + U_o^2(\cos\omega t)^2 + 2U_oUB\cos\omega t \tag{73}$$

$$U_y^2 = U^2D^2 \tag{74}$$

we have

$$|\vec{U}| = \sqrt{(U^2D^2 + U^2B^2 + U_o^2(\cos\omega t)^2 + 2U_oUB\cos\omega t)} \tag{75}$$

This can be simplified because $D^2 + B^2 = \sin^2\phi_{wc} + \cos^2\phi_{wc} = 1$, to

$$|\vec{U}| = \sqrt{(U^2 + U_o^2(\cos\omega t)^2 + 2U_oUB\cos\omega t)} \tag{76}$$

This allows each term in the transport equations to be time averaged and calculated.

$$\langle|\vec{U}|^2\tilde{U}\rangle = (1/T)\int_0^T [U^2U_o\cos(\omega t) + U_o^3(\cos\omega t)^3 + 2U_o^2UB(\cos\omega t)^2]dt = \tag{77}$$

$$\frac{1}{T\omega}\left[U^2U_o\sin(\omega T) + U_o^3\frac{1}{3}[2\sin(\omega T) + (\cos(\omega T))^2\sin(\omega T)] + 2U_o^2UB\left(\frac{1}{2}\omega T + \frac{1}{4}\sin(2\omega T)\right)\right]$$

$$= U_o^2UB$$

$$\langle|\vec{U}|^2\overline{U}\rangle = \frac{1}{T}\int_0^T [U^3B + U_o^2UB(\cos\omega t)^2 + 2U_oU^2B^2\cos\omega t]dt = \tag{78}$$

$$\frac{B}{T}\left[U^3T + U_o^2U\frac{1}{\omega}\left(\frac{1}{2}\omega T + \frac{1}{4}\sin 2\omega T\right) + 2U_oU^2B\frac{1}{\omega}\sin\omega T\right]$$

$$= U^3B + \frac{1}{2}U_o^2UB$$

$$\langle|\vec{U}|^2\bar{V}\rangle = \frac{D}{T}\int_0^T [U^3 + U_o^2U(\cos\omega t)^2 + 2U_oU^2B\cos\omega t]dt = \tag{79}$$

$$\frac{D}{T}\left[U^3T + U_o^2U\frac{1}{\omega}\left(\frac{1}{2}\omega T + \frac{1}{4}\sin 2\omega T\right) + \frac{2}{\omega}U_oU^2B\sin\omega T\right]$$

$$= U^3D + \frac{1}{2}U_o^2UD$$

$$\langle|\vec{U}|^3\tilde{U}\rangle = \frac{1}{T}\int_0^T\left[(U^2 + (U_o^2\cos\omega t + 2U_oUB)\cos\omega t)^{\frac{3}{2}}U_o\cos\omega t\right]dt \tag{80}$$

$$\langle|\vec{U}|^3\bar{U}\rangle = \frac{1}{T}\int_0^T\left[(U^2 + (U_o^2\cos\omega t + 2U_oUB)\cos\omega t)^{\frac{3}{2}}UB\right]dt \tag{81}$$

$$\langle|\vec{U}|^3\bar{V}\rangle = \int_0^T\left[(U^2 + (U_o^2\cos\omega t + 2U_oUB)\cos\omega t)^{\frac{3}{2}}UD\right]dt \tag{82}$$

Equations 80 through 82 are solved numerically. Calculating equations 77 through 82 gives all the terms needed to solve equations 63 and 64 (assuming that equations 61 and 62 have been solved). Equations 63 and 64 give the total transport in the x and y directions. The variables needed before

any calculations can take place are:

d = median sediment diameter (d_{50})

U_o = the maximum wave orbital velocity

U = the depth-averaged current velocity

g = the acceleration due to gravity

ρ_s = sediment density (assumed = 2, 650 kg/m^3 for quartz)

ρ = water density (assumed = 1, 025 kg/m^3 for seawater)

ϕ_{wc} = angle between current and wave motion

ε_B = bedload efficiency factor (assumed = 0.1)

ε_S = suspended load efficiency factor (assumed = 0.02)

C_f = friction coefficient (assumed = 0.003)

The bedload and suspended load transport rates are given separately by equations 63 and 64 (terms multiplied by K_B are bedload while those multiplied by K_S are suspended load). It is interesting to note that the bedload transport is not dependent on grain diameter and because the transport equations are time averaged, the wave period (T) is not needed to calculate the transport. It is also important to remember that ε_B, ε_S, and C_f are not universal constants, but depend on flow conditions and the bathymetry of the bed. Since, however, there is no explicit way to calculate them based on the given variables, values of these factors must be assumed, and the ones listed above yield good results from previous experiments.

4.3 Madsen

The Madsen model (1997) is unique when compared to the other two because it takes the effect of the flow on the bed into account. The flow can change the roughness of the bed by causing dunes or ripples to form, which ultimately affects the transport. Since waves have a greater effect on the current than the current does on the waves, the model begins calculations assuming pure wave motion without current. The following variables are needed to begin the needed calculations:

U_c = the current velocity at a specified height (z_r) above the bottom

z_r = the height were the current velocity is specified

U_o = maximum wave orbital velocity at the bottom (also U_{bm})

h = water depth

d = median sediment diameter (d_{50})

ρ_s = sediment density (assumed = 2, 650 kg/m^3 for quartz)

ρ = water density (assumed = 1, 025 kg/m^3 for seawater)

T = period of wave motion

ϕ_{wc} = angle between current and wave motion

β = slope of bottom measured from horizontal (positive if flow is uphill)

α = angle of wave incidence

υ = kinematic viscosity of fluid (molecular = 10^{-6} m^2/sec for seawater)

$\kappa = 0.4$

k'_n = median grain diameter

If U_c at z_r is not given, it can be calculated if the depth averaged current velocity is known, assuming a logarithmic velocity profile. U_o can also be calculated based on wave conditions if it is not given. Many of the variables in the equations contain subscripts. The meaning of these subscripts are listed below:

$()_b$ = conditions at the bottom

$()_c$ = quantity associated with current

$()_{cr}$ = quantity associated with critical conditions for initiation of sediment motion

$()_m$ = maximum value of quantity

$()_w$ = quantity associated with wave motion

$()_{wm}$ = maximum of wave-associated quantity

()' = skin friction conditions

$()_*$ = quantity associated with shear

The model begins by assuming pure wave motion without a current. This is done in order to determine whether the bed is flat or contains bedforms. The wave orbital excursion amplitude (A_o) and the frequency of wave motion are calculated from equations 52 and 53 respectively. The wave solution can now be obtained beginning with $C_\mu = 1$.

$$\frac{C_\mu U_o}{k'_n \omega} = \Gamma \tag{83}$$

If $0.2 < \Gamma < 100$

$$f'_w = C_\mu \exp\{7.02\Gamma^{-0.078} - 8.82\} \tag{84}$$

If $100 < \Gamma < 10{,}000$

$$f'_w = C_\mu \exp\{5.61\Gamma^{-0.109} - 7.30\} \tag{85}$$

Equations 84 and 85 are from Madsen (1994) and f_w is the wave friction factor.

$$U'^2_{*wm} = \frac{1}{2} f'_w U_o^2 \tag{86}$$

The prime (') designates skin friction conditions.

$$\delta'_{cw} = \kappa \frac{U'_{*wm}}{\omega} \tag{87}$$

If $k'_n U'_{*wm}/\nu > 3.3$,

$$z'_o = \frac{k'_n}{30} \tag{88}$$

If $k'_n U'_{*wm}/\nu < 3.3$,

$$z'_o = \nu/9U_{*wm} \tag{89}$$

The skin friction Shields parameter (ψ'_m) can be calculated from

$$\psi'_m = \frac{U'^2_{*wm}}{(s-1)gd} \tag{90}$$

The critical Shields parameter (ψ_{cr}), along with S_*, can be found using equations 34 through 38. If $\psi'_m < 1/2\ \psi_{cr}$, there is no sediment transport: $\eta = \lambda = 0$ and $k_n = k'_n = d$. Where η is the ripple height, λ is the ripple length, and k_n is the moveable bed roughness. If $\psi'_m > 0.35$, there is sheet

flow (which means that the shear is so strong that the ripples become eroded smooth) $\eta = \lambda = 0$ and

$$k_n = 15\psi'_m d \tag{91}$$

If $1/2\ \psi_{cr} < \psi'_m < 0.35$,

$$Z = \frac{\psi'_m}{S_*} \tag{92}$$

If $Z < 0.0016$, assume $Z = 0.0016$.

If $0.0016 \leq Z < 0.012$ use

$$\frac{\eta}{A_o} = 1.8 \times 10^{-2} Z^{-0.5} \tag{93}$$

$$\frac{\eta}{\lambda} = 1.5 \times 10^{-1} Z^{-0.009} \tag{94}$$

If $0.012 < Z < 0.18$ use

$$\eta / A_o = 7.0 \times 10^{-4} Z^{1.23} \tag{95}$$

$$\eta / \lambda = 1.05 \times 10^{-2} Z^{.065} \tag{96}$$

These results allow one to use the following equation to find k_n, the moveable bed roughness:

$$k_n = 4\eta \tag{97}$$

If $Z > 0.18$, sheet flow is assumed: $\eta = \lambda = 0$ and k_n can be solved from equation 90.

Once the moveable bed roughness has been found, the combined wave-current problem can be solved. The process is iterative, and begins with $\mu = 0$.

$$\mu = \frac{U_{*c}^2}{U_{*wm}^2} \tag{98}$$

$$C_\mu = \sqrt{(1 + (2\mu\cos\phi_{wc}) + \mu^2)} \tag{99}$$

$$\frac{(C_\mu U_o)}{k_n \omega} = \Gamma \tag{100}$$

If $0.2 < \Gamma < 100$

$$f_{wc} = C_\mu \exp\{7.02\Gamma^{-0.078} - 8.82\} \tag{101}$$

If $100 < \Gamma < 10{,}000$

$$f_{wc} = C_\mu \exp\{5.61\Gamma^{-0.109} - 7.30\} \tag{102}$$

Equations 101 and 102 are from Madsen (1994) and f_{wc} is the wave friction factor in the presence of a current.

$$U_{*wm}^2 = \frac{1}{2} f_{wc} U_o^2 \tag{103}$$

$$U_{*m}^2 = C_\mu U_{*wm}^2 \tag{104}$$

$$\delta_{cw} = \kappa \frac{U_{*\mathrm{m}}}{\omega} \tag{105}$$

If $k_n U_{*\mathrm{m}}/\nu > 3.3$

$$z_{\mathrm{o}} = \frac{k_n}{30} \tag{106}$$

If $k_n U_{*m}/\nu < 3.3$,

$$z_{\mathrm{o}} = \nu/9 U_{*\mathrm{m}} \tag{107}$$

The iterations are completed with the calculation of the shear velocity ($U_{*\mathrm{c}}$):

$$U_{*\mathrm{c}} = U_{*\mathrm{m}} \frac{\left(\ln(\frac{z_r}{\delta_{cw}})\right)}{\ln(\frac{\delta_{\mathrm{cw}}}{z_{\mathrm{o}}})} \left[-\frac{1}{2} + \sqrt{\left(\frac{1}{4} + \left(\kappa \frac{U_c(z_r)}{U_{*\mathrm{m}}} \right) \frac{\left(\ln(\frac{\delta_{\mathrm{cw}}}{z_{\mathrm{o}}})\right)}{\left(\ln\left(\frac{z_r}{\delta_{\mathrm{cw}}}\right)\right)^2} \right)} \right] \tag{108}$$

After these iterations are performed, a value for $U_{*\mathrm{c}}$ (the current shear velocity), is known. This value can be introduced into equation 98 and then equations 99 through 108 can be resolved until there is no change in the answers. $U_{*\mathrm{wm}}$ (the maximum wave shear velocity), $U_{*\mathrm{m}}$ (the maximum total shear velocity), δ_{cw} (the boundary layer thickness) and z_{o} (the bottom roughness scale in log-profile) are known. This allows the total fluid shear stress to be calculated from

$$\tau_m = \rho_w U_{*\mathrm{m}}^2 \tag{109}$$

Equations 110 and 111 give the current velocity profile:

For $z < \delta_{cw}$

$$U_c(z) = \frac{U_{*c}}{\kappa}\frac{U_{*c}}{U_{*m}}\ln\left(\frac{z}{z_o}\right) \tag{110}$$

For $z > \delta_{cw}$

$$U_c(z) = \frac{U_{*c}}{\kappa}\ln\left(\frac{z}{z_{oa}}\right) \tag{111}$$

The tangent of the phase angle of the bottom shear stress is given by equation 112 while equation 113 gives the apparent bottom roughness for currents in the presence of waves. Equation 113 can be solved after equation 110 is used to find $U_c(\delta_{cw})$.

$$\tan\varphi = \frac{(\pi/2)}{\ln\left(\kappa\frac{U_{*m}}{z_o\omega}\right) - 1.15} \tag{112}$$

$$z_{oa} = \frac{\delta_{cw}}{\exp(\kappa U_c(\delta_{cw})/U_{*c})} \tag{113}$$

After the apparent bottom roughness has been calculated from equation 113, the wave-current problem is solved again, this time for skin friction conditions. Instead of using the moveable bed roughness, $k'_n = d$ = median sediment diameter is used and the new current specification, $U_c = U_c(\delta_{cw})$ at $z = \delta_{cw}$ is used instead of the current velocity given. Once again, equations 98 through 109 need to be solved iteratively.

4.3.b Bedload Transport

The critical shear velocity (U_{*cr}) and shear stress (τ_{cr}) can be calculated from:

$$U_{*cr} = \sqrt{\psi_{cr}(s-1)gd} \tag{114}$$

$$\tau_{cr} = \rho_w U_{*cr}^2 \tag{115}$$

The skin friction Shields parameters can also be calculated:

$$\psi'_c = \frac{U'^2_{*c}}{(s-1)gd} \tag{116}$$

$$\psi'_{wm} = \frac{U'^2_{wm}}{(s-1)gd} \tag{117}$$

All the variables needed to calculate the bedload for a combined wave-current flow are now known. Equation 118 gives the bedload transport ($[\bar{q}_{sb}]_{wc}$) due to the shear stresses caused by the flow while equation 119 gives the bedload transport ($[\bar{q}_{sb}]_{\beta}$) due to the bottom slope (β is the bed-slope and α is the angle of wave incidence).

$$\left[\frac{\bar{q}_{sb}}{d\sqrt{((s-1)gd)}}\right]_{wc} = 6\psi'^{3/2}_c \frac{U'_{wm}}{U'_{*c}}\left\{\frac{3}{2}\cos\phi_{wc}, \sin\phi_{wc}\right\} \tag{118}$$

$$\beta_w = \arctan(\tan\beta\cos\alpha) \tag{119}$$

$$\mu_b = \frac{(\tan\beta_w)}{\tan\phi_m} \quad \text{where } \phi_m = 30^o \tag{120}$$

$$\left[\frac{\bar{q}_{sb}}{d\sqrt{((s-1)gd)}}\right]_{\beta} = 4.5\psi'^{3/2}_{wm}\{-\mu_b,0\} \tag{121}$$

$$\tan\varphi' = \frac{(\pi/2)}{\ln\left(\kappa\frac{U'^{*m}}{z'_o\omega}\right)-1.15} \tag{122}$$

The total bedload transport can be found by the vector addition of $[\bar{q}_{sb}]_{wc}$ and $[\bar{q}_{sb}]_{\beta}$.

4.3.c Mean Suspended Load Transport

The last thing left to calculate it the suspended load transport. This is begun with the calculation of z_R, the reference elevation for specifications of reference concentration of sediment, given by equation 123. W is the sediment fall velocity and can be found from equation 45. The mean reference concentration is given by C_R (the overbar indicates a time averaged quantity) and C_{Rwm} gives the maximum wave reference concentration. γ is the resuspension parameter.

$$z_R = 7d \tag{123}$$

$$\overline{C_R} = \gamma C_b\left[\frac{2}{\pi}\frac{\tau'_{wm}}{\tau_{cr}} - 1\right] \quad \text{where } C_b = 0.65 \tag{124}$$

$$\gamma = \begin{pmatrix} 2 \times 10^{-3} & \text{for rippled bed} \\ 2 \times 10^{-4} & \text{for flat bed} \end{pmatrix} \tag{125}$$

$$C_{Rwm} = \gamma C_b\left[\frac{4}{\pi}\frac{\tau'_c}{\tau_{cr}}\cos\phi_{wc} - \frac{\tau'_{wm}}{\tau_{cr}}\frac{(\tan\beta_w)}{\tan\phi_m}\right] \tag{126}$$

$\phi_m = 30^o$

For $z_R > z_o$:

$$\bar{q}_{sS} = \frac{U_{*c}}{\kappa}\overline{C}_R\left[\frac{\delta_{cw}}{z_R}\right]^{-\frac{W}{\kappa U_{*m}}}\delta_{cw}(I_1 + I_2) \tag{127}$$

$$I_1 = \kappa\frac{U_{*c}}{(\kappa U_{*m} - W)}\left[\ln\frac{\delta_{cw}}{z_o} - \frac{\kappa U_{*m}}{(\kappa U_{*m} - W)} - \left[\frac{z_R}{\delta_{cw}}\right]^{\frac{\kappa U_{*m} - W}{\kappa U_{*m}}}\left[\ln\frac{z_R}{z_o} - \frac{\kappa U_{*c}}{(\kappa U_{*m} - W)}\right]\right] \tag{128}$$

$$I_2 = \frac{\kappa U_{*c}}{(\kappa U_{*c} - W)}\left[\left[\frac{h}{\delta_{cw}}\right]^{\frac{\kappa U_{*c} - W}{\kappa U_{*c}}}\left[\ln\frac{h}{z_{oa}} - \frac{\kappa U_{*c}}{(\kappa U_{*c} - W)}\right] - \left[\ln\frac{\delta_{cw}}{z_{oa}} - \frac{\kappa U_{*c}}{(\kappa U_{*c} - W)}\right]\right] \tag{129}$$

For $z_R < z_o$:

$$\bar{q}_{sS} = \frac{U_{*c}}{\kappa}\overline{C}_R\left[\frac{\delta_{cw}}{z_R}\right]^{-\frac{W}{\kappa U_{*m}}}\delta_{cw}(I_3 + I_2) \tag{130}$$

$$I_3 = \frac{\ln\frac{\delta_{cw}}{z_o}}{\ln\frac{\delta_{cw}}{z_R}}\frac{\kappa U_{*c}}{(\kappa U_{*m} - W)}\left\{\ln\frac{\delta_{cw}}{z_R} - \frac{\kappa U_{*m}}{(\kappa U_{*m} - W)}\left[1 - \left[\frac{z_R}{\delta_{cw}}\right]^{\frac{\kappa U_{*m} - W}{\kappa U_m}}\right]\right\} \tag{131}$$

The vector for the mean suspended total load transport rate is given by

$$\bar{\mathbf{q}}_{sS} = \bar{q}_{sS}\{\cos\phi_{wc}, \sin\phi_{wc}\} \tag{132}$$

4.3.d Mean Wave-Associated Suspended Load Transport

If $z_R > \delta_{cw}/\pi$, this transport = 0. Otherwise,

$$\tan\varphi_s = \frac{(\pi/2)}{\ln\kappa\dfrac{U_{*m}}{z_R\omega} - 1.15} \tag{133}$$

If $z_R < z_o$:

$$\bar{q}_{sSw} = \frac{1}{\pi^2}\sin\varphi U_o C_{Rwm}\delta_{cw}\left[\cos(\varphi-\varphi')I_4 - \frac{2}{\pi}\sin\varphi_s\cos(\varphi-\varphi'-\varphi_s)I_5\right] \tag{134}$$

With

$$I_4 = \ln\frac{\delta_{cw}}{\pi z_o} - 1 - \frac{\pi z_R}{\delta_{cw}}\left[\ln\frac{z_R}{z_o} - 1\right] \tag{135}$$

$$I_5 = \ln\frac{z_R}{z_o}\left[\ln\frac{\delta_{cw}}{\pi z_R} - 1 + \frac{\pi z_R}{\delta_{cw}}\right] + \left[\ln\frac{\delta_{cw}}{\pi z_R}\right]^2 - 2\ln\frac{\delta_{cw}}{\pi z_R} + 2\left[1 - \frac{\pi z_R}{\delta_{cw}}\right] \tag{136}$$

If $z_R > z_o$:

$$\bar{q}_{sSw} = \frac{1}{\pi^2}\sin\varphi U_o C_{Rwm}\delta_{cw}\frac{\ln\dfrac{\delta_{cw}}{\pi z_o}}{\ln\dfrac{\delta_{cw}}{\pi z_R}} \times \left[\cos(\varphi-\varphi')I_6 - \frac{2}{\pi}\sin\varphi_s\cos(\varphi-\varphi'-\varphi_s)I_7\right] \tag{137}$$

With

$$I_6 = \ln\frac{\delta_{cw}}{\pi z_R} - 1 + \frac{\pi z_R}{\delta_{cw}} \tag{138}$$

$$I_7 = \left[\ln\frac{\delta_{cw}}{\pi z_R}\right]^2 - 2\ln\frac{\delta_{cw}}{\pi z_R} + 2\left[1 - \frac{\pi z_R}{\delta_{cw}}\right] \tag{139}$$

The vector for the mean wave-associated suspended load transport rate can be given by

$$\bar{q}_{sSw} = \bar{q}_{sSw}\{1, 0\} \tag{140}$$

The vector addition of $[\bar{q}_{sb}]_{wc}$, $[\bar{q}_{sb}]_{\beta}$, $\bar{q}_{sS}$ and $\bar{q}_{sSw}$ yields the total sediment transport (Q_t). This is summarized by equation 141:

$$Q_t = \bar{q}_{sSw} + \bar{q}_{sS} + [\overline{q}_{sb}]_{\beta} + [\overline{q}_{sb}]_{wc} \tag{141}$$

5.0 Comparison of Models for Combined Wave-Current Flows

5.1 Description of the Differences

The Scheffner (1996) modification to the Ackers and White model (1973) is the simplest of the three models studied. The Scheffner modification simply augments the current velocity so that the given problem can be compared to a steady unidirectional flow with a higher mean velocity. This is not a very adequate way of dealing with the new problem of having an unsteady flow that can be acting at an angle to the current. It assumes that the physics is essentially unchanged and that the sediment will react in the same way to a combined wave-current flow as it does to a steady unidirectional flow. There are many factors that suggest that this is not the case. Since there is only one velocity acting in the Scheffner model, is it impossible to take into account the fact

that wave propagation is not always in the same direction as the current. It is certain that waves contribute to transport, but they do so quite differently than a steady flow. Linear waves alone cannot transport sediment on a flat bed because there is no net shear stress on the bottom: the shear under a trough is always equal to the shear under a crest, so they cancel each other out. Waves, however, can stir up the bottom sediment, enabling the current to transport it.

Bailard (1981) accounts for waves by incorporating the wave orbital velocities into a total velocity vector that changes with time. This vector is used in the expression for transport and is then time averaged over the wave period to get the transport. The model assumes that any sediment suspension occurs instantaneously in response to fluid forcing, indicating that the fluid velocity, sediment suspension, and transport are all in phase. The wave period appears in the transport equation but drops out in the calculations because the equations are time averaged, and therefore the wave period has no effect on the transport. A peculiarity with the Bailard model is the fact that the bedload transport does not depend on grain diameter.

The suspended load in the Bailard model is calculated using the total velocity vector, which incorporates both the current velocity and wave orbital velocity. This methodology is flawed, however, because waves are only able to affect mixing within the wave bottom boundary layer and not the entire depth. Only the current shear velocity mixes sediment in the fluid water column above the wave bottom boundary layer. This will overestimate the suspended load, especially for high wave orbital velocities. This overestimation is likely to take place in the Scheffner model as well, because it also fails to differentiate between wave and current velocities. Unlike the Scheffner model, the Bailard model does take into account the angle between wave propagation and current direction and also the bed slope. The Bailard model still does not incorporate a critical flow condition that must be surpassed in order for transport to occur.

The Madsen model accounts for waves by first ignoring the existence of any current and then predicts the existence of bedforms which would change the roughness experienced by the flow and the shear stresses acting on the bottom. The model ignores the current at first because it assumes that waves play a much larger role in determining boundary layer conditions and the formation of bedforms. After the calculation of the possible existence of bedforms, this new information is used to determine the total roughness experienced by the flow, and includes the current in the calculations. This total roughness is used to determine the total shear stress and the Shields parameter. Bedload and suspended load are calculated using skin friction values, because movement of individual grains involves the roughness of the single grain and not the ripple. The Madsen model, like the Scheffner model, still incorporates a critical value that the flow must surpass in order for transport to begin, and like the Bailard model, it incorporates the bottom slope and angle between wave propagation and current direction. Unlike the other two models, the Madsen model takes into account the formation of bedforms and wave boundary layers, and also includes the calculations of phase angles. A problem with the calculation of suspended load transport is the model's dependence of knowing the highly uncertain reference concentration C_R and resuspension parameter, γ.

5.2 Discussion

The combined wave-current problem involves two more variables than the steady unidirectional flow problem: the wave period (T) and the maximum orbital wave velocity (U_o). This is assuming the simplest case where the current is in the same direction as wave propagation. These added variables make the problem much more complex than the steady unidirectional flow

because it is even more difficult to isolate which input causes which pattern of sediment transport. The manner of investigation is the same as that for the steady flow: one input is varied and the transport is plotted against it, holding all other variables constant. For this combined flow, all of the runs were performed with a water depth of 5 meters. It is logical to assume that grain diameter and current velocity have the same effect on transport as they do in a steady unidirectional flow, i.e., all the models predict increased transport with increased current velocity and the Bailard and Madsen models predict increased transport with decreasing sediment size. Therefore, the effects of wave period and orbital velocity on sediment transport are the focus, but runs were also performed to confirm that sediment diameter and current velocity have the same effect in a combined unsteady flow as they do in steady unidirectional flow.

The first analysis was performed to confirm whether grain diameter has the same effect on sediment transport in a combined unsteady flow as it does in a steady unidirectional one. Figures 16 through 18 on pages 69 through 71 plot the total sediment transport rate versus grain diameter for all three models at three different wave periods, ranging from 4 seconds (short waves) to 16 seconds (long waves). Table 5 on page 72 contains the output of these runs. The current velocity and maximum orbital velocity were held constant, both equal to 0.35 m/sec. It is interesting to note that at this low current velocity, the Madsen model and the Ackers and White model would predict no transport in a steady unidirectional flow; but when waves are present, the added shear enables the flow to easily initiate transport. This indicates the importance of waves in creating sediment transport: only a small current velocity is needed for transport when waves are present.

Figures 16 through 18 reveal the same pattern for the combined unsteady flow as for the steady unidirectional flow: the Bailard model and Madsen model predict a steady decrease in sediment transport with increased sediment diameter, with the sharpest gradient occurring with the

very fine sediments while the Ackers and White model predicts that transport peaks at a grain diameter of about 0.5 mm. This pattern holds for all three periods investigated. Though not shown on Figures 16 through 18, the Madsen model predicts zero transport for grains larger than 3 mm and the Ackers and White model predicts zero transport for grains larger than 1 mm due to the fact that these grains are too large to be moved by the given flow conditions.

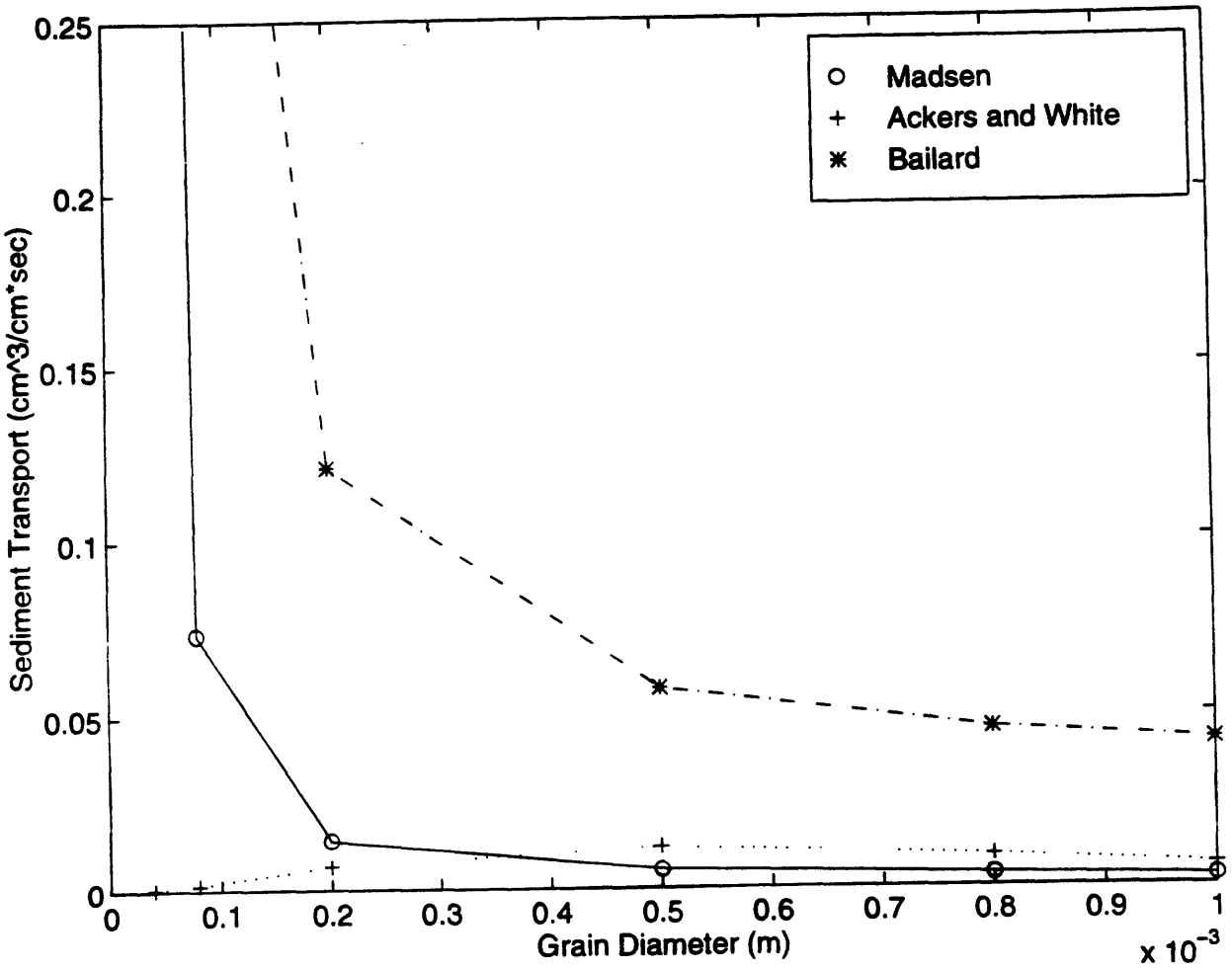

Figure 16. The total sediment transport rate versus sediment diameter for a wave period of 4 sec, an average current velocity of 0.35 m/sec and a maximum wave orbital velocity of 0.35 m/sec.

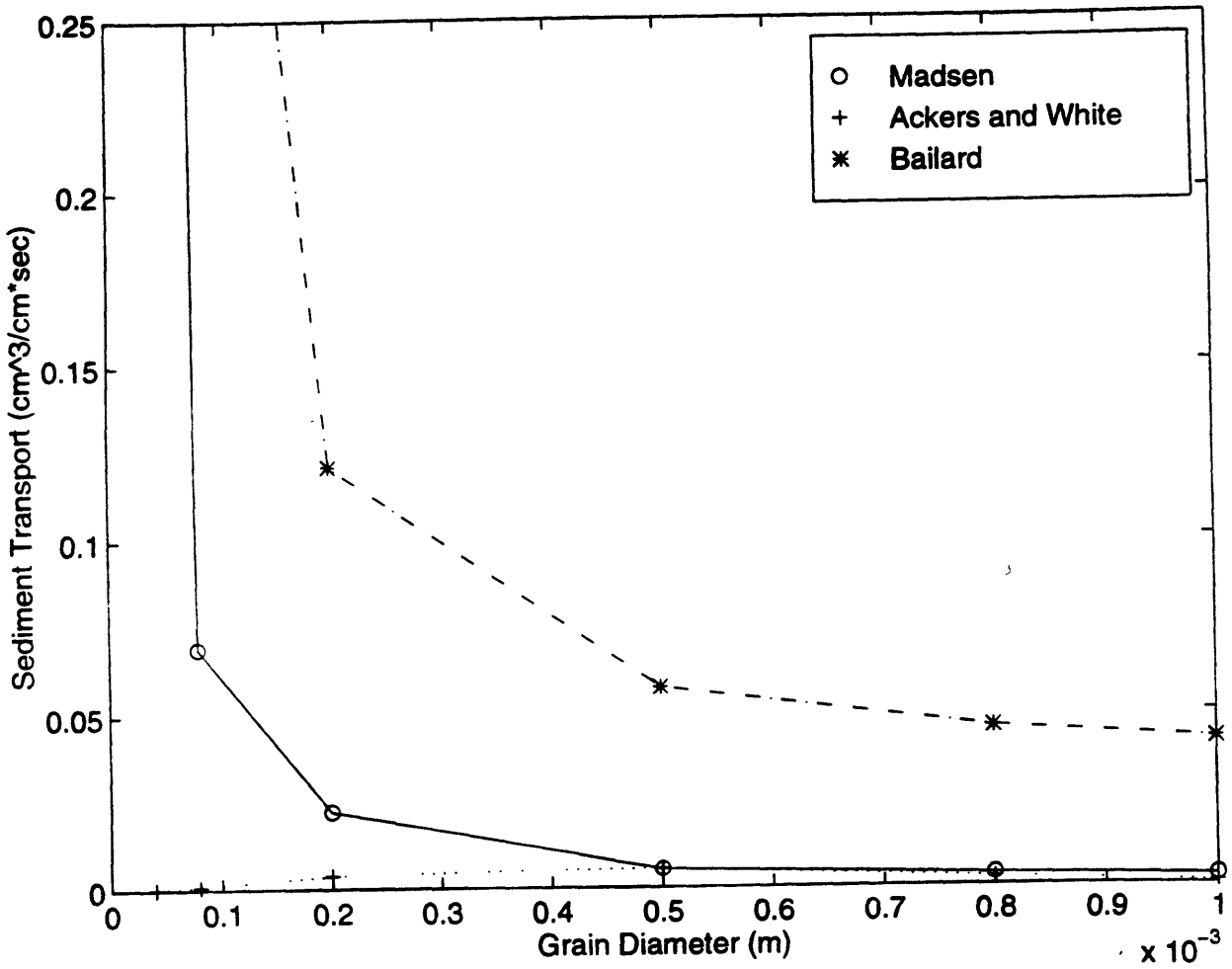

Figure 17. The total sediment transport rate versus sediment diameter for a wave period of 8 sec, an average current velocity of 0.35 m/sec and a maximum wave orbital velocity of 0.35 m/sec.

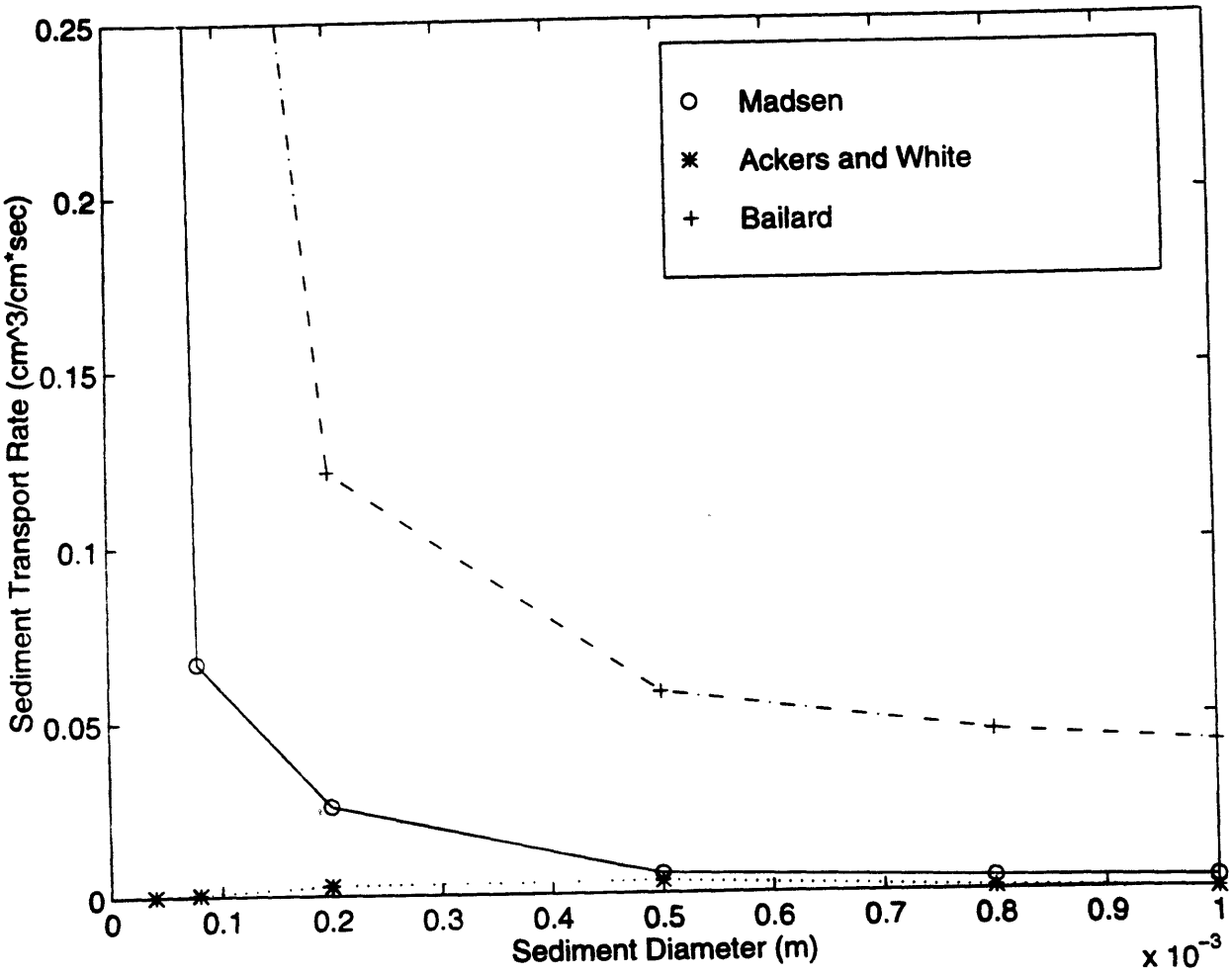

Figure 18. The total sediment transport rate versus sediment diameter for a wave period of 16 sec, an average current velocity of 0.35 m/sec and a maximum wave orbital velocity of 0.35 m/sec.

Table 5

Total Transport Rate Versus Grain Size and Wave Period, $U_c = U_o = 0.35$ m/sec.

Case #	Period (sec)	d (mm)	Madsen Total Load (m^3/m*sec)	Madsen Condition 3 = ripples 2 = sheet flow	Ackers & White Total Load (m^3/m*sec)	Bailard Total Load (m^3/m*sec)
1	4	0.04	0.000143528	2	3.95756E-08	0.000186054
2	4	0.08	7.35993E-06	2	1.52032E-07	4.83634E-05
3	4	0.2	1.4559E-06	3	6.81757E-07	1.2116E-05
4	4	0.5	5.49465E-07	3	1.2349E-06	5.75197E-06
5	4	0.8	3.59988E-07	3	9.31671E-07	4.56662E-06
6	4	1	2.78829E-07	3	6.35335E-07	4.18839E-06
7	8	0.04	0.000125456	2	1.47927E-08	0.000186054
8	8	0.08	6.94393E-06	2	7.49561E-08	4.83634E-05
9	8	0.2	2.23655E-06	3	3.81911E-07	1.2116E-05
10	8	0.5	5.47954E-07	3	5.79413E-07	5.75197E-06
11	8	0.8	3.63094E-07	3	2.58447E-07	4.56662E-06
12	8	1.0	2.92533E-07	3	6.73853E-08	4.18839E-06
13	16	0.04	0.000110108	2	6.22399E-09	0.000186054
14	16	0.08	6.50454E-06	2	3.98971E-08	4.83634E-05
15	16	0.2	2.94676E-06	3	2.22257E-07	1.2116E-05
16	16	0.5	5.8696E-07	3	2.46562E-07	5.75197E-06
17	16	0.8	4.24741E-07	3	1.64039E-08	4.56662E-06
18	16	1	4.10054E-07	3	0	4.18839E-06
19	4	0.1	3.38438E-06	2	2.31059E-07	4.13143E-05
20	6	0.1	3.40848E-06	2	1.56284E-07	4.13143E-05
21	8	0.1	3.41416E-06	2	1.20138E-07	4.13143E-05
22	10	0.1	3.41391E-06	2	9.87458E-08	4.13143E-05
23	12	0.1	3.4116E-06	2	8.45485E-08	4.13143E-05
24	14	0.1	2.56442E-06	2	7.44043E-08	4.13143E-05
25	16	0.1	2.65667E-06	2	6.67721E-08	4.13143E-05
26	18	0.1	2.65667E-06	2	6.08071E-08	4.13143E-05
27	4	0.2	1.4559E-06	3	6.38784E-07	1.28659E-05
28	6	0.2	1.82362E-06	3	4.52606E-07	1.28659E-05
29	8	0.2	2.07997E-06	3	3.5753E-07	1.28659E-05
30	10	0.2	2.70756E-06	3	2.99205E-07	1.28659E-05
31	12	0.2	2.93012E-06	3	2.59479E-07	1.28659E-05
32	14	0.2	3.1565E-06	3	2.30521E-07	1.28659E-05
33	16	0.2	3.38486E-06	3	2.08383E-07	1.28659E-05
34	18	0.2	3.61406E-06	3	1.90852E-07	1.28659E-05
35	4	0.5	5.49465E-07	3	1.2349E-06	5.75197E-06
36	6	0.5	5.44256E-07	3	8.00147E-07	5.75197E-06
37	8	0.5	5.47954E-07	3	5.79413E-07	5.75197E-06
38	10	0.5	5.55533E-07	3	4.4613E-07	5.75197E-06
39	12	0.5	5.65084E-07	3	3.5719E-07	5.75197E-06
40	14	0.5	5.75717E-07	3	2.93831E-07	5.75197E-06
41	16	0.5	5.8696E-07	3	2.46562E-07	5.75197E-06
42	18	0.5	5.98538E-07	3	2.10066E-07	5.75197E-06

It makes sense for the Madsen model and the Bailard model to predict a large increase in transport at very fine sediment sizes because both models predict large suspended load transports for very fine sediments, which is especially true when there are waves present. Waves do a good job at scouring fine sediment off of the bed floor, and it makes sense that there would be a very large transport when suspended load transport dominates in relation to bedload transport, which is the case for very fine sediment.

Since the modification made to the Ackers and White model to account for waves makes it virtually identical to the steady unidirectional flow model, one would expect the model to exhibit the same properties in both cases, which is exactly what happens. Changing the grain diameter has two effects: it changes the roughness felt by the flow and it changes the critical shear stress needed to initiate movement. Increasing the grain diameter increases both the roughness (and therefore the total shear stress on the bed) and the critical shear stress of the sediment. These counteract each other, making the effect of transport uncertain, leading to a prediction that increases transport with grain diameter up to a certain point, after which transport decreases as the sediment size increases to the stage where it is too large to be transported by the given flow conditions.

Figures 19 through 21 on pages 74 through 76 break down the total sediment transport versus grain diameter into a suspended load transport and a bedload transport for the Madsen and Bailard models. Table 6 on page 77 contains the output for these runs. The results are the same for the combined flow as it was for steady unidirectional flow: suspended load decreases sharply as sediment size increases while the bedload is much flatter, and increases slightly for the Madsen model at the very large grain diameters. Since the suspended load dominates, especially for the fine grains, transport always decreases with increased sediment size for these two models. Again,

in a real world situation where the sediment is probably not well sorted, each grain size would experience the same shear stress and one would expect larger transport for the smaller sediments.

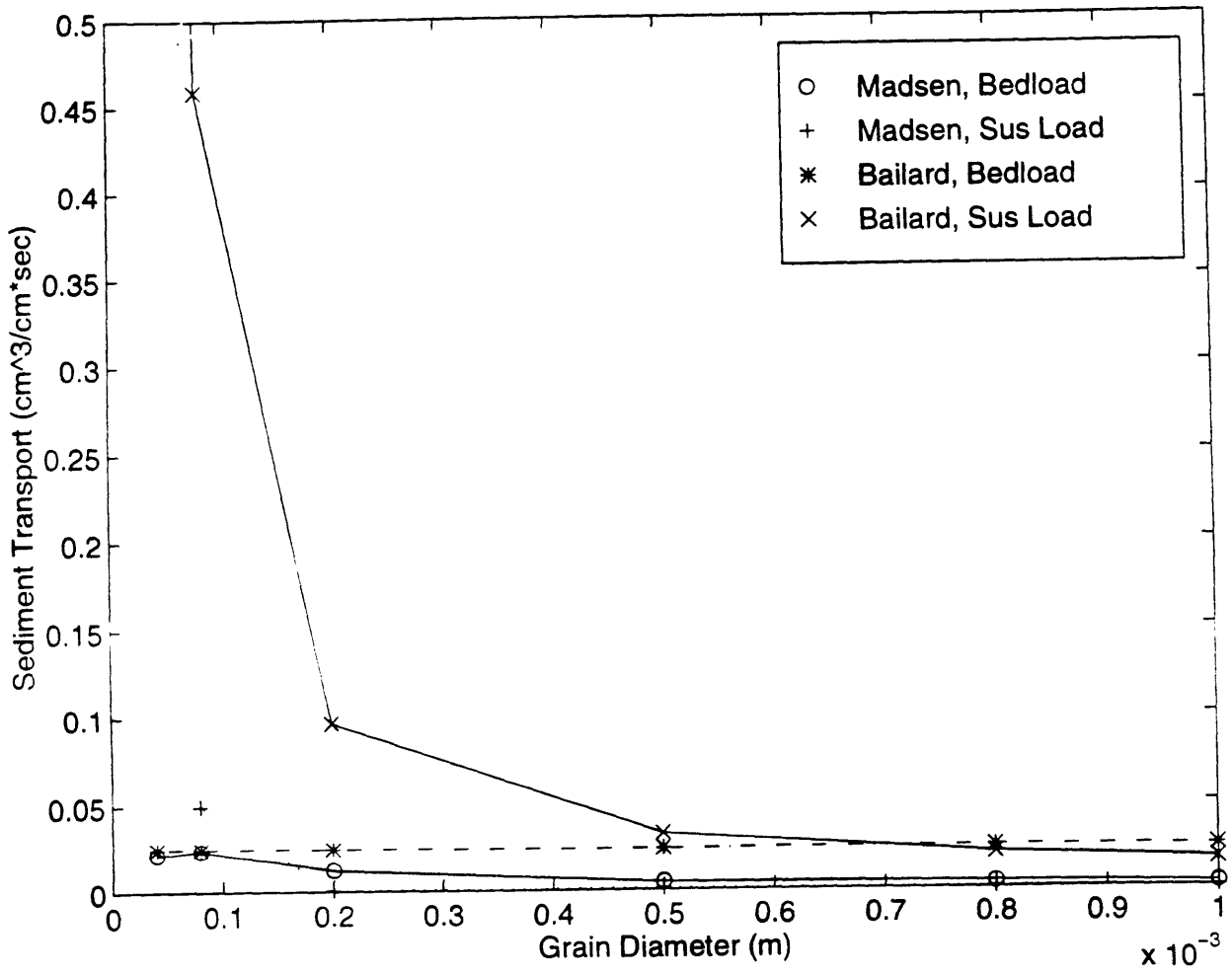

Figure 19. Break down of the total sediment transport rate versus sediment diameter for a wave period of 4 sec, an average current and a maximum wave orbital velocity of 0.35 m/sec.

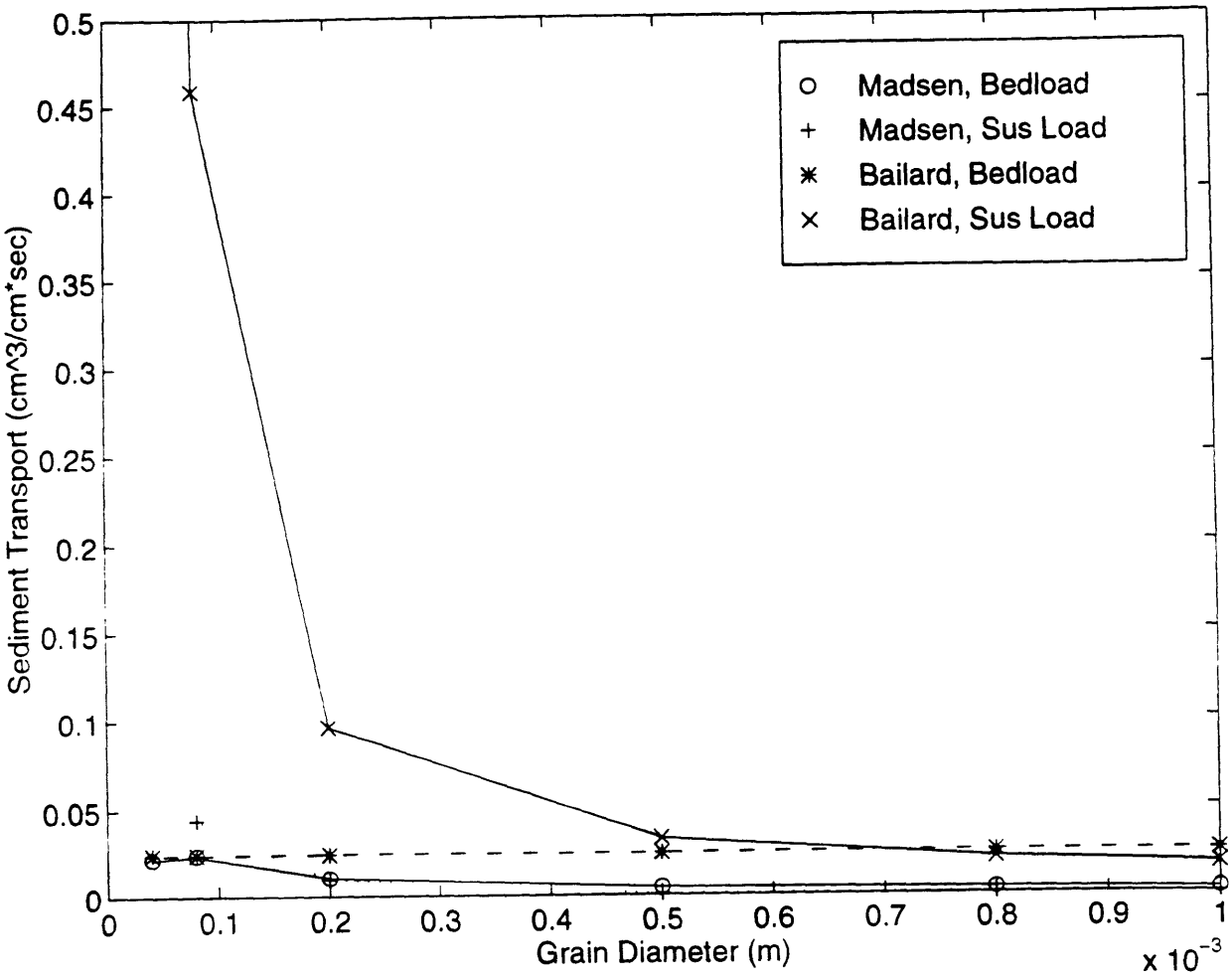

Figure 20. Break down of the total sediment transport rate versus sediment diameter for a wave period of 8 sec, an average current and a maximum wave orbital velocity of 0.35 m/sec.

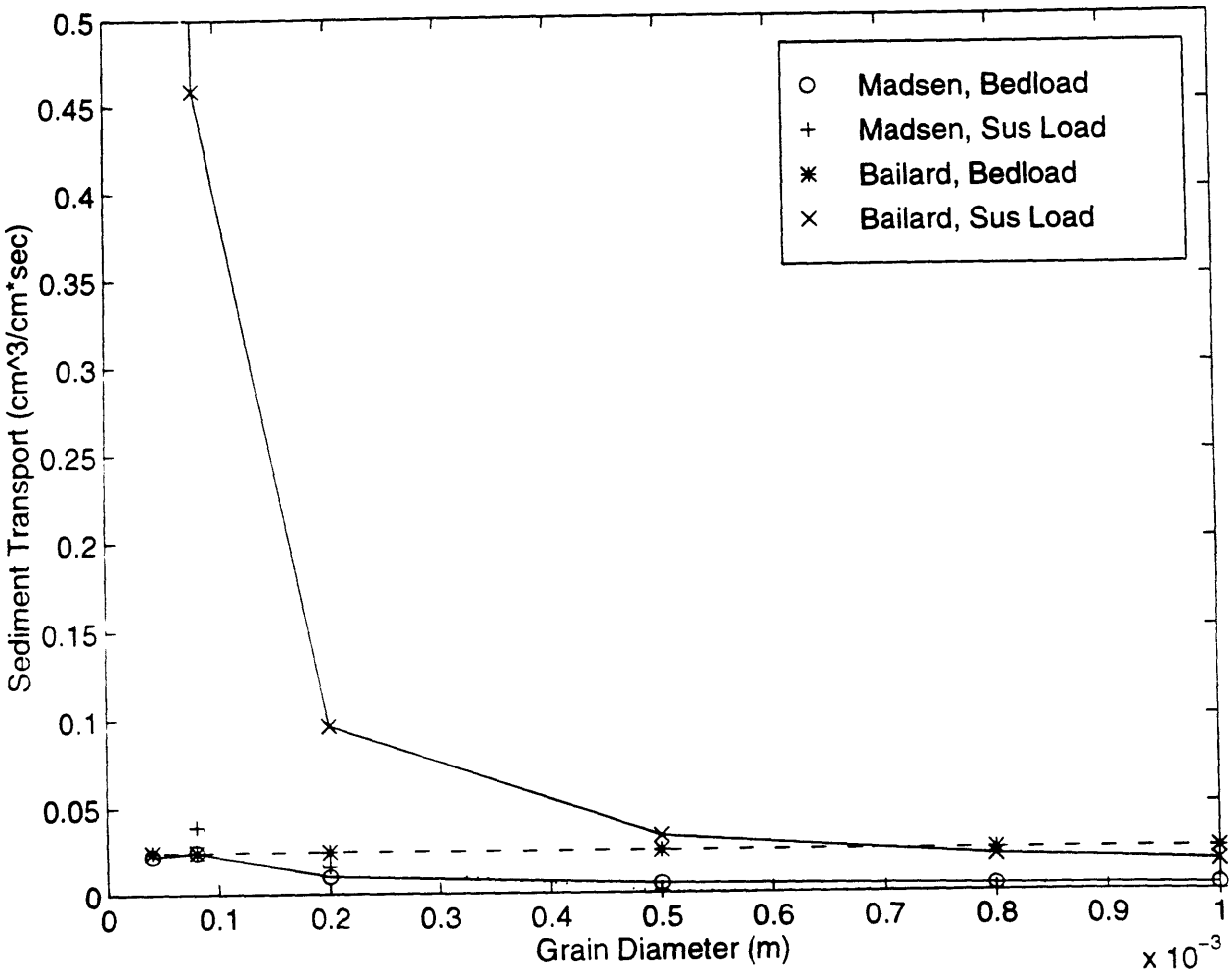

Figure 21. Break down of the total sediment transport rate versus sediment diameter for a wave period of 16 sec, an average current and a maximum wave orbital velocity of 0.35 m/sec.

Table 6

Bedload and Suspended Load Versus Grain Size and Wave Period, $U_c = U_o = 0.35$ m/sec.

Case #	Period (sec)	d (mm)	Madsen Bedload (m^3/m*sec)	Madsen Sus Load (m^3/m*sec)	Bailard Bedload (m^3/m*sec)	Bailard Sus Load (m^3/m*sec)
1	4	0.04	2.14035E-06	0.000141333	2.46659E-06	0.000183587
2	4	0.08	2.37879E-06	4.93625E-06	2.46659E-06	4.58968E-05
3	4	0.2	1.21492E-06	5.16284E-08	2.46659E-06	9.6494E-06
4	4	0.5	4.63448E-07	8.27897E-08	2.46659E-06	3.28539E-06
5	4	0.8	3.35356E-07	2.46935E-08	2.46659E-06	2.10003E-06
6	4	1	2.69041E-07	9.90478E-09	2.46659E-06	1.72181E-06
7	8	0.04	2.21481E-06	0.000123145	2.46659E-06	0.000183587
8	8	0.08	2.44383E-06	4.41838E-06	2.46659E-06	4.58968E-05
9	8	0.2	1.05512E-06	9.72879E-07	2.46659E-06	9.6494E-06
10	8	0.5	4.74756E-07	7.67927E-08	2.46659E-06	3.28539E-06
11	8	0.8	3.48361E-07	1.31331E-08	2.46659E-06	2.10003E-06
12	8	1	2.89334E-07	0	2.46659E-06	1.72181E-06
13	16	0.04	2.25417E-06	0.000107687	2.46659E-06	0.000183587
14	16	0.08	2.46922E-06	3.89335E-06	2.46659E-06	4.58968E-05
15	16	0.2	1.02252E-06	1.60811E-06	2.46659E-06	9.6494E-06
16	16	0.5	5.39857E-07	7.16153E-08	2.46659E-06	3.28539E-06
17	16	0.8	4.11759E-07	0	2.46659E-06	2.10003E-06
18	16	1	3.94061E-07	0	2.46659E-06	1.72181E-06
19	4	0.1	2.4675E-06	8.74873E-07	2.46659E-06	3.88477E-05
20	6	0.1	2.5091E-06	8.38065E-07	2.46659E-06	3.88477E-05
21	8	0.1	2.52852E-06	8.07217E-07	2.46659E-06	3.88477E-05
22	10	0.1	2.53865E-06	7.8104E-07	2.46659E-06	3.88477E-05
23	12	0.1	2.54412E-06	7.58404E-07	2.46659E-06	3.88477E-05
24	14	0.1	1.96115E-06	4.99413E-07	2.46659E-06	3.88477E-05
25	16	0.1	2.01191E-06	5.28575E-07	2.46659E-06	3.88477E-05
26	18	0.1	2.01191E-06	5.28575E-07	2.46659E-06	3.88477E-05
27	4	0.2	1.21492E-06	5.16284E-08	2.46659E-06	1.03993E-05
28	6	0.2	1.13006E-06	4.76347E-07	2.46659E-06	1.03993E-05
29	8	0.2	1.08961E-06	7.63998E-07	2.46659E-06	1.03993E-05
30	10	0.2	1.06853E-06	1.37968E-06	2.46659E-06	1.03993E-05
31	12	0.2	1.05774E-06	1.58136E-06	2.46659E-06	1.03993E-05
32	14	0.2	1.05312E-06	1.78224E-06	2.46659E-06	1.03993E-05
33	16	0.2	1.05249E-06	1.98217E-06	2.46659E-06	1.03993E-05
34	18	0.2	1.05458E-06	2.18097E-06	2.46659E-06	1.03993E-05
35	4	0.5	4.63448E-07	8.27897E-08	2.46659E-06	3.28539E-06
36	6	0.5	4.64542E-07	7.92578E-08	2.46659E-06	3.28539E-06
37	8	0.5	4.74756E-07	7.67927E-08	2.46659E-06	3.28539E-06
38	10	0.5	4.88759E-07	7.49882E-08	2.46659E-06	3.28539E-06
39	12	0.5	5.04728E-07	7.36057E-08	2.46659E-06	3.28539E-06
40	14	0.5	5.21887E-07	7.25089E-08	2.46659E-06	3.28539E-06
41	16	0.5	5.39857E-07	7.16153E-08	2.46659E-06	3.28539E-06
42	18	0.5	5.58437E-07	7.08726E-08	2.46659E-06	3.28539E-06

The next analysis is an examination of how the sediment transport varies with wave period. Figures 22 through 24 on pages 79 through 81 plot the total sediment transport rate versus period for the three models studied. Table 5 on page contains the output of these runs. The current velocity and maximum orbital wave velocity were both held constant at 0.35 m/sec. Figure 22 plots the transport for a sediment having a diameter equal to 0.1 mm, figure 23 plots the transport for 0.2 mm and figure 24 plots the transport for 0.5 mm sediment (these are the same sizes examined for the steady unidirectional flow).

Since the Bailard model does not depend on wave period, transport versus wave period for every sediment examined is flat. The Bailard model predicts no change in transport when the wave period is changed. For the 0.1 mm sediment, the Ackers and White model and the Madsen model predict a very similar occurrence: transport varies little with wave period. For the other two grain sizes, however, the Ackers and White model and the Madsen model diverge. For the larger two sediments, the Madsen model predicts that transport increases slightly with increasing wave period, while the Ackers and White model predicts that transport decreases with increasing wave period.

It appears from these results that the Bailard model is more accurate than at least one of these models for assuming that transport does not depend on wave period. Figures 30 through 32 on pages 82 through 84, which break down the total sediment transport rate versus period into a bedload and a suspended load for the Bailard and Madsen models, provide some insight into the predictions made by the Madsen model. Table 6 on page 77 contains the output of these runs. The figures show that when the Madsen model predicts a positive correlation between transport and wave period, it is the suspended load that is greatly changing with wave period while the bedload remains relatively unchanged. When the wave period increases, this allows the wave boundary

layer to also increase, which leads to an increased shear velocity and shear stress. This allows the wave to scour more of the bottom and therefore produce a larger suspended load transport, which is exactly what the Madsen model predicts.

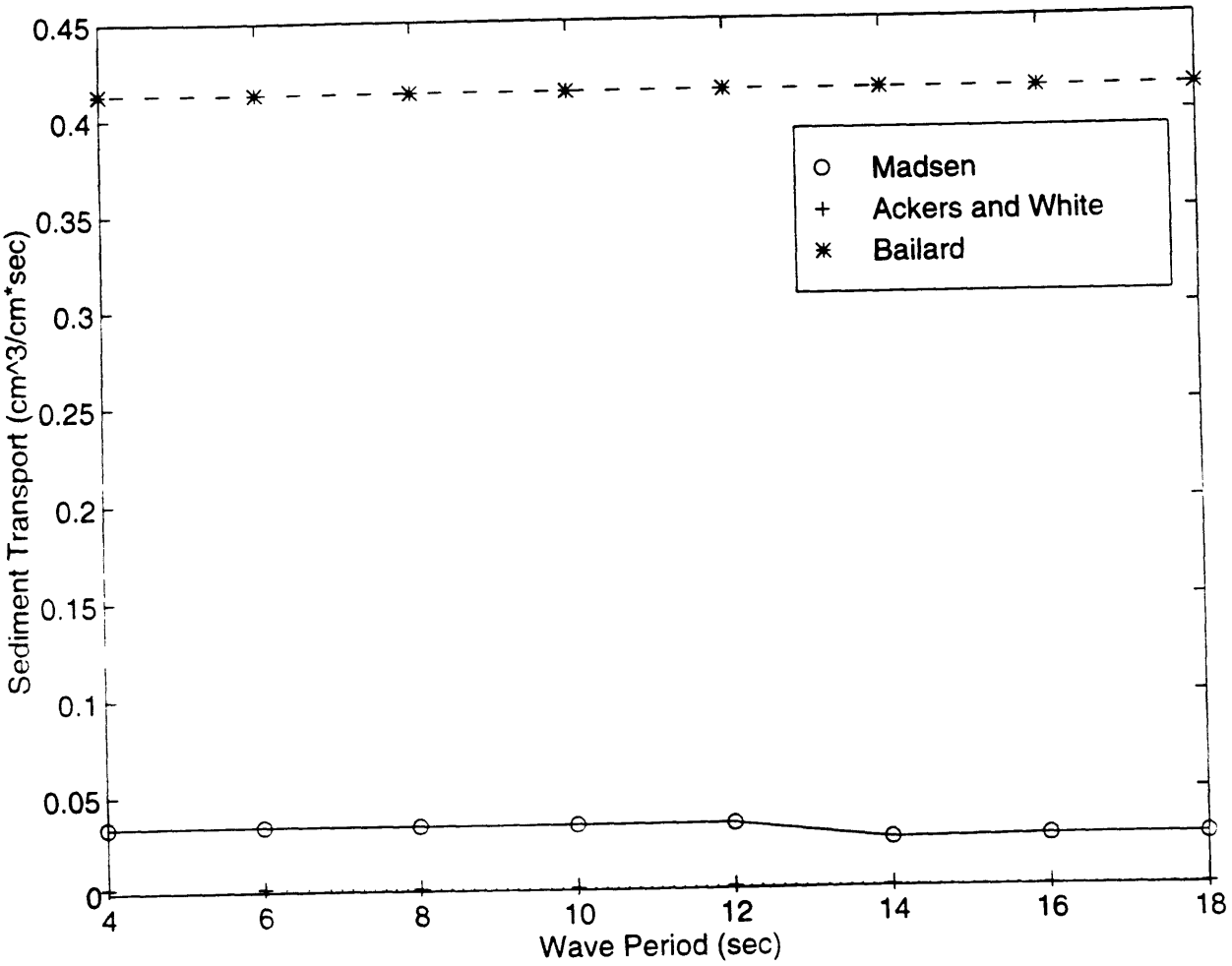

Figure 22. The total sediment transport rate versus wave period, for 0.1 mm diameter sediment, an average current velocity of 0.35 m/sec and a maximum wave orbital velocity of 0.35 m/sec.

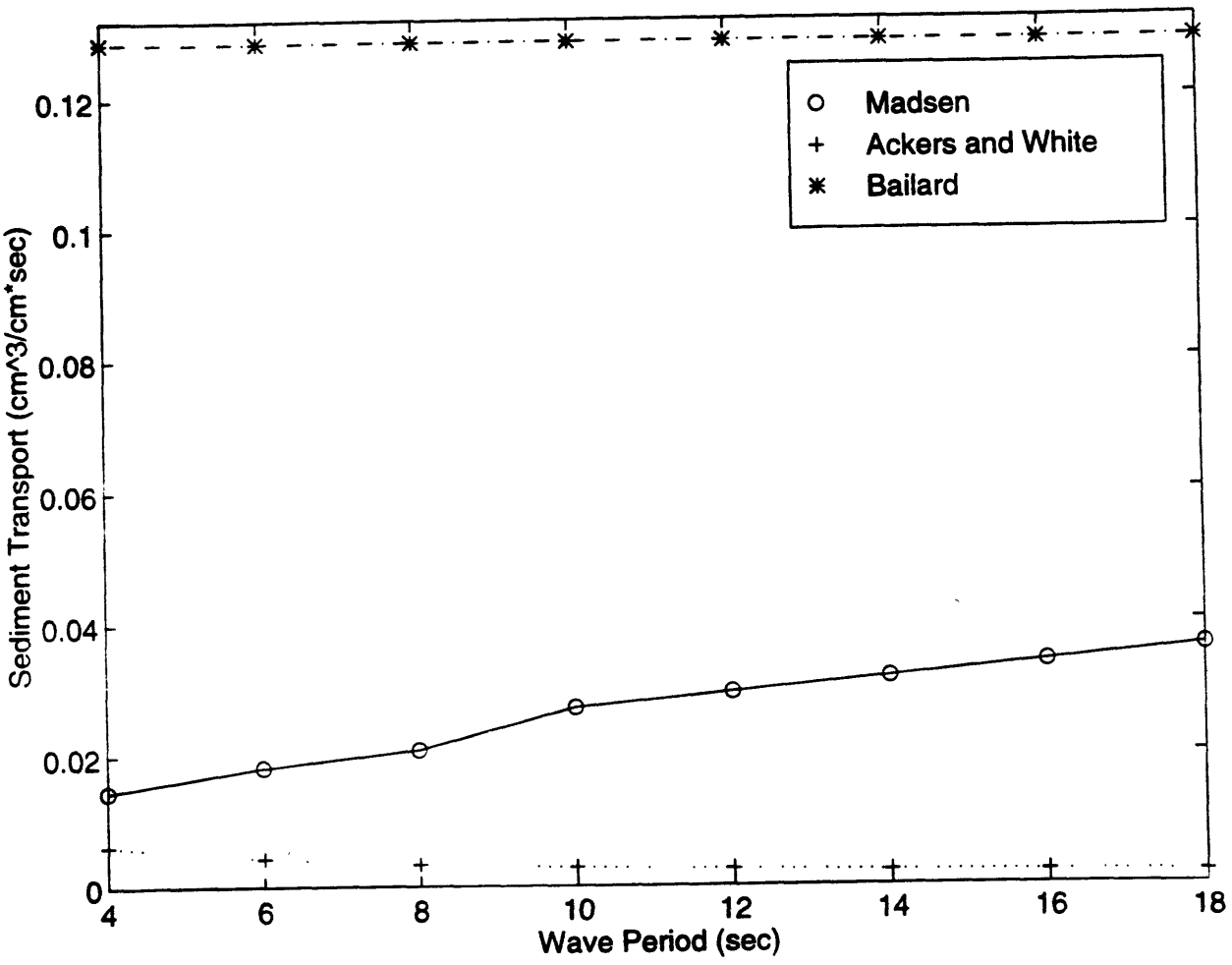

Figure 23. The total sediment transport rate versus wave period, for 0.2 mm diameter sediment, an average current velocity of 0.35 m/sec and a maximum wave orbital velocity of 0.35 m/sec.

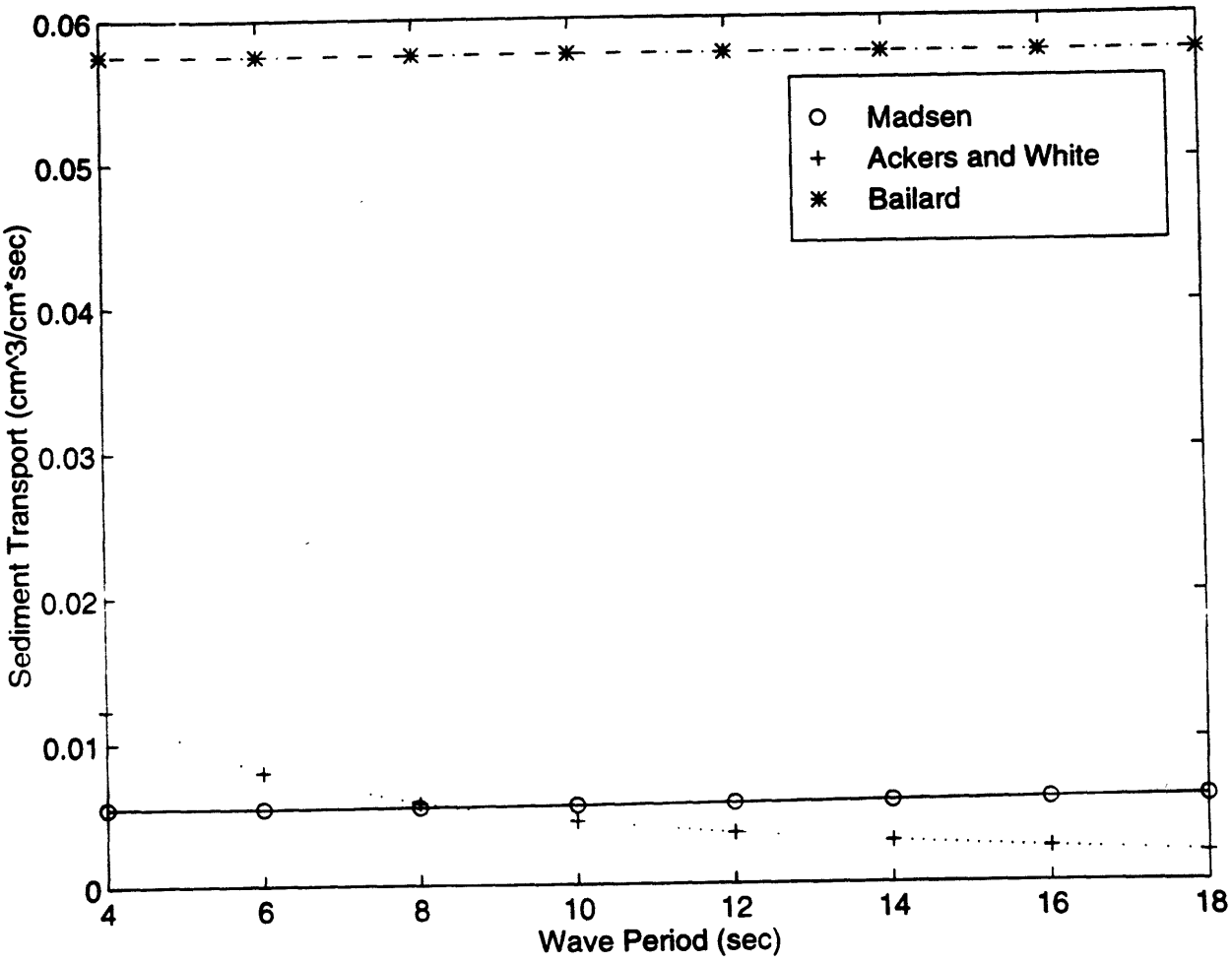

Figure 24. The total sediment transport rate versus wave period, for 0.5 mm diameter sediment, an average current velocity of 0.35 m/sec and a maximum wave orbital velocity of 0.35 m/sec.

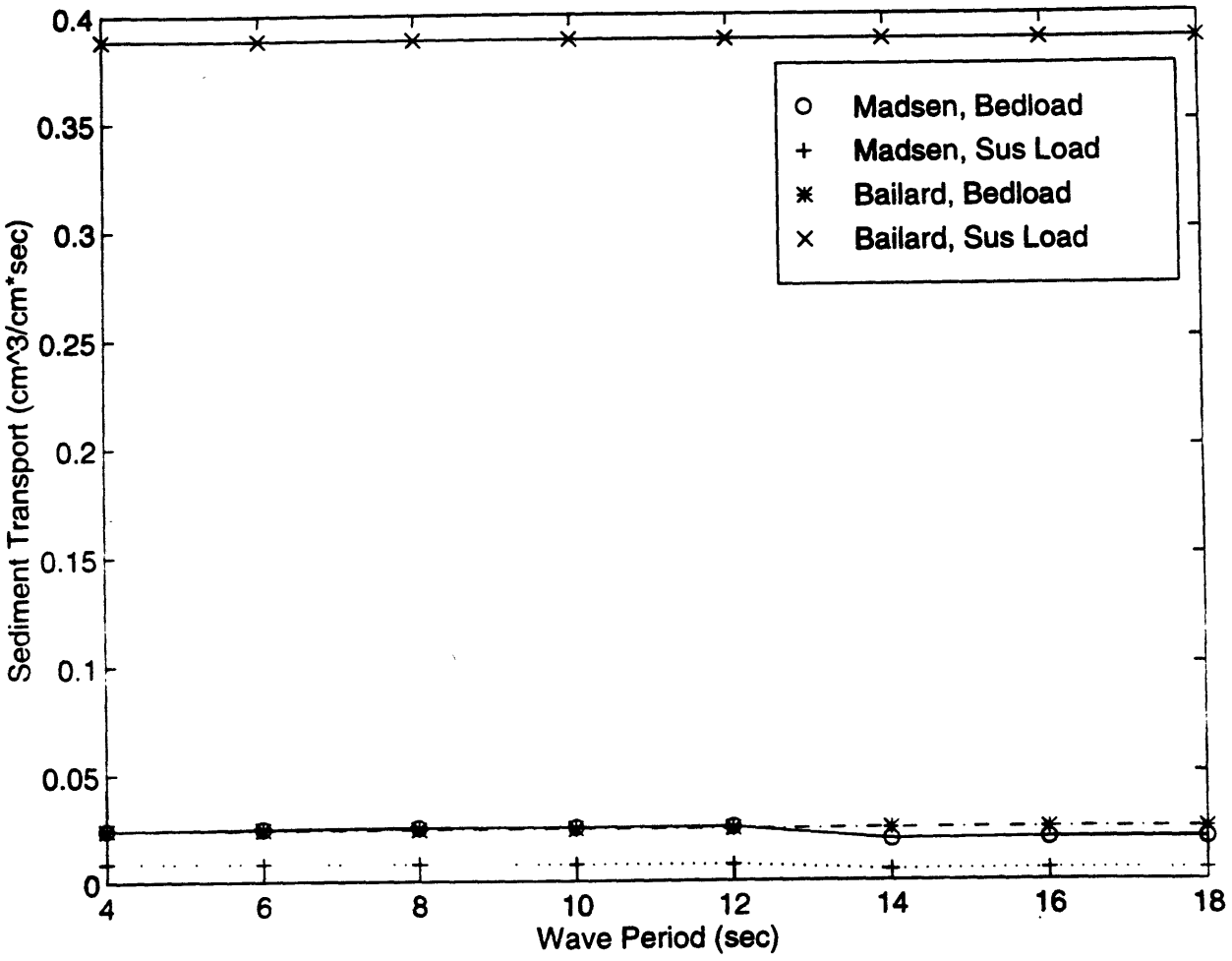

Figure 25. Break down of the total sediment transport rate versus wave period for 0.1 mm diameter sediment, an average current and a maximum wave orbital velocity of 0.35 m/sec.

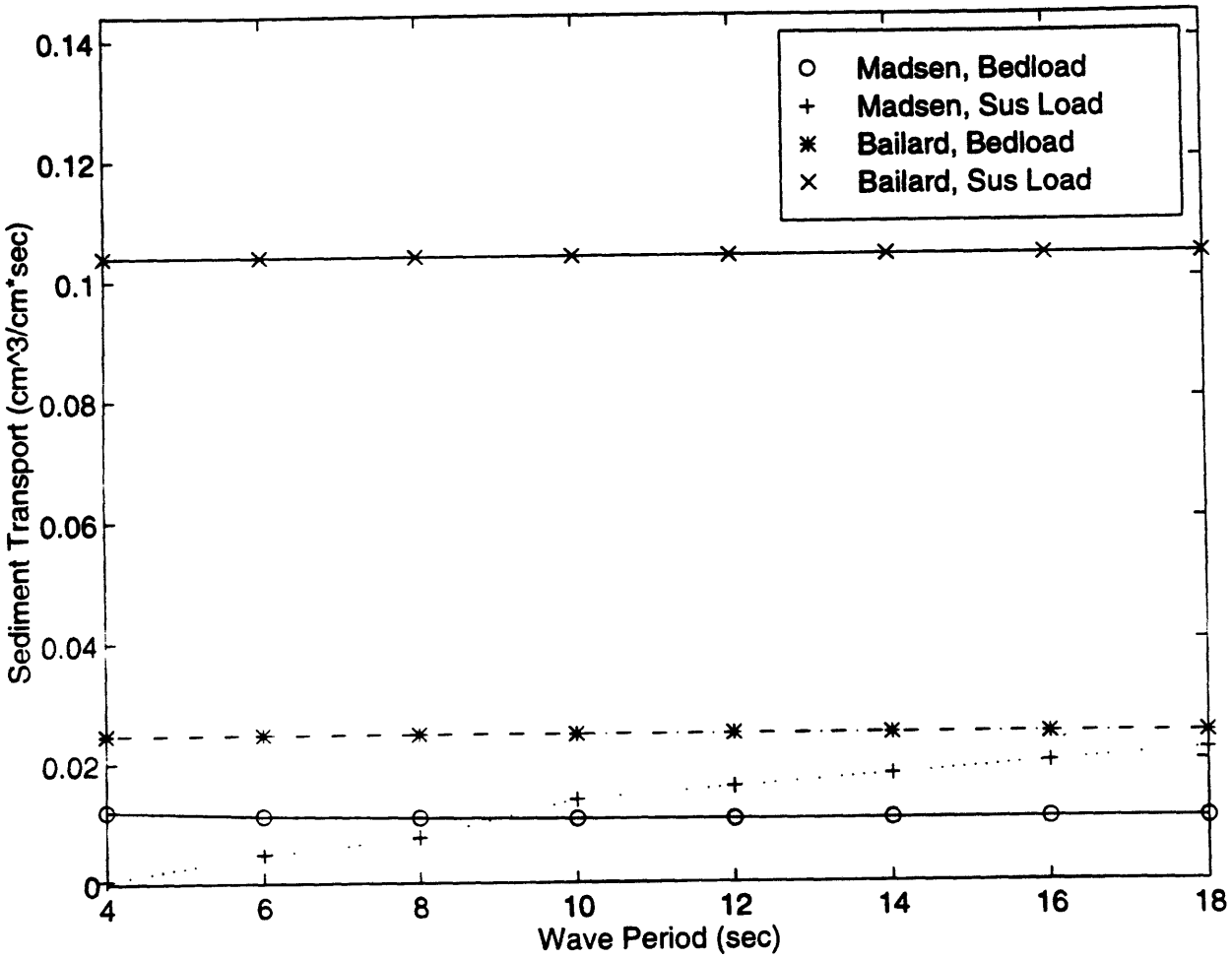

Figure 26. Break down of the total sediment transport rate versus wave period for 0.2 mm diameter sediment, an average current and a maximum wave orbital velocity of 0.35 m/sec.

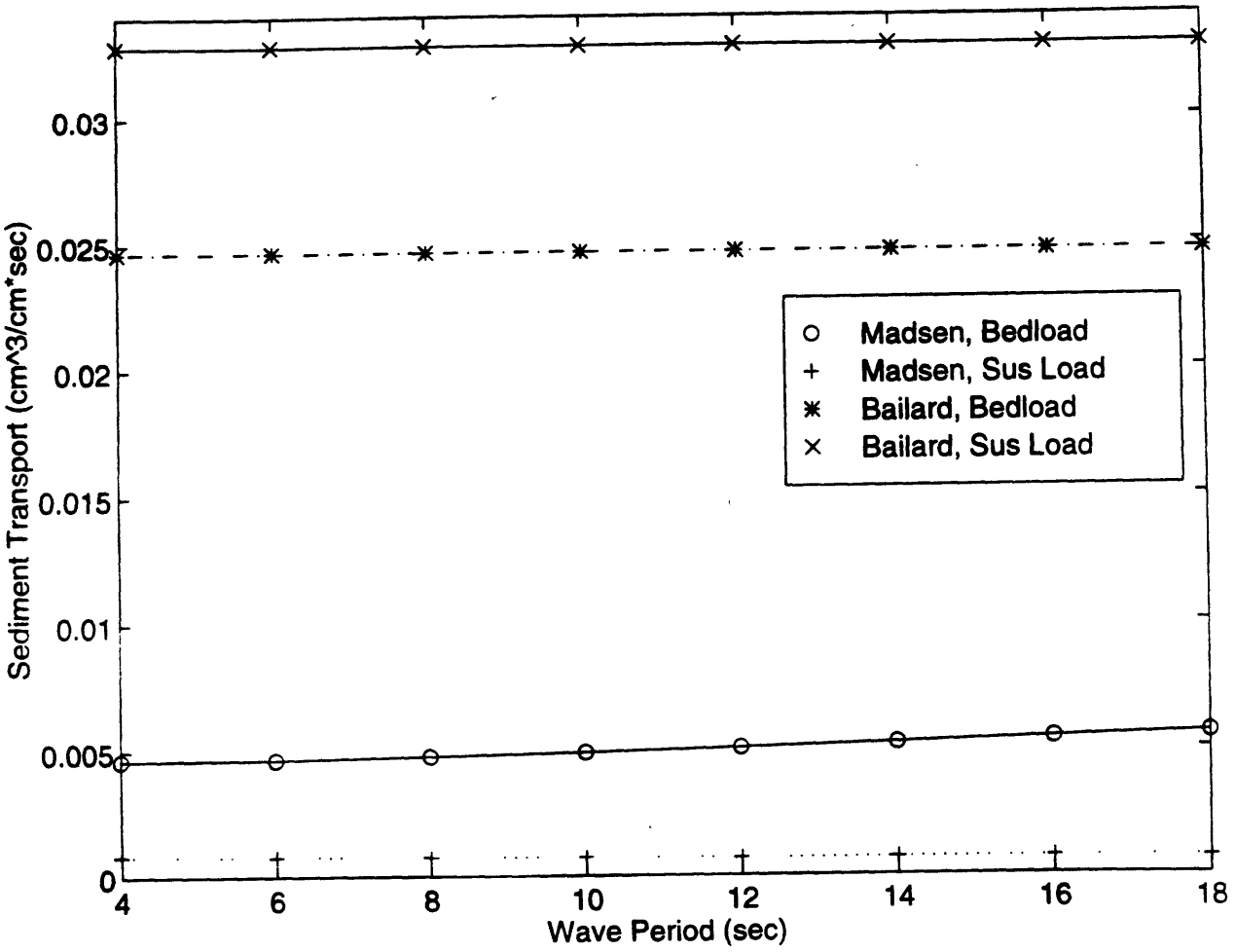

Figure 27. Break down of the total sediment transport rate versus wave period for 0.5 mm diameter sediment, an average current and a maximum wave orbital velocity of 0.35 m/sec.

The bedload, however, is not as affected by the wave period. The total shear velocity does not necessarily increase, and therefore the bedload does not necessarily increase. The larger wave boundary layer is compensated for by the fact that the wave friction factor decreases with increasing period (because the friction factor is related to angular frequency, which decreases with increasing wave period). Therefore, when bedload plays a larger role in the transport, as is the case for larger sediments (0.5 mm), the transport is less dependent on the wave period. This appears to be contradicted by the fact that the flattest Madsen curve occurs for the smallest grain size examined, the 0.1 mm diameter sediment. Suspended load usually dominates for small sediment, especially when ripples are present. Table 5, reveals that there are no ripples in this case because the flow is strong enough to completely wash them away (condition 2 indicates sheet flow while condition 3 indicates flow over ripples). The Madsen model predicts that bedforms begin as soon as transport starts and grow until a certain stage is reached where the flow begins to break the ripples down, and when the flow is strong enough, the ripples are eroded completely (this is referred to as sheet flow). Suspended load transport increases with the flow while ripples are present because the increased roughness enables more sediment to be held in suspension. However, when the ripples are eroded the roughness is decreased, and while bedload greatly increases at this stage, suspended load greatly decreases. Since sheet flow is occurring for this run (figure 25), the suspended load is less than the bedload and therefore the fact that transport does not vary with period at this grain size supports the assumption that suspended load transport, and not bedload transport, should vary with the wave period.

The Ackers and White prediction of decreased transport with increasing wave period is more pronounced the larger the grain size becomes. The reason can be traced to the Scheffner modification of the Ackers and White model. From equations 52 and 53 it is obvious that the

wave orbital excursion amplitude (A_o) increases with increasing wave period. This causes the bottom friction coefficient (f_w) to also go down. Since calculating ξ is dependent on f_w and C_z, which does not change, this leads to a smaller U_{wc} with increased period, and since this new velocity is what is used to calculate the total shear stress, and ultimately the total transport, increasing the period therefore leads to a decreased transport rate. The reason why the effect is magnified with increasing grain diameter is because sand grain diameter is used in the calculation of the bottom friction coefficient and a larger grain diameter increases the effect of the orbital excursion amplitude on the calculation of f_w. Since the Ackers and White model does not specifically account for a suspended load and the effects of increasing the wave boundary layer, it will always predict a decreased transport for an increased wave period.

The last thing that needs to be determined is the effect of the flow velocity on sediment transport. If the pattern follows that of the steady unidirectional flow, it can be expected that sediment transport will rise sharply with increasing flow conditions. Figures 28 through 30 (pages 87 through 89) plot the total sediment transport versus the maximum orbital wave velocity. These figures plot the transport for grain diameters of 0.1 mm, 0.2 mm, and 0.5 mm, and a wave period 8 seconds. Table 7 on page 90 contains the output of these runs. The current velocity is held constant at 0.35 m/sec. As expected, the Bailard model predicts the largest transport for the lower orbital velocities, adhering to the pattern of predicting the most transport when there is a low flow rate. This can still be attributed to the fact that the Bailard model does not incorporate a critical parameter that must be overcome in order for transport to begin.

Another similarity between the combined flow results and the results obtained from the steady unidirectional flow is the large dependency that the Ackers and White model has on flow velocities. Since this model is essentially unchanged from the steady flow model, increasing the

wave orbital velocity has the same effect as increasing the current velocity for the steady unidirectional flow: the transport begins to increase exponentially at the higher flow velocities.

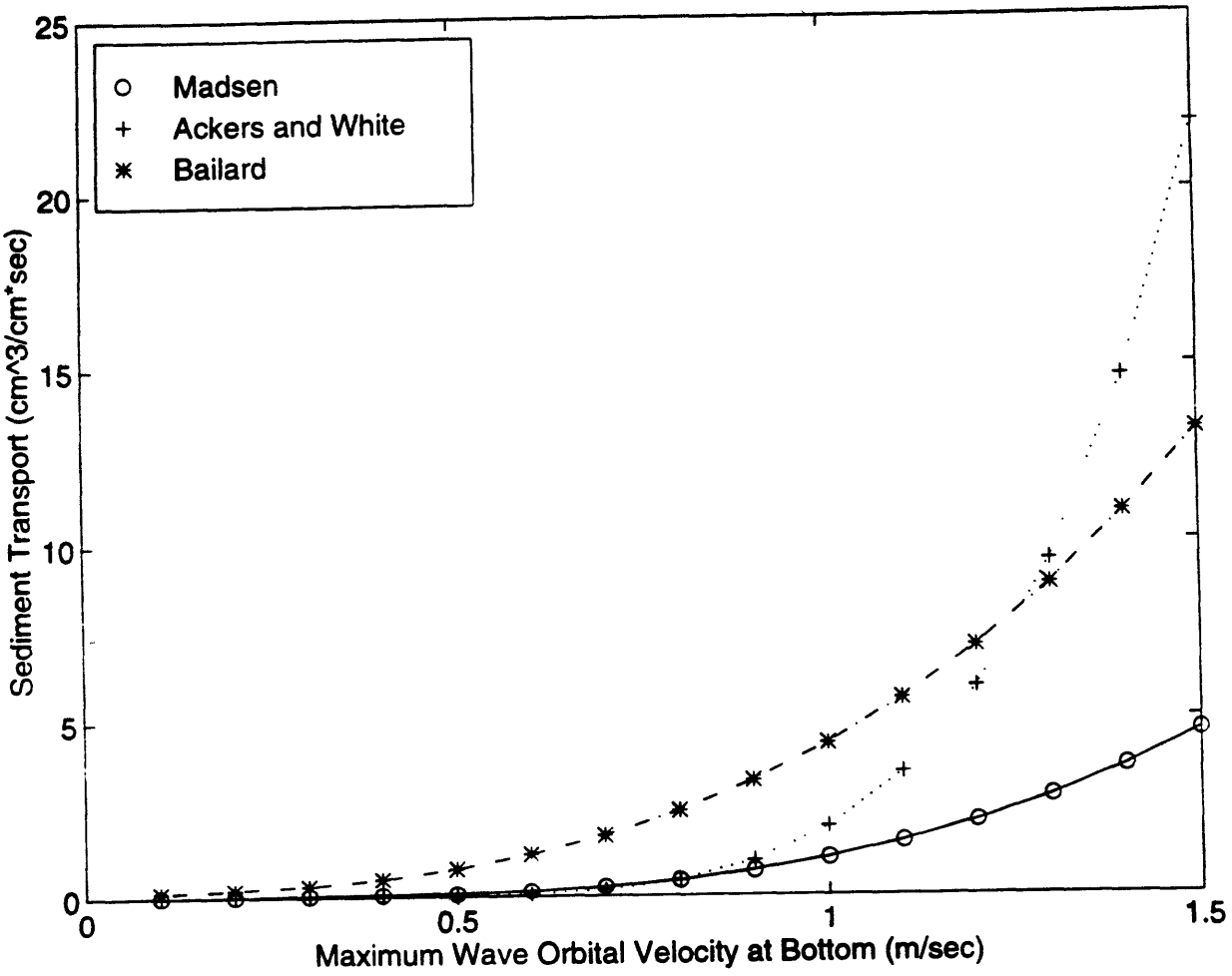

Figure 28. The total sediment transport rate versus maximum wave orbital velocity for a wave period of 8 sec, 0.1 mm diameter sediment, and an average current velocity of 0.35 m/sec.

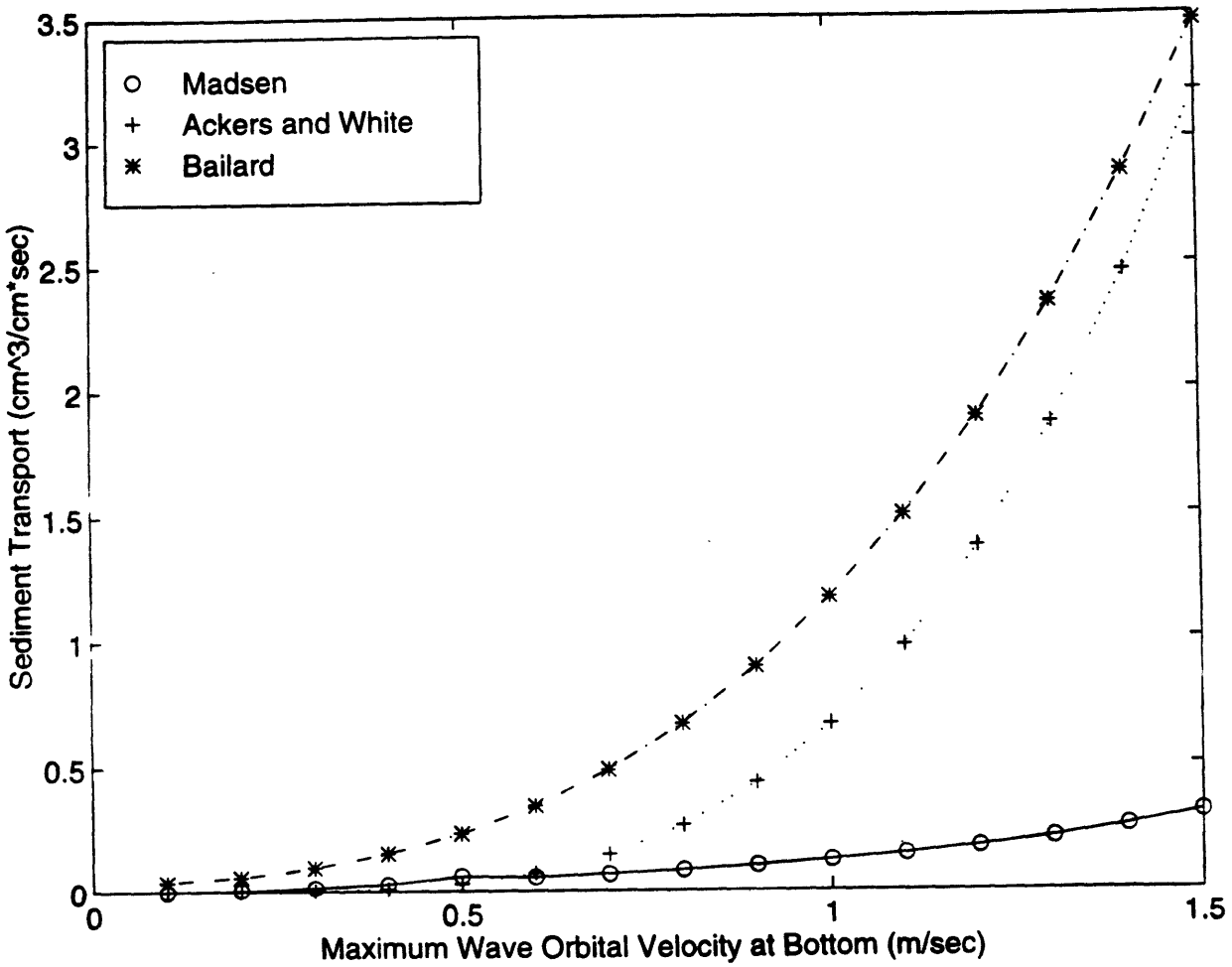

Figure 29. The total sediment transport rate versus maximum wave orbital velocity for a wave period of 8 sec, 0.2 mm diameter sediment, and an average current velocity of 0.35 m/sec.

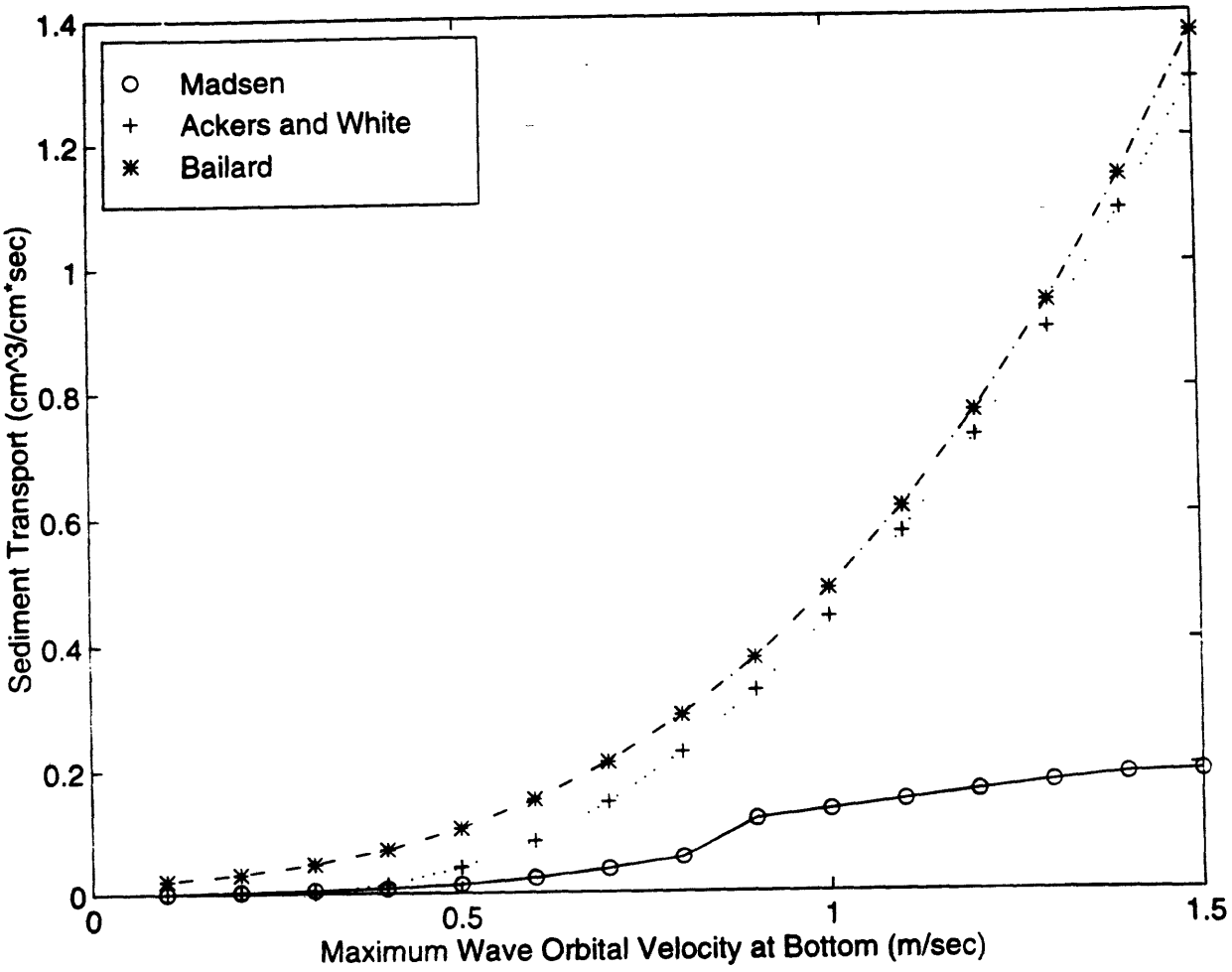

Figure 30. The total sediment transport rate versus maximum wave orbital velocity for a wave period of 8 sec, 0.5 mm diameter sediment, and an average current velocity of 0.35 m/sec.

Table 7

Total Sediment Transport vs. Wave Orbital Velocity and Sediment Diameter, U_c = 0.35 m/sec.

Case #	Period (sec)	d (mm)	Madsen Total Load (m^3/m*sec)	Madsen Condition 3 = ripples 2 = sheet flow	Ackers & White Total Load (m^3/m*sec)	Bailard Total Load (m^3/m*sec)
1	4	0.04	0.000143528	2	3.95756E-08	0.000186054
2	4	0.08	7.35993E-06	2	1.52032E-07	4.83634E-05
3	4	0.2	1.4559E-06	3	6.81757E-07	1.2116E-05
4	4	0.5	5.49465E-07	3	1.2349E-06	5.75197E-06
5	4	0.8	3.59988E-07	3	9.31671E-07	4.56662E-06
6	4	1	2.78829E-07	3	6.35335E-07	4.18839E-06
7	8	0.04	0.000125456	2	1.47927E-08	0.000186054
8	8	0.08	6.94393E-06	2	7.49561E-08	4.83634E-05
9	8	0.2	2.23655E-06	3	3.81911E-07	1.2116E-05
10	8	0.5	5.47954E-07	3	5.79413E-07	5.75197E-06
11	8	0.8	3.63094E-07	3	2.58447E-07	4.56662E-06
12	8	1.0	2.92533E-07	3	6.73853E-08	4.18839E-06
13	16	0.04	0.000110108	2	6.22399E-09	0.000186054
14	16	0.08	6.50454E-06	2	3.98971E-08	4.83634E-05
15	16	0.2	2.94676E-06	3	2.22257E-07	1.2116E-05
16	16	0.5	5.8696E-07	3	2.46562E-07	5.75197E-06
17	16	0.8	4.24741E-07	3	1.64039E-08	4.56662E-06
18	16	1	4.10054E-07	3	0	4.18839E-06
19	4	0.1	3.38438E-06	2	2.31059E-07	4.13143E-05
20	6	0.1	3.40848E-06	2	1.56284E-07	4.13143E-05
21	8	0.1	3.41416E-06	2	1.20138E-07	4.13143E-05
22	10	0.1	3.41391E-06	2	9.87458E-08	4.13143E-05
23	12	0.1	3.4116E-06	2	8.45485E-08	4.13143E-05
24	14	0.1	2.56442E-06	2	7.44043E-08	4.13143E-05
25	16	0.1	2.65667E-06	2	6.67721E-08	4.13143E-05
26	18	0.1	2.65667E-06	2	6.08071E-08	4.13143E-05
27	4	0.2	1.4559E-06	3	6.38784E-07	1.28659E-05
28	6	0.2	1.82362E-06	3	4.52606E-07	1.28659E-05
29	8	0.2	2.07997E-06	3	3.5753E-07	1.28659E-05
30	10	0.2	2.70756E-06	3	2.99205E-07	1.28659E-05
31	12	0.2	2.93012E-06	3	2.59479E-07	1.28659E-05
32	14	0.2	3.1565E-06	3	2.30521E-07	1.28659E-05
33	16	0.2	3.38486E-06	3	2.08383E-07	1.28659E-05
34	18	0.2	3.61406E-06	3	1.90852E-07	1.28659E-05
35	4	0.5	5.49465E-07	3	1.2349E-06	5.75197E-06
36	6	0.5	5.44256E-07	3	8.00147E-07	5.75197E-06
37	8	0.5	5.47954E-07	3	5.79413E-07	5.75197E-06
38	10	0.5	5.55533E-07	3	4.4613E-07	5.75197E-06
39	12	0.5	5.65084E-07	3	3.5719E-07	5.75197E-06
40	14	0.5	5.75717E-07	3	2.93831E-07	5.75197E-06
41	16	0.5	5.8696E-07	3	2.46562E-07	5.75197E-06
42	18	0.5	5.98538E-07	3	2.10066E-07	5.75197E-06

There is a difference, however, when one looks at the predictions made by the Madsen model: it no longer predicts the largest transport for the finest sediment as it had done in the steady unidirectional flow. According to the Madsen model, the combined wave-current flow is quite different from the steady unidirectional case, and increasing the maximum orbital velocity does not produce the same effect as increasing the average current velocity in a stream or river.

Waves, though important for initiating sediment transport and bedload, are more important for influencing the suspended load. When the wave velocity is increased, more and more sediment will be put into suspension, but unless the sediment is coarse, the relative effect on bedload will be small, and even though currents have the same effect on fine sediment, it is not as pronounced. Figures 31 through 33 (pages 92 through 94) break down the total transport given by figures 28 through 30 into a bedload transport and suspended load transport for the Bailard model and the Madsen model. Table 8 on page 95 contains the output from these runs. This breakdown reveals the usual trend: suspended load dominates for the small sediment. There is an interesting difference, however, when the sediment is coarser. As the bedload and suspended load increase with orbital velocity, there is a sudden hitch in the Madsen prediction, and the suspended load actually decreases as the bedload jumps up rapidly. There is a physical explanation for this phenomenon: it represents the onset of sheet flow, when the bedforms are entirely eroded off of the bottom. Figure 33 clearly shows when this happens, at a wave orbital velocity of about 0.9 m/sec. When this happens, the bedload increases greatly as the suspended load decreases because of the decreased roughness. In real life, however, this transition is smoother than it is portrayed in the model, which is why it appears so abruptly in the plots. After sheet flow has occurred, the bedload predictions of the Madsen model and the Bailard become much closer in magnitude.

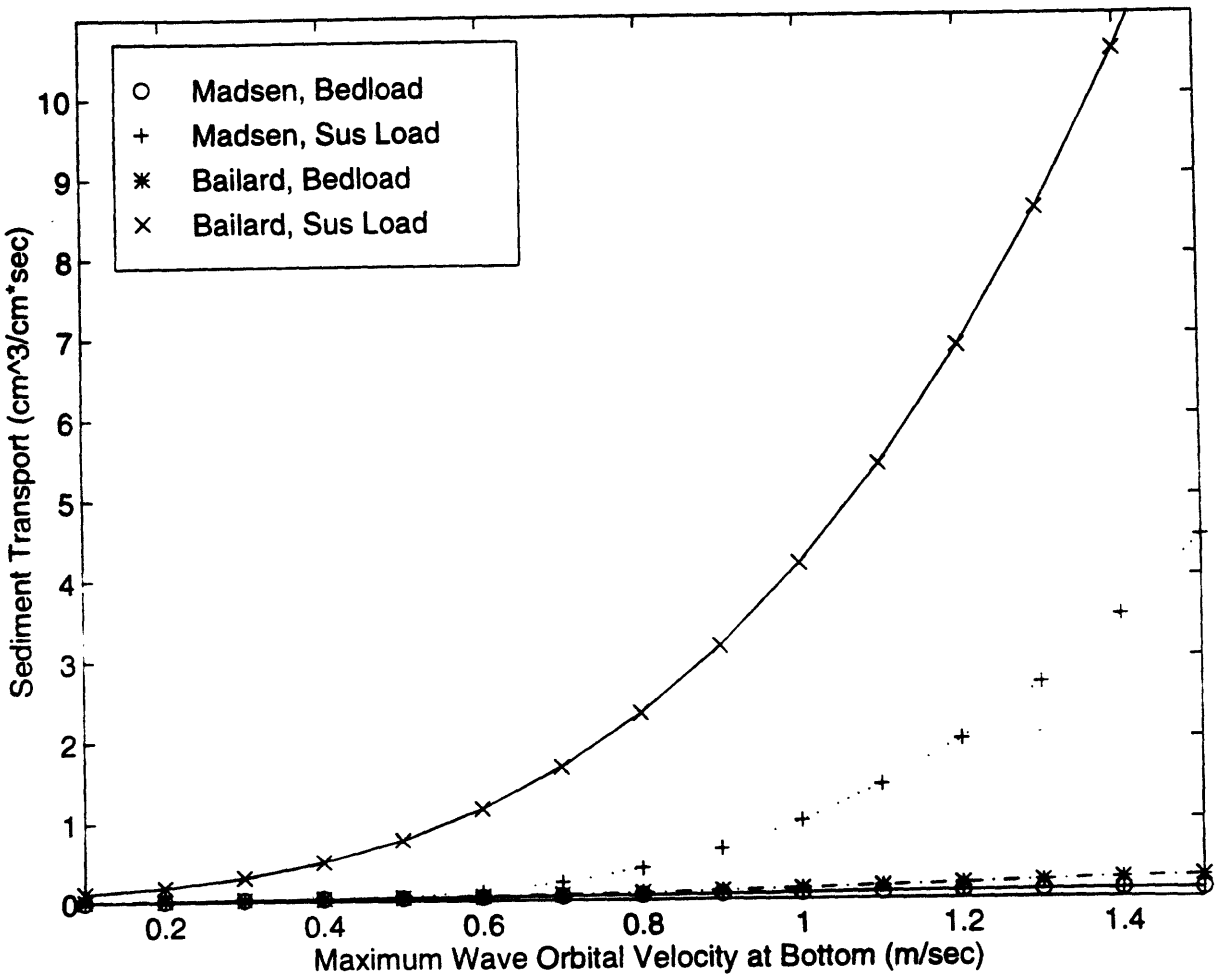

Figure 31. Break down of the sediment transport rate versus maximum wave orbital velocity for a wave period of 8 sec, 0.1 mm diameter sediment, and an average current velocity of 0.35 m/sec.

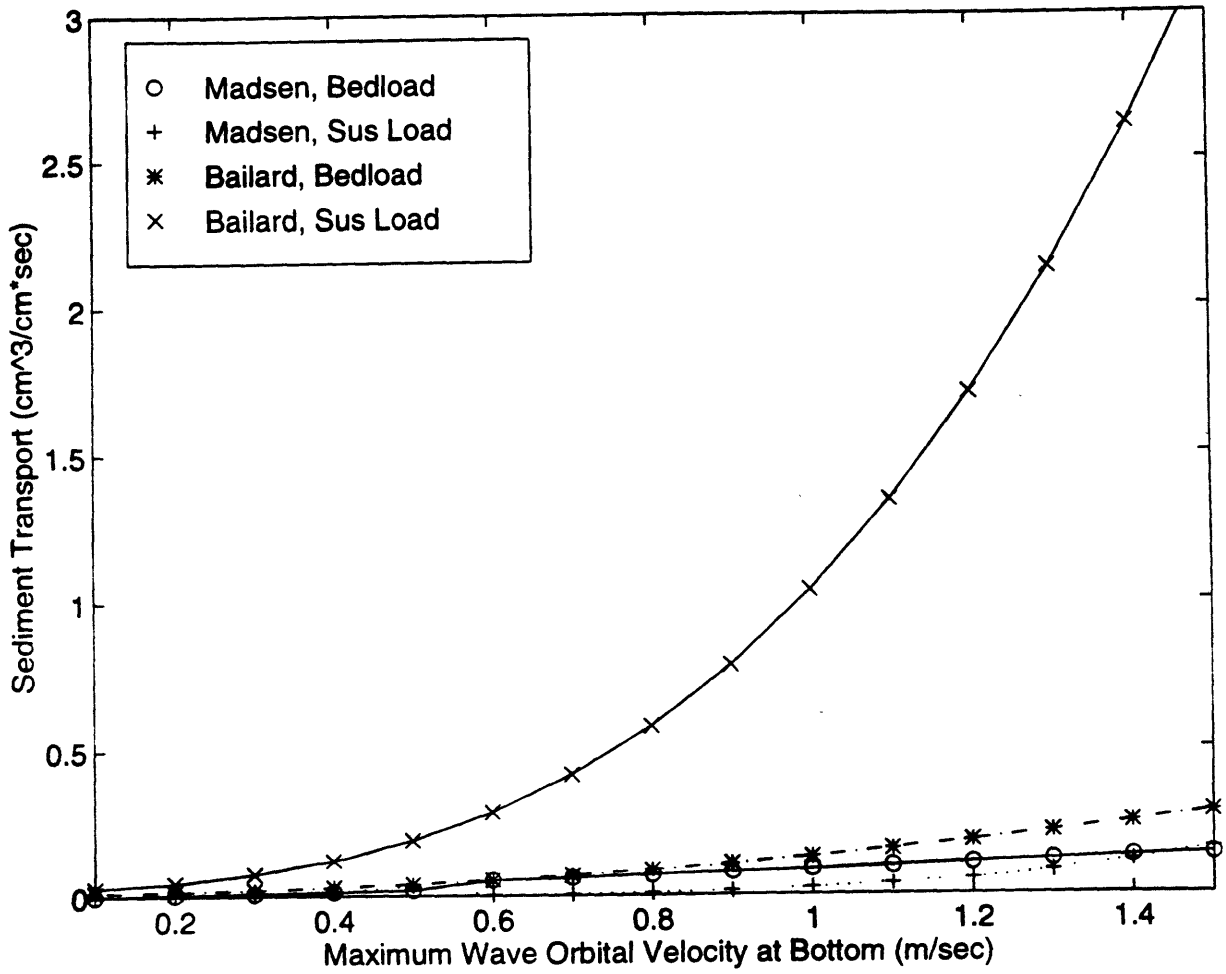

Figure 32. Break down of the sediment transport rate versus maximum wave orbital velocity for a wave period of 8 sec, 0.2 mm diameter sediment, and an average current velocity of 0.35 m/sec.

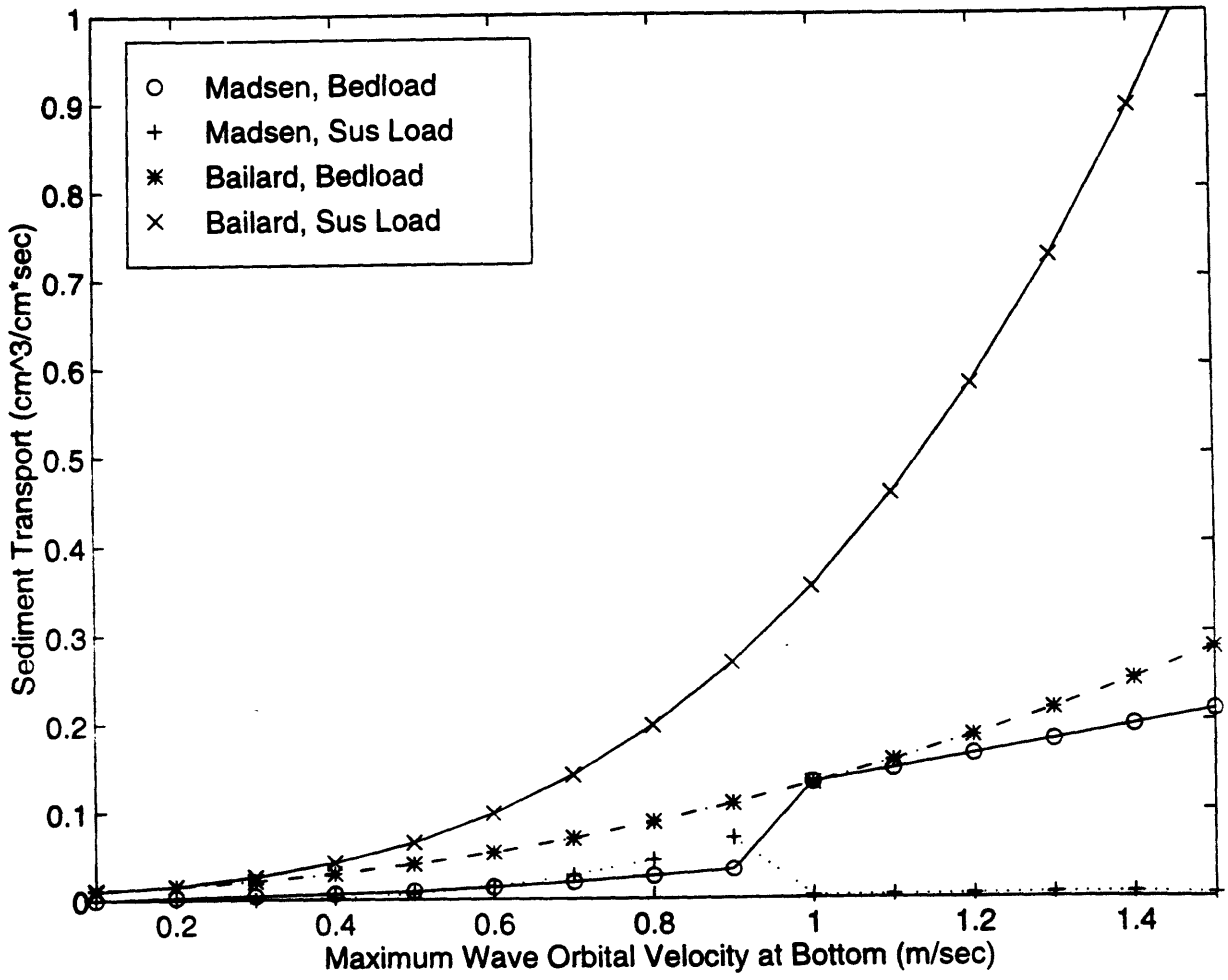

Figure 33. Break down of the sediment transport rate versus maximum wave orbital velocity for a wave period of 8 sec, 0.5 mm diameter sediment, and an average current velocity of 0.35 m/sec.

Table 8

Break Down of the Transport vs. Wave Orbital Velocity and Sediment Diameter, U_c=.35m/sec.

Case #	Uo (m/sec)	d (mm)	Madsen Bedload (m^3/m*sec)	Madsen Sus Load (m^3/m*sec)	Bailard Bedload (m^3/m*sec)	Bailard Sus Load (m^3/m*sec)
1	0.1	0.1	0	0	1.10745E-06	1.10762E-05
2	0.2	0.1	6.98782E-07	0	1.46988E-06	1.79328E-05
3	0.3	0.1	2.2269E-06	3.37898E-07	2.07395E-06	3.02479E-05
4	0.4	0.1	2.83575E-06	1.60845E-06	2.91963E-06	4.93525E-05
5	0.5	0.1	3.46528E-06	4.72226E-06	4.00694E-06	7.70516E-05
6	0.6	0.1	4.16787E-06	1.08653E-05	5.33588E-06	0.00011537
7	0.7	0.1	4.90071E-06	2.13598E-05	6.90644E-06	0.000166386
8	0.8	0.1	5.64975E-06	3.76011E-05	8.71863E-06	0.000232192
9	0.9	0.1	6.41226E-06	6.10027E-05	1.07724E-05	0.000314891
10	1	0.1	7.18606E-06	9.29556E-05	1.30679E-05	0.000416587
11	1.1	0.1	7.96941E-06	0.000134804	1.56049E-05	0.000539387
12	1.2	0.1	8.76092E-06	0.000187833	1.83836E-05	0.000685397
13	1.3	0.1	9.55946E-06	0.000253258	2.14039E-05	0.000856725
14	1.4	0.1	1.03641E-05	0.000332227	2.46659E-05	0.001055482
15	1.5	0.1	1.11742E-05	0.000425817	2.81694E-05	0.001283774
16	0.1	0.2	0	0	1.10745E-06	2.75123E-06
17	0.2	0.2	3.92616E-07	0	1.46988E-06	4.45433E-06
18	0.3	0.2	8.06767E-07	4.41185E-07	2.07395E-06	7.5133E-06
19	0.4	0.2	1.32843E-06	1.10218E-06	2.91963E-06	1.22587E-05
20	0.5	0.2	1.9466E-06	3.46647E-06	4.00694E-06	1.91389E-05
21	0.6	0.2	5.2437E-06	2.3175E-07	5.33588E-06	2.86569E-05
22	0.7	0.2	6.14259E-06	4.56838E-07	6.90644E-06	4.13286E-05
23	0.8	0.2	7.05772E-06	6.99221E-07	8.71863E-06	5.76744E-05
24	0.9	0.2	7.98596E-06	1.42474E-06	1.07724E-05	7.8216E-05
25	1	0.2	8.92486E-06	2.38793E-06	1.30679E-05	0.000103476
26	1.1	0.2	9.87249E-06	3.7253E-06	1.56049E-05	0.000133979
27	1.2	0.2	1.08273E-05	5.5664E-06	1.83836E-05	0.000170246
28	1.3	0.2	1.17881E-05	8.05698E-06	2.14039E-05	0.000212803
29	1.4	0.2	1.27539E-05	1.13647E-05	2.46659E-05	0.000262172
30	1.5	0.2	1.3724E-05	1.56814E-05	2.81694E-05	0.000318877
31	0.1	0.5	0	0	1.10745E-06	9.36727E-07
32	0.2	0.5	2.11881E-07	0	1.46988E-06	1.51659E-06
33	0.3	0.5	3.8012E-07	2.36062E-08	2.07395E-06	2.55809E-06
34	0.4	0.5	5.75594E-07	1.64661E-07	2.91963E-06	4.17379E-06
35	0.5	0.5	8.38133E-07	4.79573E-07	4.00694E-06	6.51632E-06
36	0.6	0.5	1.2665E-06	9.96424E-07	5.33588E-06	9.75696E-06
37	0.7	0.5	1.76593E-06	1.77782E-06	6.90644E-06	1.40714E-05
38	0.8	0.5	2.33383E-06	2.88172E-06	8.71863E-06	1.96367E-05
39	0.9	0.5	1.09889E-05	2.13031E-07	1.07724E-05	2.66307E-05
40	1	0.5	1.22305E-05	2.79822E-07	1.30679E-05	3.52312E-05
41	1.1	0.5	1.34782E-05	3.46023E-07	1.56049E-05	4.56164E-05
42	1.2	0.5	1.47301E-05	3.88398E-07	1.83836E-05	5.79646E-05
43	1.3	0.5	1.59851E-05	3.469E-07	2.14039E-05	7.24541E-05
44	1.4	0.5	1.72422E-05	7.12738E-07	2.46659E-05	8.92631E-05
45	1.5	0.5	1.85005E-05	9.60985E-07	2.81694E-05	0.00010857

Since linear waves (which is assumed for the analysis) alone cannot yield a net sediment transport, it can be expected that the Scheffner modification to the Ackers and White model will lead to an over-estimation of the transport for high orbital wave velocities. This occurs because the new current velocity is artificially high and since it is used in calculations of the actual transport, will lead to high predictions. It must be remembered, however, that it is unclear whether this new current velocity should be used everywhere in equation 1, and that the over-estimation made by the Ackers and White model would be reduced if the new current velocity replaced only one of the two current velocities in equation 1.

Figures 34 through 36 (pages 98 through 100) plot the total sediment transport versus the average current velocity for the three models. They contain the same conditions as Figures 28 through 30: a wave period of 8 seconds, the same three sediment diameters (0.1 mm, 0.2 mm, and 0.5 mm) and the maximum wave orbital velocity is held constant at 0.35 m/sec. Table 9 on page 101 contains the output of these runs. Figures 28 through 30 reveal how the models account for waves when predicting sediment transport. Figures 34 through 36 reveal how the models account for the current when predicting sediment transport. Comparing the two sets of figures pinpoints the main difference between the Madsen model and the Bailard and the Ackers and White models. The predictions made by the Madsen model differ greatly according to whether the wave orbital velocity is increased or whether the current velocity is increased. When the current velocity is increased, the Madsen model predicts a much larger transport than when the wave orbital velocity is increased. The Bailard results and the Ackers and White results look very similar for both scenarios. The pattern of exponential sediment transport with increasing flow velocity occurs when either the current velocity is increased or the wave orbital velocity is increased. The Madsen model, on the other hand, only predicts exponential growth when the current velocity is increased;

when the wave orbital velocity is increased, the Madsen model predicts a more linear relationship, one that is much flatter than the predictions made by the other two models. The prediction made by the Madsen model makes more physical sense because waves can only keep sediment in suspension in the wave bottom boundary layer and not throughout the entire water column. The current shear stress, on the other hand, can keep sediment in suspension throughout the entire water column, and therefore, increasing the current velocity should have a much larger influence on the sediment transport rate than increasing the wave orbital velocity.

Though the Ackers and White model and the Bailard model predict larger sediment transport rates for the cases where the current velocity is increased, the output looks very similar to the cases where the wave orbital velocity is increased. This makes sense because both models do not differentiate between the effects of waves and currents when calculating the transport. The Madsen model is usually more sensitive to grain size than the other two models, and the Madsen model usually predicts the largest transport for small sediment. Figure 34 appears to contradict this because the Madsen model predicts quite a small sediment transport rate compared to the other models. The Madsen model result for the 0.1 mm sediment follows the pattern of the prediction made for the 0.5 mm sediment and not the 0.2 mm sediment. The reason for this is the fact that sheet flow is occurring for the 0.1 mm sediment so the suspended load transport is quite small, and since suspended load usually dominates for small sediment, this greatly reduces the total sediment transport rate for this sediment. The same thing is occurring for the 0.5 mm sediment: bedload dominates. This is not the case, however, for the 0.2 mm sediment. The suspended load dominates in this case, and as Figure 35 reveals, the total transport rate predicted by the Madsen model rises rapidly with the wave orbital velocity, matching the predictions made by the other two models. The main cause for the difference between suspended load transport rates changing

with sheet flow is the fact that the Madsen resuspension parameter decreases from 0.002 to 0.0002 for a flat bed. Figure 37 (page 102) is identical to Figure 34 except that the resuspension parameter for the Madsen model was set to 0.002, even though sheet flow is occurring. The results are remarkably similar to Figure 35, where suspended load dominates. This shows the importance of the resuspension parameter and the effect of sheet flow.

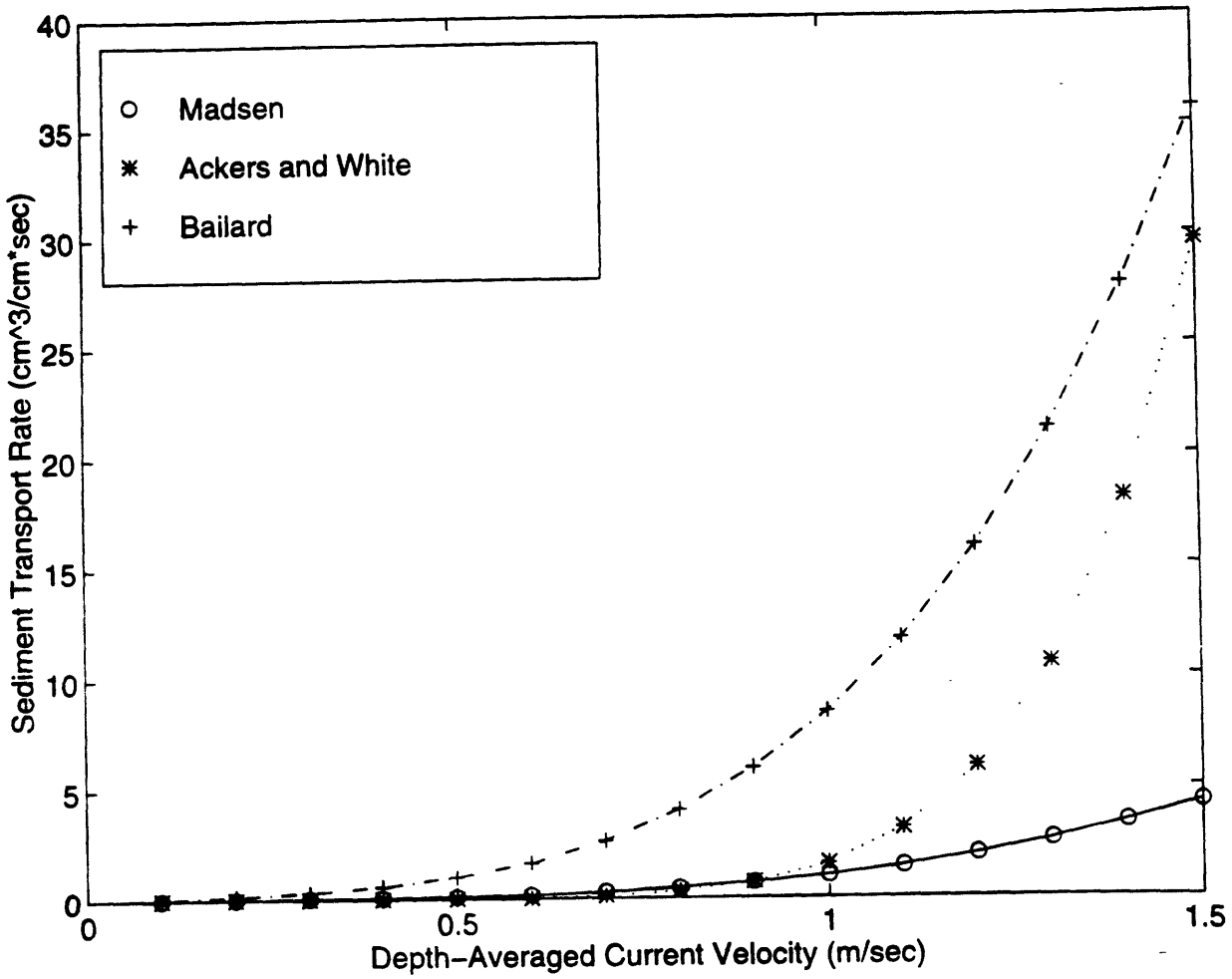

Figure 34. The total sediment transport rate versus the average current velocity for a maximum wave orbital velocity of 0.35 m/sec, a wave period of 8 sec, and 0.1 mm diameter sediment.

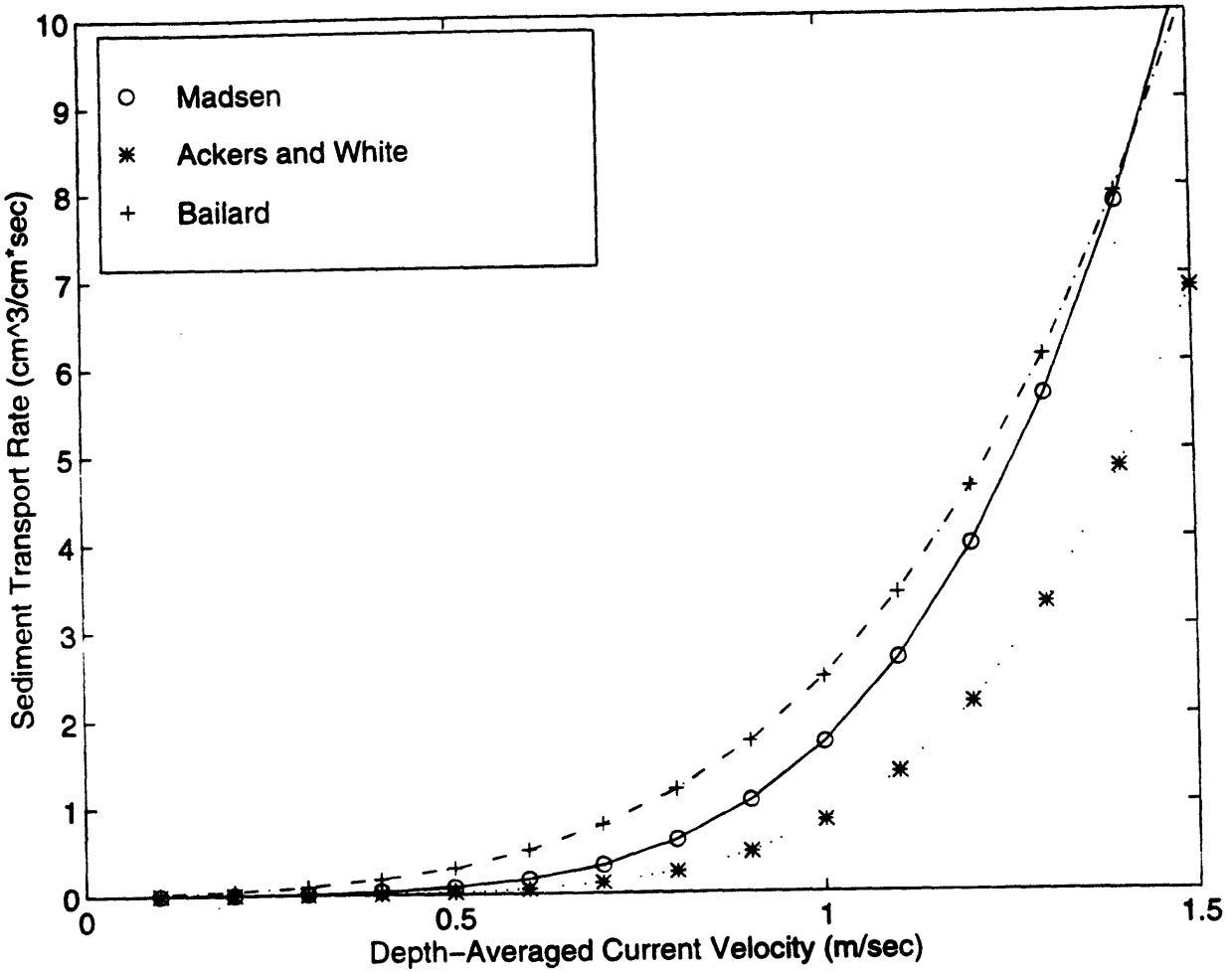

Figure 35. The total sediment transport rate versus the average current velocity for a maximum wave orbital velocity of 0.35 m/sec, a wave period of 8 sec, and 0.2 mm diameter sediment.

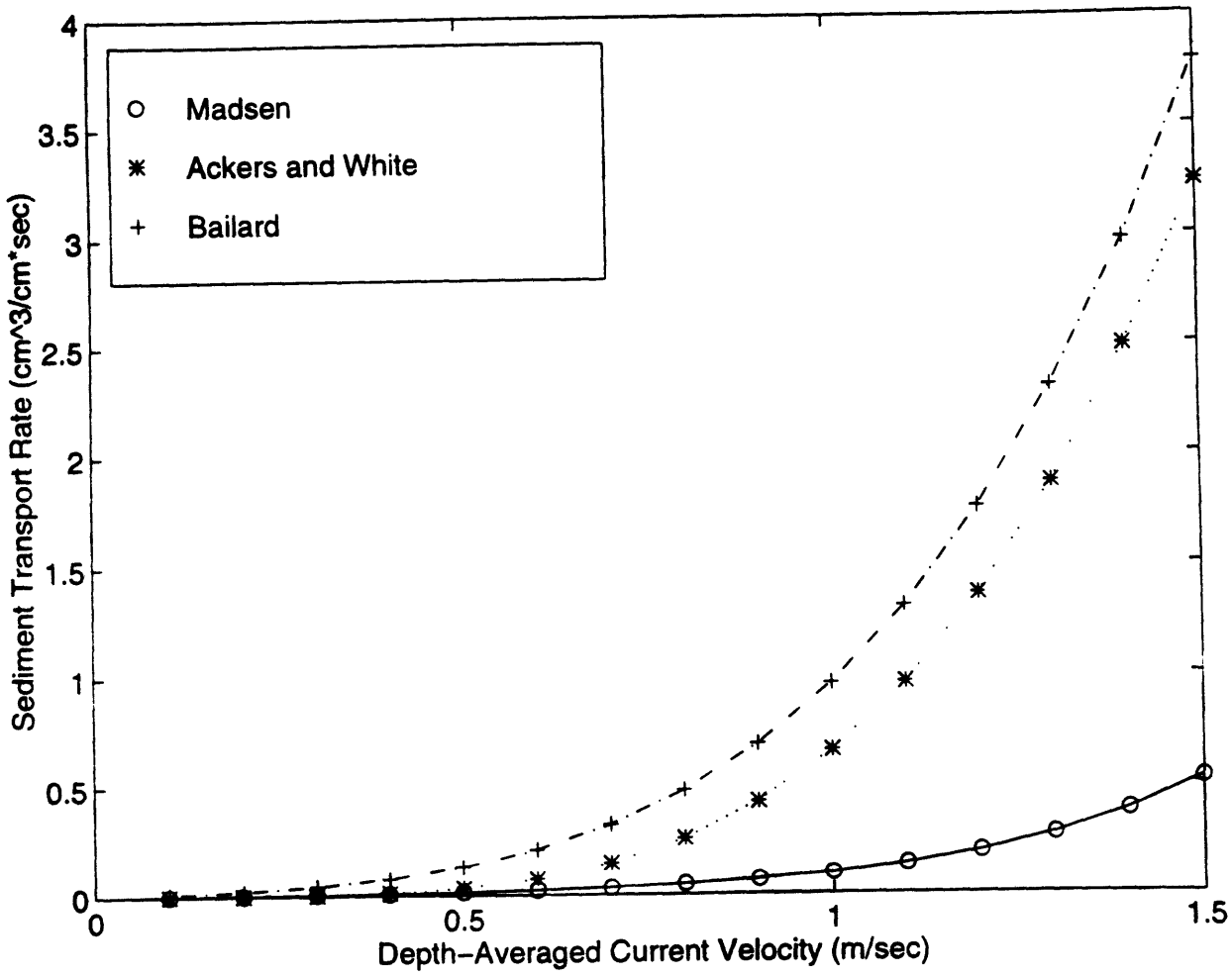

Figure 36. The total sediment transport rate versus the average current velocity for a maximum wave orbital velocity of 0.35 m/sec, a wave period of 8 sec, and 0.5 mm diameter sediment.

Table 9

The Sediment Transport Rate Versus Current Velocity and Sediment Diameter, U_o= 0.35 m/sec.

Case #	Uc (m/sec)	d (mm)	Madsen Total Load (m^3/m*sec)	Madsen Condition 3 = ripples 2 = sheet flow 1 = no flow	Ackers & White Total Load (m^3/m*sec)	Bailard Total Load (m^3/m*sec)
1	0.1	0.1	3.12556E-07	2	1.56278E-09	5.28232E-06
2	0.2	0.1	1.07096E-06	2	9.2376E-09	1.39321E-05
3	0.3	0.1	2.39478E-06	2	5.25896E-08	2.95832E-05
4	0.4	0.1	4.79362E-06	2	2.63198E-07	5.6435E-05
5	0.5	0.1	9.10571E-06	2	1.10138E-06	9.96671E-05
6	0.6	0.1	1.64018E-05	2	3.86196E-06	0.000165809
7	0.7	0.1	2.80523E-05	2	1.15959E-05	0.000262808
8	0.8	0.1	4.53872E-05	2	3.05637E-05	0.000400035
9	0.9	0.1	6.96988E-05	2	7.2307E-05	0.000588277
10	1	0.1	0.000102277	2	0.000156403	0.000839745
11	1.1	0.1	0.000144346	2	0.000313949	0.001168067
12	1.2	0.1	0.000197046	2	0.000591813	0.001588293
13	1.3	0.1	0.000261431	2	0.001057686	0.002116893
14	1.4	0.1	0.000338462	2	0.001805956	0.002771755
15	1.5	0.1	0.000429019	2	0.002964426	0.00357219
16	0.1	0.2	4.03252E-08	3	8.024E-09	1.74055E-06
17	0.2	0.2	2.74246E-07	3	4.10324E-08	4.48366E-06
18	0.3	0.2	1.22687E-06	3	1.81683E-07	9.30319E-06
19	0.4	0.2	3.33139E-06	3	6.7031E-07	1.74244E-05
20	0.5	0.2	7.77508E-06	3	2.05112E-06	3.0335E-05
21	0.6	0.2	1.6634E-05	3	5.33692E-06	4.98839E-05
22	0.7	0.2	3.29546E-05	3	1.21653E-05	7.82999E-05
23	0.8	0.2	6.07323E-05	3	2.49341E-05	0.000118192
24	0.9	0.2	0.000104816	3	4.69164E-05	0.00017255
25	1	0.2	0.00017077	3	8.23577E-05	0.000244743
26	1.1	0.2	0.000264724	3	0.00013656	0.000338521
27	1.2	0.2	0.000393215	3	0.000215953	0.000458013
28	1.3	0.2	0.000563053	3	0.000328167	0.000607729
29	1.4	0.2	0.000781193	3	0.000482084	0.000792559
30	1.5	0.2	0.00105463	3	0.000687899	0.001017774
31	0.1	0.5	5.29821E-07	3	9.03765E-10	8.5488E-07
32	0.2	0.5	1.7083E-06	3	3.48582E-08	2.12095E-06
33	0.3	0.5	3.4163E-06	3	2.71132E-07	4.2319E-06
34	0.4	0.5	5.66689E-06	3	1.10618E-06	7.6693E-06
35	0.5	0.5	8.49155E-06	3	3.17403E-06	1.29976E-05
36	0.6	0.5	1.19247E-05	3	7.30653E-06	2.08953E-05
37	0.7	0.5	1.60005E-05	3	1.4483E-05	3.21611E-05
38	0.8	0.5	2.07519E-05	3	2.57883E-05	4.77136E-05
39	0.9	0.5	2.62107E-05	3	4.23834E-05	6.85918E-05
40	1	0.5	3.24075E-05	3	6.5485E-05	9.59546E-05
41	1.1	0.5	3.9372E-05	3	9.63521E-05	0.000131081
42	1.2	0.5	4.7133E-05	3	0.000136278	0.00017537
43	1.3	0.5	5.57186E-05	3	0.000186582	0.000230341
44	1.4	0.5	6.51566E-05	3	0.000248609	0.000297633
45	1.5	0.5	7.54742E-05	3	0.000323721	0.000379007

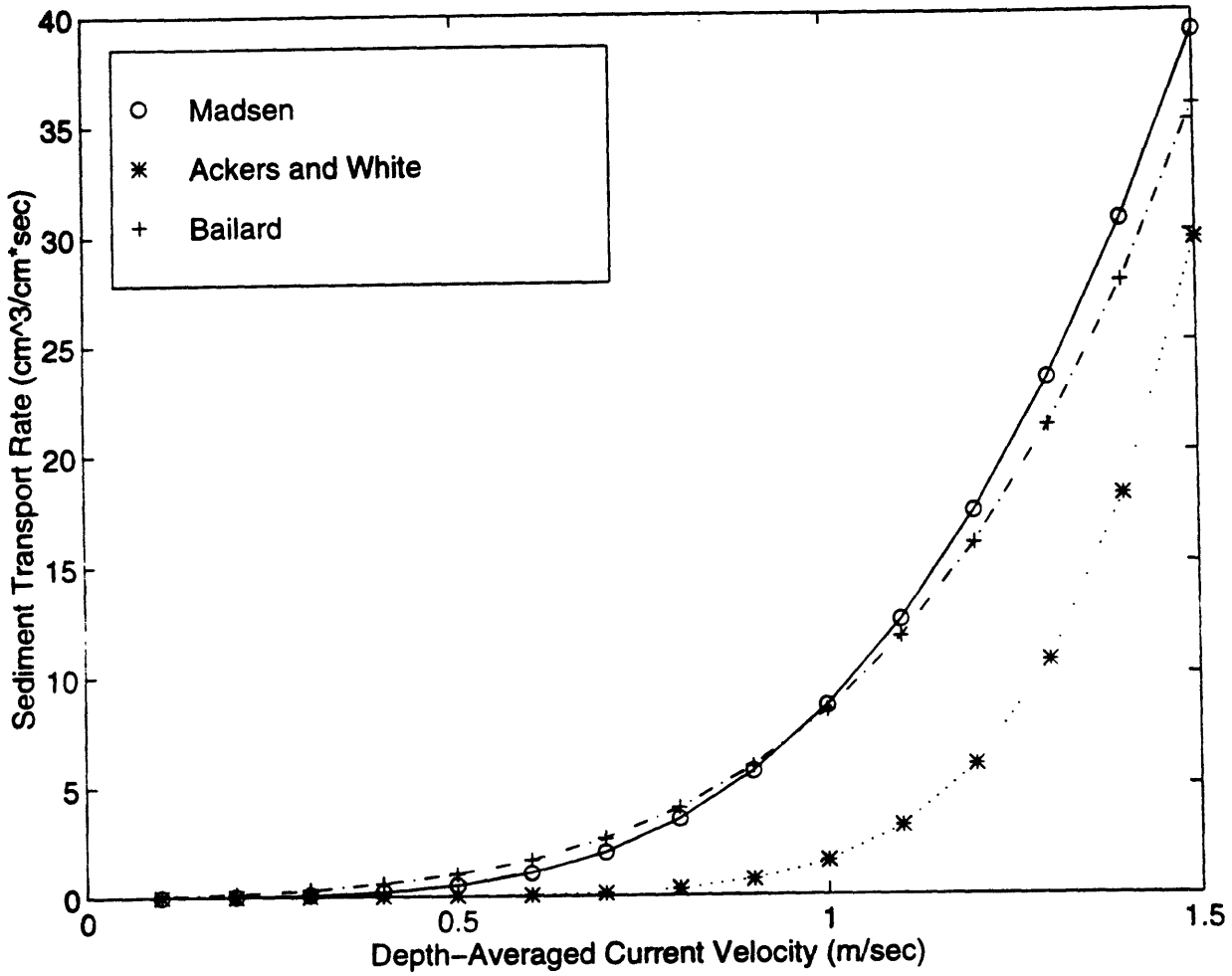

Figure 37. The total sediment transport rate versus the average current velocity for a maximum wave orbital velocity of 0.35 m/sec, a wave period of 8 sec, and 0.1 mm diameter sediment. Same as Figure 34 except that the Madsen resuspension parameter has increased from 0.0002 to 0.002

It appears from all of the runs that the Madsen model usually predicts significantly less transport than the other two, especially in terms of suspended load transport when compared to the Bailard model. This result is especially pronounced at the higher flow velocities. This makes sense, because the main difference between the Madsen model and the other two is how suspended load is calculated and the effect that the wave orbital velocities have in the calculation of the suspended load transport. Since the suspended load transport is more important than the bedload transport for high flow velocities or small sediment, the divergence between the models is the most pronounced at the higher flow velocities.

Other differences between the models arise from the Madsen model's incorporation of bedforms in the calculation of total roughness experienced by the flow, and at the higher flow conditions, the Madsen model predicts the erosion of these bedforms, making it more similar to the other two models by assuming that the bed is flat. It may appear that this should lead the Madsen model's suspended load transport to converge with that of the Bailard model's. The Madsen model, however, constantly takes the changing floor conditions into account; the Bailard model and the Ackers and White model do not. It is important to remember that the Bailard model has three factors that were determined experimentally, probably from flows with bedforms, so they probably apply to flows with bedforms, and not to sheet flow conditions. This could contribute to the divergence. Another possible cause of divergence is the uncertainty of the Madsen model's reference concentration and resuspension parameter. The difference between Figures 34 and 37 show how changing the resuspension parameter can greatly alter the magnitude of the Madsen model results.

It is impossible to judge which model gives the best answer by looking at the magnitude of each result. Predicting sediment transport is highly uncertain, and it is logical to examine the

methodology of each model and the patterns that arise from the results. This would suggest that the Madsen model and the Ackers and White model would give the best results for low flow rates. The Madsen model appears to do the best job of accounting for wave period and changes in the bed, as well as in predicting the suspended load transport, which the Bailard model appears to over-estimate. Also, the Ackers and White model does not seem very appropriate for the real coastal environment because of its prediction that transport does not always increase with decreasing sediment diameter and also its failure to incorporate the effects of bed slope and the angle between wave propagation and current velocity.

6.0 Conclusion

The prediction of sediment transport is complex and depends on many variables that constantly change. There are many models that predict sediment transport based on these variables, and the models vary greatly in their complexity. The Ackers and White model is the simplest of the three models examined while the Madsen models is the most complex, attempting to incorporate all of the factors that influence the calculation of the sediment transport rate.

Comparing the predictions of the three models for pure unidirectional flow reveal differences between the models, but the overall patterns are quite similar. Increased flow velocities lead to greater sediment transport rates for all three models, and even though the models differ on the absolute values of the transport, they do predict similar patterns. There are differences when the transport is broken down, however. The Madsen and Bailard models differ on the method of calculating suspended load transport, since the Bailard model does not incorporate a flow depth in its

calculations while in the Madsen model, the flow depth is an important factor in determining the suspended load transport rate. This difference is magnified for the combined current-wave flow. The Ackers and White model differs from the other two by not predicting that the transport rate always decreases with increased sediment diameter. The Bailard model differs from the others by not incorporating a flow depth and a critical parameter for the initiation of movement in its calculations. Despite these differences, the models do not predict great differences for low to moderate flow rates (flows with a current velocity that is less than 1 m/sec).

The differences between the models are magnified when the predictions for combined current-wave flows are analyzed. Both the Bailard model and the Ackers and White model fail to differentiate between the effect the current has on the sediment transport rate and the effect that waves have on the sediment transport rate. Waves and currents contribute to sediment transport in different ways, and a large current can transport more sediment than a large wave can. In fact, no linear wave can produce a net sediment transport, no matter how large it is. The Madsen model does take these differences into account when calculating the sediment transport rate. The Bailard model and the Ackers and White model combine the current velocity and the maximum wave orbital velocity into one velocity vector that is used to determine sediment transport. The Madsen model uses both velocities to determine the amount of sediment scoured into suspension and uses both velocities to determine the initiation of bedload, but it uses only the current velocity for determining the suspended transport of these loads.

The main difference between the Madsen model and the other two arises mainly from the suspended load sediment transport, where the flow depth and the differentiation between the current and wave velocities is quite important. From the patterns of the predictions and the methods used by the three models, it appears that the Madsen model does the best job at incorporating all

of the factors that go into the sediment transport rate. Unlike the other two models, the Madsen model predicts the roughness of the bottom (whether there are ripples or dunes present) and uses this information to further refine its predictions.

The Bailard model is limited by the fact that is does not incorporate a flow depth or differentiate between the current and wave velocities in its calculations. The Ackers and White model (with the Scheffner modification to account for waves) is limited by the fact that it oversimplifies the current-wave problem by assuming that the wave orbital velocity and the current velocity are in the same direction, by assuming that the waves approach the shore directly and by accounting for waves with the simple augmentation of the average current velocity. The Bailard model and the Ackers and White model would over-predict the total sediment transport rate when there are large waves because of these deficiencies. The Madsen model does the best job at incorporating all of the factors that go into determining sediment transport and its use is recommended when attempting to predict sediment transport.

7.0 References

1. Ackers, P., "Sediment Transport in Channels: An Alternative Approach", Report INT 102, Hydraulics Research Station, Wallingford, England, Mar., 1972

2. Ackers, P. and White, W.R., "Sediment transport: new approach and analysis", *Journal of the Hydraulics Division*, ASCE, 99(11), 2041-2060, 1973.

3. Bagnold, R.A., "An Approach to the sediment transport problem from general physics", *U.S. Geological Survey Prof. Paper*, 422-I, 1966.

4. Bailard, J.A., "An Energetics total load sediment transport model for a plane sloping beach", *Journal of Geophysical Research*, Vol 86, 10938-10954, 1981.

5. Madsen, O.S., "Spectral Wave-Current Bottom Boundary Layer Flows", *24th International Conference Coastal Engineering Research Council/ASCE*, 1994.

6. Madsen, O. S., Course notes for class 1.67 at the Massachusetts Institute of Technology, fall semester 1997.

7. Scheffner, N.W., "Systematic analysis of long-term fate of disposed dredged material", *Journal of Waterway, Port, Coastal, and Ocean Engineering*, 127-133, 1996.